Studies toward the Total Synthesis of Biselides & Radical Fluorination of Aliphatic Compounds

by

Hope Fan

B.Sc. (Hons., Biochemistry), University of Waterloo, 2011

Thesis Submitted in Partial Fulfillment of the
Requirements for the Degree of
Master of Science

in the
Department of Chemistry
Faculty of Science

SIMON FRASER UNIVERSITY

Spring 2014

Approval

Name: **Hope Fan**

Degree: **Master of Science**

Title of Thesis: ***Studies toward the Total Synthesis of Biselides & Radical Fluorination of Aliphatic Compounds***

Examining Committee: **Chair:** Dr. Krzysztof Starosta
Associate Professor

Dr. Robert A. Britton
Senior Supervisor
Associate Professor

Dr. Charles J. Walsby
Supervisor
Associate Professor

Dr. Peter D. Wilson
Supervisor
Associate Professor

Dr. Robert N. Young
Internal Examiner
Professor

Date Defended/Approved: January 24, 2014

Partial Copyright Licence

Abstract

Modern pharmaceuticals originate predominately either from natural products or totally synthetic compounds. The rich variety of marine life found in the Earth's oceans have especially allowed our access to increasingly more and intriguing biologically active marine natural products, such as haterumalides and biselides. The lack of materialistic return associated with natural product isolation from marine organisms has prompted the need for practical laboratory synthesis. The same demand holds true for synthetic drugs, as more novel synthetic methods are required to complement the increasingly target- and diversity-oriented approach to synthetic drug discovery.

Biselides, isolated from the Okinawan ascidian *Didemnidae* sp., are marine macrolides which have demonstrated potent cytotoxicity towards a variety of human cancer cell lines while being non-toxic towards brine shrimp. They contain a 2,5-disubstituted-3-oxygenated tetrahydrofuran functionality and a (*Z*,*Z*)-1,4-diene as part of a 14-membered macrocyclic molecular skeleton. A proposed total synthesis of biselide A involves the cyclization of chloropolyols to form the substituted tetrahydrofuran and metathesis for construction of the (*Z*,*Z*)-1,4-diene. Specifically, direct ring-closing metathesis (RCM), relay ring-closing metathesis (RRCM), and cross metathesis (CM) strategies were examined, with only the CM strategy allowing us to construct the 1,4-diene with desired geometry.

The second part of this thesis describes the development of a novel methodology for the direct conversion of C(sp^3)-H bonds to C(sp^3)-F bonds. This radical-based, photocatalytic process yielded monofluorinated products from various small molecule aliphatic substrates, and has showed further potential with other chemical systems. Improvement and expansion of this methodology could hold positive future implications with regards to fluoropharmaceuticals.

Keywords: marine natural products; tetrahydrofurans; total synthesis; biselide; metathesis; fluorination

Acknowledgements

First and foremost, I would like to acknowledge the support and mentorship of my senior supervisor, Dr. Robert Britton, without whom I would not be here. I am deeply grateful for the confidence he had shown in me, and for his infectious enthusiasm, optimism, high scientific standards, endless knowledge, and constant encouragement. I am especially inspired by his never-say-die attitude, which served as motivation during times of struggle in a long total synthesis project.

I would like to thank the members of my supervisory committee, Profs. Peter Wilson and Charles Walsby, for their support and guidance during my M.Sc. studies. It was also a pleasure to work for Dr. Wilson as a teaching assistant, and to obtain muscle-building secrets from Dr. Walsby at the gym. I would also like to thank Prof. Robert Young for serving as the internal examiner.

I would like to extend my thanks to Prof. Regine Gries for her kind assistance with chiral gas chromatography, as well as her patient willingness to practice speaking German with me.

I would like to acknowledge the assistance of the NMR staff, Dr. Andrew Lewis and Colin Zhang, for helping me set up various complex NMR experiments. I further want to thank the departmental secretaries Lynn Wood and Evon Khor for all their assistance, ever-positive attitude, and flawless organization.

I would also like to thank the Britton Group members from past and present: Dr. Bal Kang, Dr. Jeff Mowat, Stanley Chang, Shira Halperin, Milan Bergeron-Brlek, Jason Draper, Michael Holmes, Vijay Dhand, Lee Belding, Jarod Moore, Steve Hur, and Matthew Taron; I was truly fortunate to work alongside these intelligent and easy-going people who during this journey have become good friends. I would also like to thank other friends in the department, especially Thanh Nguyen, Nevena Cekic, and Dr. Lubomir Vezenkov, for their support and generosity throughout my graduate studies.

I would like to thank my parents for giving me the freedom to pursue my interests in life, for allowing me to develop my own independence and personality. I would also like to thank all my friends for their unshaken support.

Lastly, I would like to thank my former supervisor at the University of Waterloo, Prof. Michael Chong, for getting this all started. I am deeply grateful for the opportunities given to me during my undergraduate studies, and for his continued support for my career. As well, I would like to thank NSERC and SFU for their generous and much-needed financial support.

Table of Contents

List of Tables

List of Figures

List of Schemes

List of Abbreviations

9-BBN	9-Borabicyclo[3.3.1]nonane
$[\alpha]_D$	Specific rotation at the sodium D line (589 nm)
δ	Chemical Shift in ppm from tetramethylsilane
°C	Degrees Celsius
Ac	Acetyl
aq	Aqueous
Bn	Benzyl
Bu	Butyl
BuLi	*n*-Butyl lithium
Bz	Benzoyl
cat	Catalytic amount
Cbz	Carboxybenzyl
COSY	Correlation Spectroscopy
CSA	Camphorsulfonic acid
dba	Dibenzylidene acetone
DCE	Dichloroethane
de	Diastereomeric excess
DIBAL-H	Diisobutylaluminium hydride
DIC	*N,N'*-Diisopropylcarbodiimide
DIPA	Diisopropylamine
DIPEA	Diisopropylethylamine
DMAP	*N,N*-Dimethylaminopyridine
DMP	Dess-Martin periodinane
DMPM	Dimethoxylphenylmethyl
DMSO	Dimethylsulfoxide
dr	Diastereomeric ratio
ee	Enantiomeric excess
eq	Equivalents
er	Enantiomeric ratio
Et	Ethyl
HPLC	High-performance liquid chromatography
HRMS	High-resolution mass spectrometry
HSQC	Heteronuclear Single Quantum Coherence
Hz	Hertz
i	Iso-
LDA	Lithium diisopropylamide

LiHMDS	Lithium hexamethyldisilazide
M	Molar
m-CPBA	*meta*-Chloroperoxybenzoic acid
Me	Methyl
Mes	Mesityl
mmol	Millimole (s)
mol	Mole (s)
m.p.	Melting Point
MW	Microwave
NCS	*N*-chlorosuccinimide
NFSI	*N*-fluorobenzenesulfonimide
NMR	Nuclear Magnetic Resonance
nOe	Nuclear Overhauser Effect
Nu	Nucleophile
PG	Protecting group
Ph	Phenyl
PMB	*para*-Methoxybenzyl
ppm	Parts-per-million
PPTS	Pyridinium *para*-toluenesulfonate
Pr	Propyl
RCM	Ring-closing metathesis
RRCM	Relay ring-closing metathesis
r.t.	Room temperature
SCUBA	Self-Contained Underwater Breathing Apparatus
SOMO	Singly Occupied Molecular Orbital
t	Tertiary
TBADT	Tetrabutylammonium decatungstate
TBAF	Tetra-*n*-butylammonium fluoride
TBDPS	*tert*-Butyldiphenylsilyl
TBHP	*tert*-Butyl hydroperoxide
TBS	*tert*-Butyldimethylsilyl
TES	Triethylsilyl
Tf	Trifluoromethanesulfonyl
THF	Tetrahydrofuran
TIPS	Triisopropylsilyl

1. Introduction

Throughout much of our history, humans have relied on medicinal substances for the treatment of illnesses and diseases. During this time, our means of drug discovery has undergone revolutionary changes, from the trial-and-error practice of ingesting animal and herbal products for much of human history, to the current era of modern pharmacology in the Developed World, where a wide range of drug discovery methods are employed.[1] In 2007, Newman and Cragg published a comprehensive analysis of the sources of new and approved drugs from the 25-year window between 1981 and 2006. This report highlights the influence of synthetic and natural product based/derived drugs on the drug discovery and development process during this period of time (Table 1.1).[2] Totally synthetic drugs (i.e., pharmaceutical entities discovered through random screening of synthetic compound libraries)[3,4] account for the largest percentage of drug origins at 31%. Natural products, including their analogs with semisynthetic variations, make up for a combined 27%, while synthetic drugs based on natural pharmacophores or natural substrate mimics comprise another 26%.[2–4] It is evident that, despite the growing importance of totally synthetic drugs, natural products remain an important player in the drug discovery process.

Table 1.1 New chemical entities by source of compound, 1981-2006[2]

origin of drug	number of drugs	percentage of grand total
Biological (usually large protein or peptide isolated from organism/cell line or produced by biotechnological means in a surrogate host)	124	12%
Natural product	43	4%
Natural product derived (usually with a semisynthetic modification)	232	23%
Totally synthetic (often found by random screening or modification of an existing agent)	310	31%
Synthetic but with natural product pharmacophore or natural product mimic	262	26%
Vaccine	39	4%
grand total	1010	100%

Natural products are defined as compounds that are derived from natural sources.[5] Traditionally, these natural sources have been terrestrial organisms such as plants, animals, and microorganisms. However, with the introduction of SCUBA in the 1960s and subsequent technological advances, researchers have increasingly explored the marine environment as a source of novel and diverse biologically active natural products.[6] Covering roughly 70% of the Earth's surface, the planet's oceans represent the largest habitat for the world's species. Today, marine invertebrates (e.g., sponges, molluscs, tunicates, and bryozoans), bacteria, and algae have become well-known sources of natural products which have served as drugs or drug leads.[7] Two such examples include ecteinascidin 743 (**1**), a European Commission approved anti-tumor drug and natural product isolated from the sea squirt *Ecteinascidia turbinata*, and bryostatin 1 (**2**), isolated from the bryozoan *Bugula neritina* and currently in Phase II trials for treating Alzheimer's disease (Figure 1.1).[8]

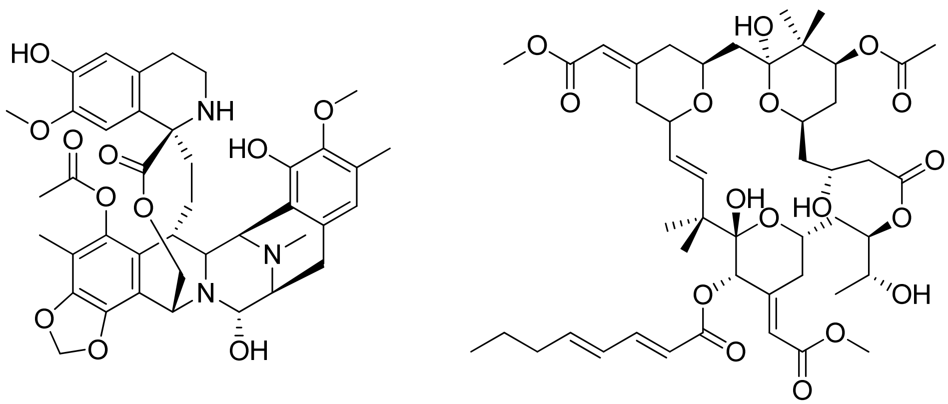

ecteinascidin 743 (**1**)   bryostatin 1 (**2**)

Figure 1.1 Examples of marine natural products as drugs or drug leads

The biggest difficulty facing the development of drug candidates from marine natural products is the procurement of sufficient and sustainable quantities of these rare compounds. Since many chemically diverse marine sponges are primitive metazoans that live almost exclusively in marine habitats, their microbial fauna are largely unculturable.[9] As a result, the valuable compounds produced by these marine sponges must be extracted and purified from specimens collected by hand using scuba diving or other related techniques. Also, since biologically active marine natural products are generally produced in small quantities as secondary metabolites, even when a large

quantity of the marine organism is obtained, the tedious extraction process (repeated fractionation, concentration, and purification) often means the eventual isolation of only micro- to milligram quantities of a natural product, usually barely enough for structure determination and basic biological testing.[10] This challenge has spurred many efforts in organic synthesis, although the level of structural complexity presented by many marine natural products has rendered synthetic efforts impractical.[11] Therefore, it is imperative that new synthetic methodologies be developed to allow improved access to a wide variety of natural product skeletons, and to uncover the promising biological properties of these compounds.

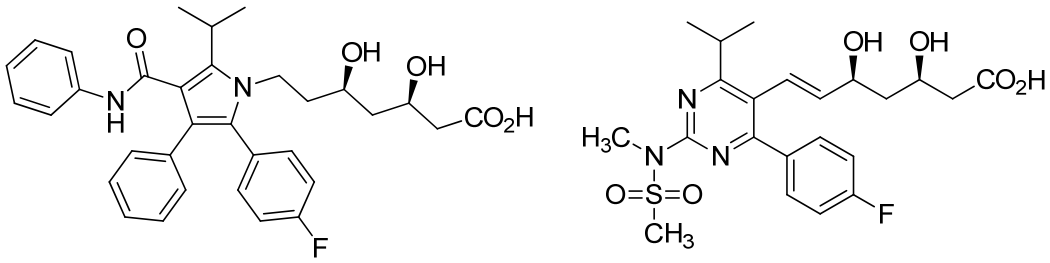

Lipitor (**3**) Crestor (**4**)

Figure 1.2 Examples of globally top-selling pharmaceuticals containing fluorine

While the use of natural products as the source for drug discovery is common practice, it is through recent advances in drug discovery technology that totally synthetic drugs have gained prominence. Since the second half of the 20th century, advances in molecular biology and genetics, coupled with the development of new synthetic chemistry methodologies brought target- and variety-oriented approaches to drug research.[12,13] Thus, the introduction of high-throughput screening (HTS) against defined molecular targets and the development of combinatorial chemistry provided even more tools for the pharmaceutical industry, resulting in the creation of enormous synthetic chemical libraries.[10] The improvement and expansion of existing synthetic methodologies has been crucial for keeping pace with demand for novel synthetic molecules. This is especially true for fluorine-containing molecules, which make up 15-20% of all new chemical entities licensed for the clinical market in the past 60 years,[14] and include globally top-selling pharmaceuticals such as Lipitor (**3**) and Crestor (**4**) (Figure 1.2).[15]

1.1. Thesis Overview

The research described in this thesis relates to synthetic efforts toward molecular targets that possess therapeutic potential. Specifically, this thesis focuses on the development of a marine natural product synthesis, as well as a fluorination methodology that may have promising future implications.

In Chapter 2, a detailed discussion of our efforts toward the first total synthesis of biselide A (Figure 2.3), a member of a family of marine macrolides that have demonstrated various anticancer activities, is presented. Applying the versatile tetrahydrofuran formation methodology previously developed in the Britton group, we were able to access the 2,5-disubstituted-3-hydroxytetrahydrofuran core of biselides in a direct and efficient manner. The bulk of these investigations focused on the construction of the challenging (*Z*,*Z*)-1,4-diene function via various types of metathesis reactions. Specifically, direct ring-closing metathesis (RCM), relay ring-closing metathesis (RRCM), and cross metathesis (CM) strategies were examined, with only the CM strategy allowing us to construct the 1,4-diene with desired geometry. Successful construction of the (*Z*,*Z*)-1,4-diene functionality represented a conquering of the most significant obstacle in this work, with the subsequent steps required to finish the synthesis unlikely to cause any major problems.

In Chapter 3, the development of a novel, mild, photocatalytic methodology for the radical fluorination of aliphatic C(sp^3)-H bonds, using tetrabutylammonium decatungstate (TBADT) as catalyst and *N*-fluorobenzenesulfonimide (NFSI) as the fluorine source, is detailed. A number of small molecule aliphatic substrates with multiple C(sp^3)-H bonds were subjected to a set of optimized reaction conditions, with monofluorination occurring predominantly at the most sterically accessible methylene and methine centers and electronically favourable positions.

2. Studies toward the Total Synthesis of Biselides

2.1. Tetrahydrofuran-Containing Marine Natural Products

Oxygen-containing heterocycles are ubiquitous motifs in biologically active marine natural products. Historically, tetrahydropyran (THP)-containing polyketide macrolides have attracted considerable attention as leads for drug discovery.[16] For example, THP-containing marine macrolides such as bryostatin 1 (**2**, Figure 1.1)[17] has reached the clinical trial stage as an anticancer agent. More recently, however, an increasing number of tetrahydrofuran (THF)-containing marine natural products have joined this prominent class of new and exciting bioactive marine macrolides.[16] These THF-containing macrolides tend to be of smaller molecular weight and lower structural and stereochemical complexity in comparison with their THP-containing counterparts and, as a result, have inspired much synthetic effort. Figure 2.1 depicts several examples of THF-containing marine natural products possessing anticancer activities that have been isolated and synthesized.

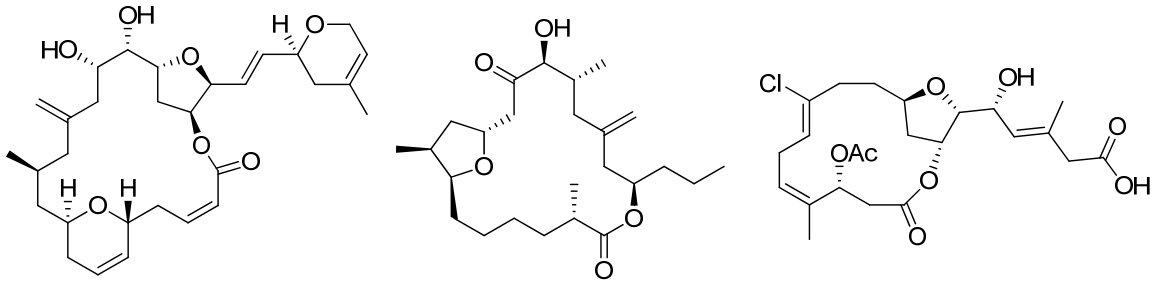

Fijianolide A (**5**) Amphidinolide T1 (**6**) Haterumalide NA (**7**)

Figure 2.1 Several THF-containing marine natural products

Fijianolide A (**5**) is a member of the fijianolide series of 20-membered ring marine macrolides, first isolated in 1988 from the marine sponge *Cacospongia mycofijiensis*.[18]

Fijianolides A and B exhibited cytotoxicity against human colon tumor cells and murine lymphoma cells. Total synthesis of fijianolide A (**5**) was completed by Mulzer and co-workers in 2008, using Sharpless asymmetric epoxidation[19] followed by stereospecific epoxide opening to generate the 2,5-disubstituted-3-oxygenated tetrahydrofuran functionality (Scheme 2.1).[20]

Scheme 2.1 Mulzer's method for constructing the THF ring in the synthesis of fijianolide A

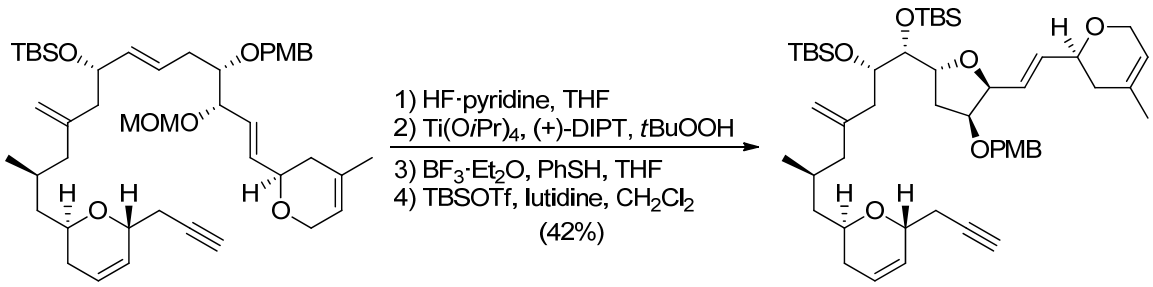

8 **9**

Scheme 2.2 Yadav's method for constructing the THF ring in the synthesis of amphidinolide T1

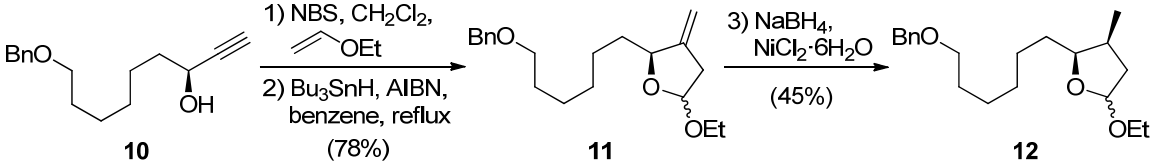

10 **11** **12**

Amphidinolide T1 (**6**) is a member of the amphidinolide T series of 19-membered macrolactones isolated from the marine dinoflagellates *Amphidinium* sp. in 1999, and contains a 2,3,5-trisubstituted tetrahydrofuran ring and an exocyclic methylidene group.[21,22] Amphidinolide T1 (**6**) was shown to possess *in vitro* cytotoxicity against murine leukemia L 1210 cells. Several total syntheses of amphidinolides T have been reported, with construction of the tetrahydrofuran ring most commonly accomplished via diastereoselective oxocarbenium allylation.[23,24] In the synthesis of amphidinolide T1 by Yadav and Reddy,[23] alkynol **10** was first converted to its corresponding bromo acetal with NBS and ethyl vinyl ether, followed by radical cyclization initiated with Bu_3SnH and AIBN to generate alkene lactol ether **11**, which was subsequently reduced[25] to afford

lactol ether **12** (Scheme 2.2). This latter material was eventually converted into the tetrahydrofuran ring in amphidinolide T1 via further transformations.

Haterumalide NA (**7**) is a member of the haterumalide family of 14-membered marine macrolides, first isolated in 1999 from the Okinawan marine sponge *Ircinia* sp.[26] Early studies on haterumalide NA (**7**) showed its cytotoxicity towards human leukemia cells. Like fijianolide A, haterumalide NA also contains a 2,5-disubstituted-3-oxygenated tetrahydrofuran core. Several syntheses of haterumalide NA have been achieved to date and will be described in detail in Section 2.3.

Although biologically active THF-containing marine natural products are increasingly prevalent, and numerous different synthetic methods have evolved to construct these molecular scaffolds, there remains room for improvement. For example, many of the processes used to synthesize substituted tetrahydrofuran rings require lengthy synthetic sequences necessary to prepare elaborate cyclization precursors, the use of chiral pool starting materials (which limits application to diastereomeric congeners), or numerous functional group manipulations. These factors limit the broader utility of tetrahydrofuran syntheses which are normally tailored for a specific synthetic target with a defined configuration and substitution pattern, or decrease the overall efficiency of the synthesis.[27] Therefore, there remains significant interest in the development of more general synthetic methods to access functionalized tetrahydrofurans and related natural products.

2.1.1. Application of α-Chloroaldehydes to the Synthesis of Tetrahydrofuran-Containing Natural Products

Considering the potential importance of many THF-containing natural products as leads in different therapeutic areas, we have had a long standing interest in the development of efficient and stereoselective synthetic methods to access substituted tetrahydrofurans. Specifically, our approach to tetrahydrofurans exploits the enantioselective methods for α-chloroaldehyde synthesis developed independently by Jørgensen[28] and MacMillan,[29] using L-prolinamide or an imidazolidinone respectively, as chiral organocatalysts (Scheme 2.3).[30] An aldol reaction between the enantiomerically enriched α-chloroaldehyde and a lithium enolate affords *anti*-configured β-

ketochlorohydrin in good yield and excellent diastereoselectivity,[27,31,32] which can be rationalized by the Evans-Cornforth model for acyclic stereocontrol.[33,34] In this model, it is proposed that in the energetically favored transition structure for reactions of α-chloroaldehydes with nucleophiles, the dipoles of the C=O and C-Cl bonds in the α-chloroaldehyde are opposed in order to minimize the molecule's net dipole moment (Scheme 2.4). The nucleophile (in our case a lithium enolate) then attacks from the less sterically hindered face of the α-chloroaldehyde, resulting in the formation of a product with an *anti*-relationship between adjacent hydroxymethine and chloromethine stereocenters.

Scheme 2.3 Synthesis of β-ketochlorohydrins from α-chloroaldehydes

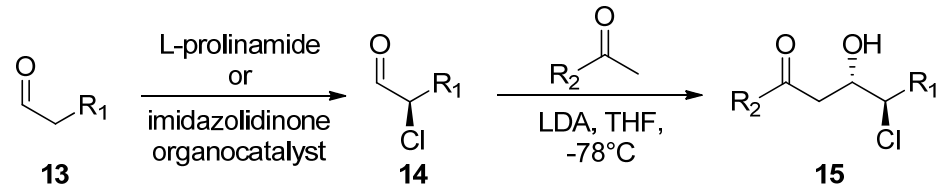

Scheme 2.4 Evans-Cornforth model for rationalizing the stereochemical outcome of aldol additions to α-chloroaldehydes

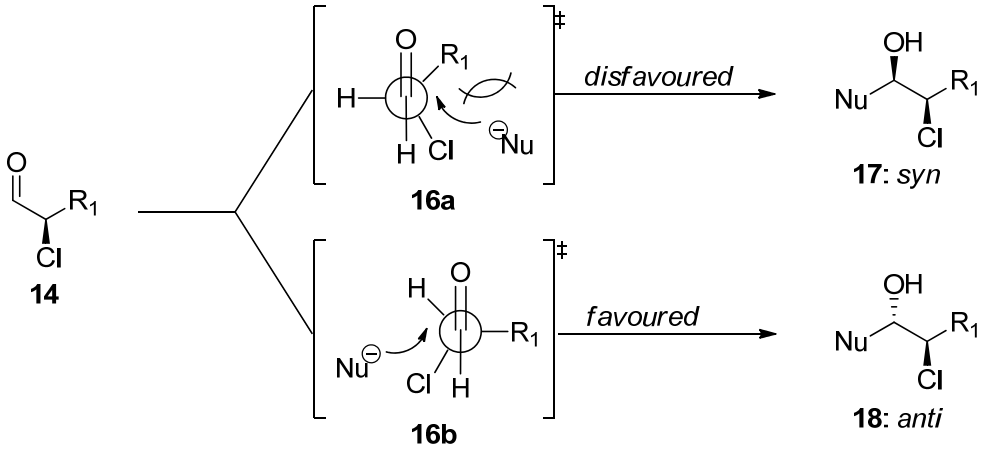

Stereoselective reduction of the resulting β-ketochlorohydrin **15** in either a 1,3-*anti*[35] or 1,3-*syn*[36] fashion then gives diastereomeric chlorodiols **19** and **20**, respectively (Scheme 2.5). Silver-promoted direct S_N2 displacement of the C2 chlorine by the C5

hydroxyl group gives tetrahydrofuranols **21** and **23**, while epoxidation under basic conditions followed by Lewis acid-promoted epoxide opening/rearrangement affords tetrahydrofuranols **22** and **24**. Thus, following any combination of these steps we are able to obtain all four possible 2,5-disubstituted-3-hydroxytetrahydrofuran diastereomers from a single 1,2-*anti*-chlorohydrin starting material (**15**). This stereochemically flexible sequence represents a highly efficient method with which one can rapidly access 2,5-disubstituted-3-hydroxytetrahydrofurans of any configuration.

Scheme 2.5 Synthesis of all diastereomers of the 2,5-disubstituted-3-hydroxytetrahydrofuran scaffold from its 1,2-anti-chlorohydrin precursor

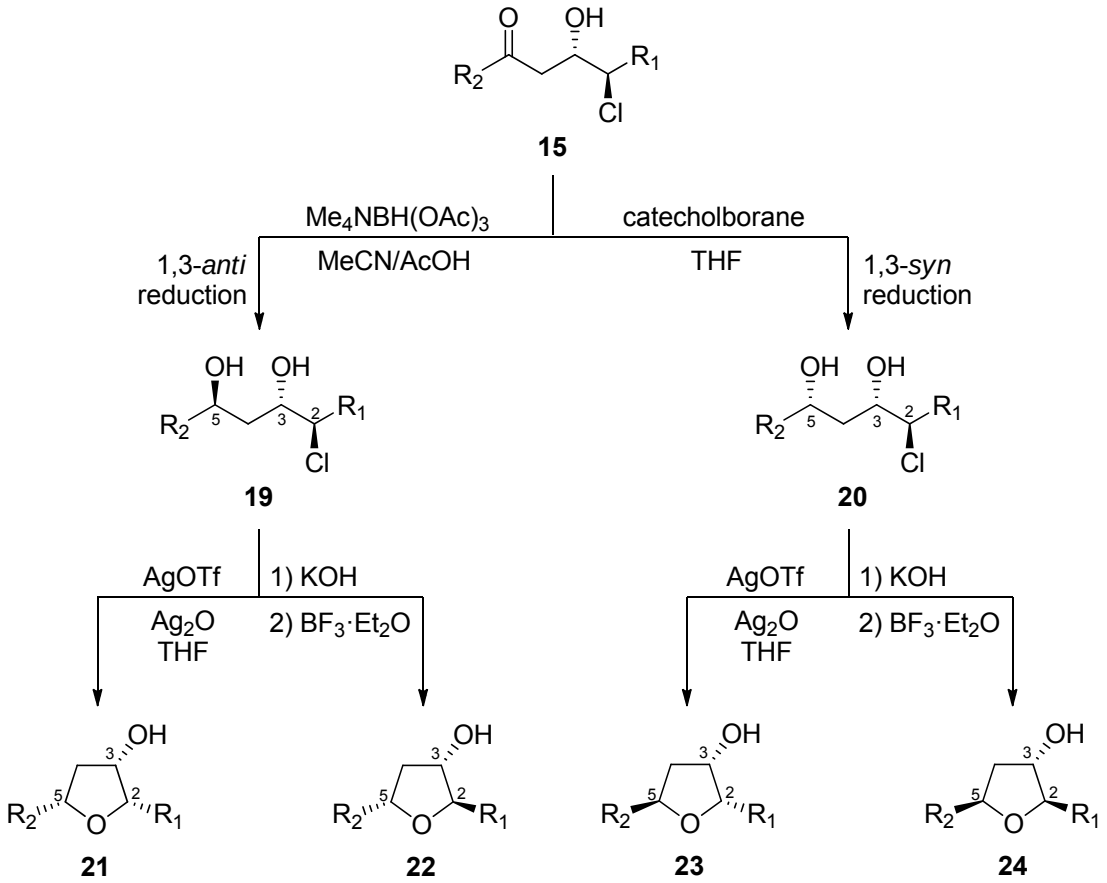

Soon after the development of this sequence, members of the Britton group (Dr. Bal Kang and Stanley Chang) discovered an alternative method for the direct cyclization of chloropolyols that does not require silver.[31] Thus, it was found that a variety of chloropolyols undergo direct cyclization to the corresponding tetrahydrofurans simply by

heating them in water or other common polar solvents. This simple and economical process effectively removes the need for stoichiometric amounts of silver salts, a notable drawback of our previous procedure. To demonstrate the effectiveness of this method, this process was applied to the synthesis of (+)-goniothalesdiol (**29**), a cytotoxic THF-containing natural product isolated from the bark of the Malaysian tree *Goniothalamus borneensis* (Scheme 2.6).[31,37]

Scheme 2.6 Application of chloropolyol cyclization methodology to the synthesis of (+)-goniothalesdiol

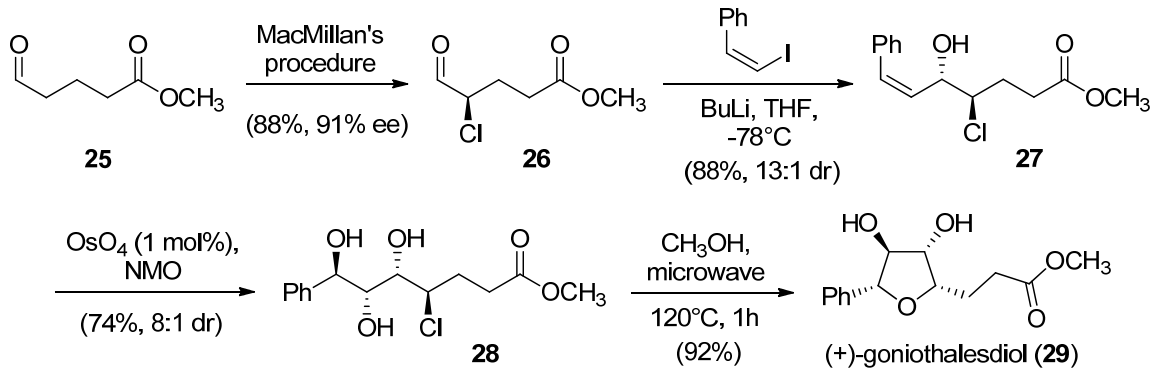

Our group went on to further demonstrate the utility of these chloropolyol cyclization processes in the synthesis of several other natural products and carbohydrates, including (+)-cephalosporolide E (**30**), (+)-pachastrissamine (**31**), and laurefurenyne A (**32**) (Figure 2.2). This chapter is dedicated to our current studies toward the total synthesis of biselides (close relatives of haterumalides, Figure 2.3), which also utilizes our chloropolyol cyclization method for tetrahydrofuran construction.

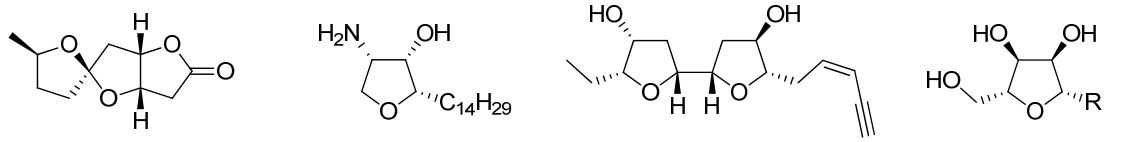

(+)-cephalosporolide E (**30**) (+)-pachastrissamine (**31**) laurefurenyne A (**32**) carbohydrates (**33**)

Figure 2.2 Various natural products synthesized in the Britton group using the chloropolyol cyclization methodology

2.2. Haterumalide and Biselide Marine Natural Products

The biselides and haterumalides are members of the cytotoxic marine macrolide family of natural products, with the key difference being oxidation at C20.[38] This family of marine macrolides has many unique structural features, including a 14-membered macrocycle (except in biselide E), a vinyl chloride functionality as part of a 1,4-diene, and a core tetrahydrofuran ring (Figure 2.3). Aside from biselide E, each member of the biselides and haterumalides possesses 5 stereogenic centers.

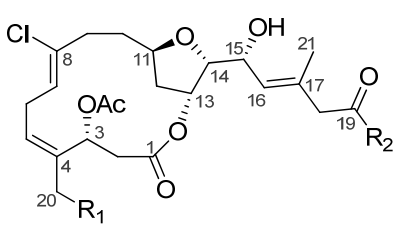

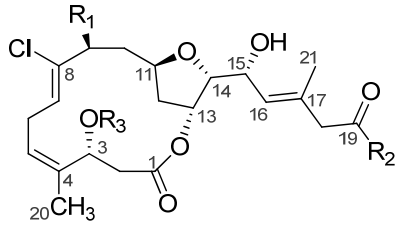

	R_1	R_2
Biselide A (**34**)	OAc	OH
Biselide B (**35**)	OAc	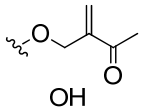
Biselide C (**36**)	OH	OH
Biselide D (**37**)	H	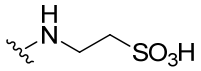

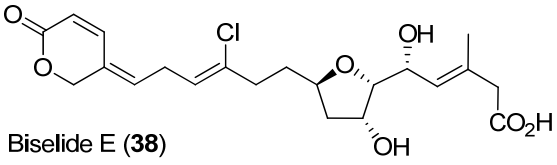

Biselide E (**38**)

	R_1	R_2	R_3
Haterumalide NA (**7**)	H	OH	Ac
Haterumalide NB (**39**)	H	OBu	Ac
Haterumalide NC (**40**)	OH	OBu	Ac
Haterumalide ND (**41**)	OH	OH	Ac
Haterumalide NE (**42**)	H	OH	H
Haterumalide B (**43**)	H	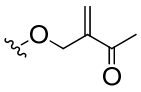	Ac

Figure 2.3 Structures of biselides and haterumalides

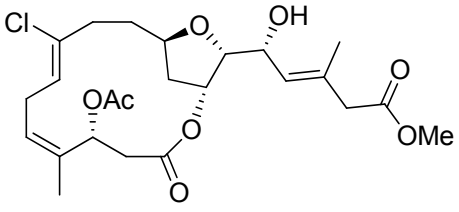

Haterumalide NA methyl ester (**44a**)

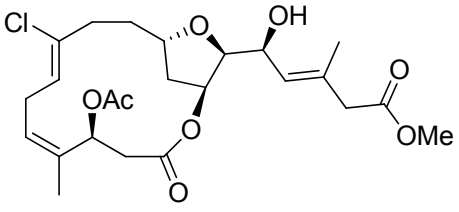

ent-Haterumalide NA methyl ester (**44b**)
(first synthesis by Kigoshi et al. in 2003)

Figure 2.4 Structures of haterumalide NA methyl ester and its enantiomer

In 1999, the first examples of haterumalide natural products were reported, separately, by two groups of researchers. Haterumalide B (**43**) was isolated from the Okinawan ascidian *Lissoclinum* sp. by Ueda and Hu[39], while at the same time haterumalides NA (**7**), NB (**39**), NC (**40**), ND (**41**), and NE (**42**) were isolated from the Okinawan sponge *Ircinia* sp. by Takada *et al*.[26] Notably, haterumalide NA exhibited cytotoxicity against P388 leukemia cancer cells, with an IC_{50} of 0.32 μg/mL, and moderate acute toxicity against mice, with an LD_{99} of 0.24 g/kg. Later, by completing the first total synthesis of what turned out to be the enantiomer of haterumalide NA methyl ester (**44b**) in 2003 (Figure 2.4), Kigoshi *et al*. were able to revise the structures of haterumalides with the correct absolute and relative stereochemistry.[40] Subsequently, in 2004, Kigoshi *et al*. isolated biselides A (**34**) and B (**35**) from the Okinawan ascidian *Didemnidae* sp.[41] They reported the isolation of three more analogs, biselides C (**36**), D (**37**), and E (**38**) a year later.[42] Biselides A (**34**) and C (**36**) showed cytotoxicity toward a variety of cancer cell lines, while the cytotoxic activities of biselides B (**35**), D (**37**), and E (**38**) could not be examined due to a lack of material available through isolation. Between biselide A (**34**), biselide C (**36**), and haterumalide NA methyl ester (**44a**), haterumalide NA methyl ester (**44a**) demonstrated the most potent cytotoxicity towards a variety of cancer cell lines, while biselide C was the least toxic (Table 2.1).[42] In fact, the LD_{50} values for haterumalide NA methyl ester (**44a**) and biselide A (**34**) are comparable to those of Cisplatin and Adriamycin, two common chemotherapy drugs. Interestingly, biselides A (**34**) and C (**36**) showed no toxicity towards brine shrimp, whereas haterumalide NA methyl ester (**44a**) was strongly toxic to brine shrimp, with an LD_{50} of 0.6 μg/mL. These results suggest that haterumalides, and especially biselides, can potentially serve as leads for novel anticancer drugs without severe side effects.[43] The unique structural properties and biological activities of these natural products, as well as the clear need for greater quantities of material for biological testing, have inspired several efforts toward their synthesis.

Table 2.1 Cytotoxicity values of biselide A, C, and haterumalide NA methyl ester

Cell line	Biselide A (34)	Biselide C (36)	Haterumalide NA methyl ester (44a)	Cisplatin	Adriamycin
MDA-MB-231 (breast)	3.72	25.5	0.406	4.83	0.186
HOP18 (lung)	9.35	82.7	0.739	4.08	0.159
NCI-H460 (lung)	3.53	18.0	0.135	0.600	0.00823
A498 (renal)	1.79	16.3	0.335	4.01	0.166
PC-3 (prostate)	2.07	18.2	0.539	4.01	0.357
DLD-1 (colon)	0.513	17.1	0.141	2.11	0.190
HCT116 (colon)	3.01	18.0	0.292	2.23	0.0629
P388 (leukemia)	3.72	21.2	0.408	0.0754	0.0252
P388/ADR (leukemia)	7.78	34.6	0.621	0.271	5.79
Mean	3.94	27.9	0.402	2.47	0.772

Note: Displayed are IC_{50} values (μM)

2.3. Previous Syntheses of Haterumalides and Biselides

2.3.1. Kigoshi's 2003 Synthesis of *ent*-Haterumalide NA Methyl Ester

The first publication concerning the synthesis of haterumalides came from the laboratory of Kigoshi in 2003, where an enantioselective synthesis of *ent*-haterumalide NA methyl ester (**44b**) was completed (Scheme 2.7).[40] This synthesis contributed to the revision of the absolute and relative stereochemistry of the haterumalide series. The synthesis began with a commercially available chiral pool material, (+)-2,3-*O*-isopropylidene-L-threitol (**45**), which was transformed over 7 steps to give diol **46**, the precursor to the key tetrahydrofuran ring functionality. Michael addition/cyclization of the diol **46** followed by silyl protection gave the tetrahydrofuran-containing intermediate **47**, establishing the stereochemistry at C11, C13, and C14. Tetrahydrofuran intermediate **47** was converted to the alkyl bromide **48**, which was coupled to vinyl bromide **49** to generate vinyl silane **50**. Via a modified Tamao protocol,[44] vinyl silane **50** was converted

directly into the vinyl chloride **51**, which was subsequently transformed into the *Z*-unsaturated ester **53** in three steps – acidic hydrolysis, Dess-Martin oxidation, and the Still-modified Horner-Wadsworth-Emmons reaction.[45] Following a series of functional group interconversions, the *Z*-unsaturated ester **53** was converted into the conjugated aldehyde **54**, the key precursor for a subsequent intramolecular Reformatsky-type reaction. Macrocyclization under Honda's conditions,[46] followed by trapping of the reactive intermediates with Ac_2O and removal of the MPM group afforded Kigoshi's key intermediate **55**, albeit in poor yield (8%). Oxidation of the primary alcohol followed by Nozaki-Hiyama-Kishi coupling[47,48] with vinyl iodide **56** afforded *ent*-haterumalide NA methyl ester (**44b**) (11:1 dr).

Scheme 2.7 Kigoshi's synthesis of ent-haterumalide NA methyl ester

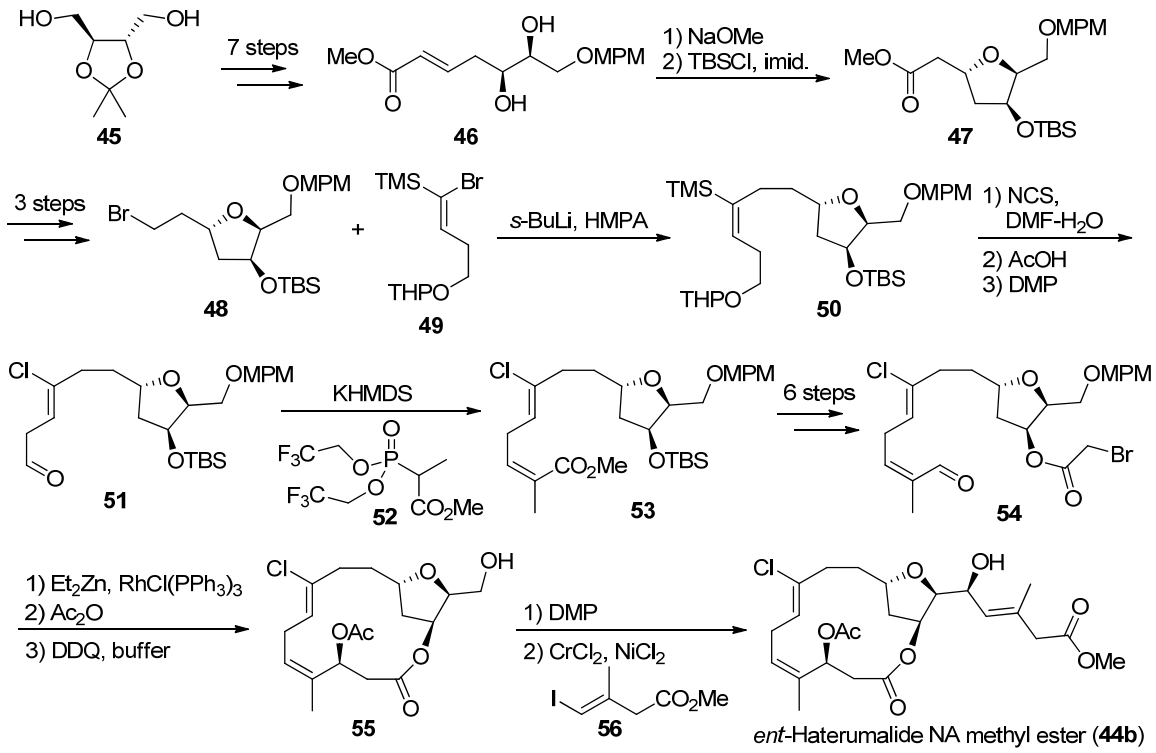

The entire synthesis was achieved in 26 steps (0.2% overall yield) from commercially available starting materials. The major isomer produced was found to display identical spectral data to the naturally occurring sample, except for the sign of the optical rotation. Further analysis by Kigoshi *et al*. revealed the major product to be

ent-haterumalide NA methyl ester (**44b**), and hence confirming the absolute stereochemistry of the naturally occurring haterumalide NA methyl ester (**44a**).

2.3.2. Snider's 2003 Synthesis of *ent*-Haterumalide NA Methyl Ester

Several months after Kigoshi *et al.* reported the first total synthesis of *ent*-haterumalide NA methyl ester (**44b**), Gu and Snider published their synthesis of the same compound.[49] The synthesis began with the preparation of enantiomerically enriched vinylstannane **62** starting from propargyl alcohol (Scheme 2.8). Propargyl alcohol (**57**) was treated with MeMgBr and catalytic CuI, followed by trapping with I_2 to afford allylic alcohol **58**.[50] Oxidation of allylic alcohol **58** followed by asymmetric aldol reaction with ketene silyl acetal **59** using Kiyooka's procedure[51] afforded the β-hydroxy phenyl ester **61**. Silyl protection of the secondary alcohol followed by a coupling reaction with hexamethylditin furnished the vinylstannane **62**.

Scheme 2.8 Snider's synthesis of chiral vinylstannane 62

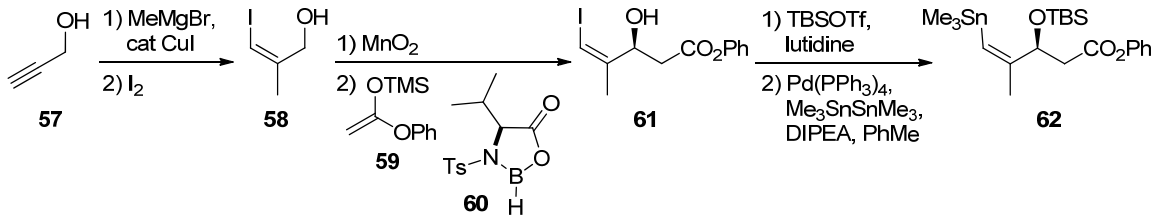

The tetrahydrofuran fragment **70** was synthesized as shown in Scheme 2.9. Allylic alcohol **65** was prepared via a Carreira asymmetric aldol reaction[52] from the OTMS dienolate **63** and acrolein (**64**). This material was then converted to the diol **66** by removal of the acetonide protecting group followed by asymmetric reduction with Et_2BOMe and $NaBH_4$. The resulting diol was then transformed into the TBS-protected propargyl alcohol **67**, which was subsequently cyclized via a stereoselective intramolecular iodoetherification, to produce the tetrahydrofuranol **68**. This latter material was converted into the propargyl alcohol **69** in 5 steps. The vinyl chloride functionality was finally introduced via a regioselective hydroalumination of the propargyl alcohol **69** with Red-Al followed by quenching with NCS. Conversion of the allylic

alcohol (not shown) to a mesylate followed by substitution with LiCl afforded the dichloride **70**.

Scheme 2.9 Snider's synthesis of dichloride 70

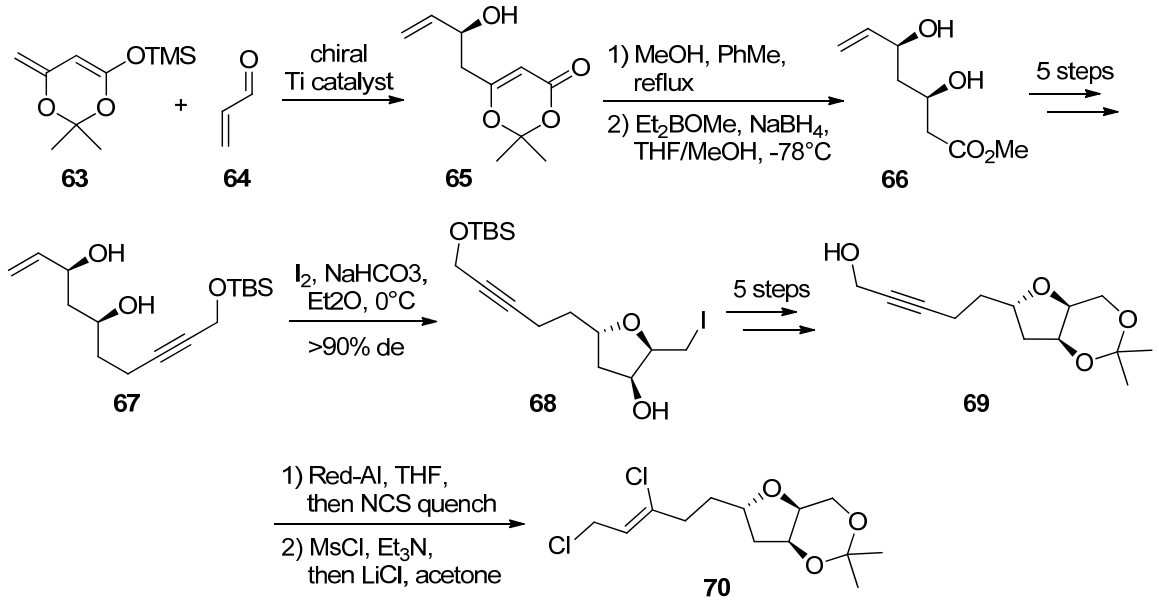

The key step in this synthesis is a Stille coupling[53] of vinylstannane **62** and dichloride **70**, under a set of conditions optimized by the authors (Scheme 2.10). The Stille coupling product **71** was subjected to CSA for removal of the acetonide, followed by trityl-protection of the primary alcohol and hydrolysis of the phenyl ester, to give hydroxy acid **72**. Macrocyclization was effected using standard Yamaguchi macrolactonization conditions[54] to give **73**. Several straightforward functional group manipulations eventually afforded Kigoshi's key intermediate **55** (Scheme 2.7), which was converted into *ent*-haterumalide NA methyl ester (**44b**) by the same NHK coupling sequence as used by Kigoshi *et al*.[40] Overall, Snider's synthesis was completed in 28 steps (0.7% overall yield) from commercially available start materials, with the spectra of the final product matching those of Kigoshi's.

Scheme 2.10 Completion of Snider's synthesis

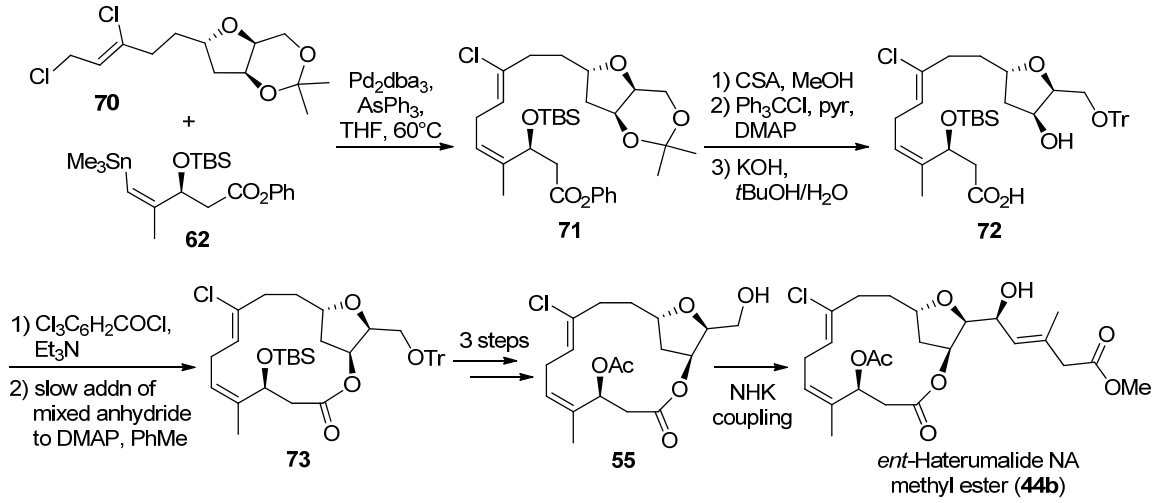

2.3.3. Hoye's 2005 Synthesis of Haterumalide NA

In 2005, Hoye and Wang achieved the first total synthesis of correctly configured haterumalide NA (**7**) (Scheme 2.11).[55] They began the synthesis by constructing the tetrahydrofuran-containing intermediate **76** following Roush's method that had been reported for the synthesis of pectenotoxin II,[56] which involves a key $SnCl_4$-catalyzed [3 + 2]-annulation. Transformation of the tetrahydrofuran-containing intermediate **76** to the ene-yne intermediate **77** set the stage for the crucial intramolecular macrocyclization step. The macrocyclization was accomplished via the Kaneda alkyne haloallylation reaction[57] using $PdCl_2(PhCN)_2$ as catalyst, to give a 1:1.4 mixture of *Z* and *E* isomers, of which the *Z* isomer **78** is desired. Luche reduction[58] of the ketone function in **78** provided the desired alcohol as a single diastereomer. In this reduction, it was proposed that the observed diastereoselectivity results from a facial bias imposed in the lowest energy conformation of the macrocycle. Subsequent acetylation and removal of the PMB protecting group afforded the enantiomer of Kigoshi's key intermediate, *ent*-**55**. The ensuing DMP oxidation and NHK coupling were similar to that employed in Kigoshi's synthesis, except that Hoye and Wang used the PMB ester **79** in the coupling step rather than the methyl ester **56**. Hoye's choice of the PMB ester allowed for mild hydrolysis to afford haterumalide NA (**7**), whereas in Kigoshi's and Snider's work they were unable to hydrolyze the methyl ester. Overall, Hoye's synthesis of haterumalide

NA (**7**) was completed in 32 steps (0.2% overall yield) from commercially available starting materials.

Scheme 2.11 Hoye's synthesis of haterumalide NA

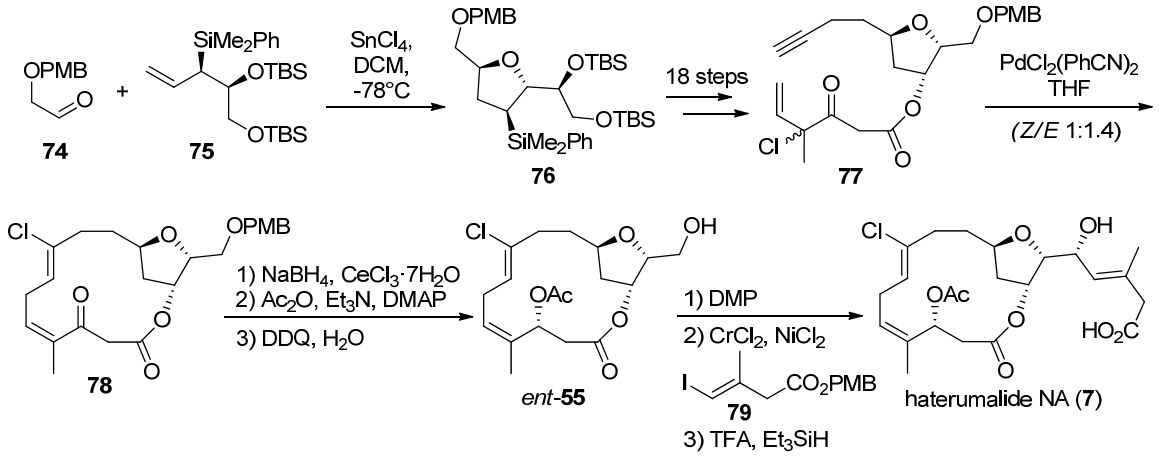

2.3.4. Roulland's 2008 Synthesis of Haterumalide NA

In early 2008, Roulland reported a total synthesis of haterumalide NA (**7**) involving the formation of the C8-C9 bond via a key Suzuki-Miyaura cross-coupling reaction.[59] The synthesis began with the chiral D-tartrate ester **80**, the sole source of chirality in the synthesis, which was converted through a sequence of steps to the diol **81** as an *E*/*Z* mixture (Scheme 2.12). The diol **81** was then cyclized via a palladium-catalyzed intramolecular etherification reaction with excellent diastereoselectivity (24:1 dr), followed by benzoyl protection of the free hydroxyl group to give the mixture of compounds **82** and **83**. These latter materials were separable by flash chromatography, and the diastereomer **82** could be readily obtained in preparation for the Suzuki-Miyaura coupling.

Scheme 2.12 Roulland's synthesis of the tetrahydrofuran 82

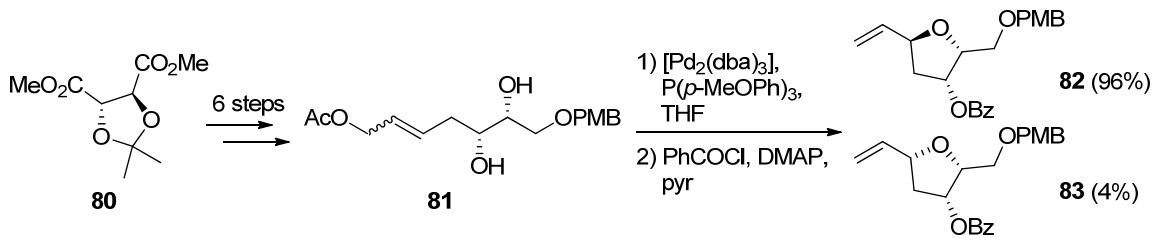

Meanwhile, the other Suzuki-Miyaura coupling partner **85** was synthesized in 10 steps from alcohol **84**[60] (Scheme 2.13). With the two coupling partners in hand, the Suzuki-Miyaura cross-coupling reaction[61] was carried out using 9-BBN and catalytic [$Pd_2(dba)_3$], followed by hydrolysis to give the seco acid **86**. Yamaguchi[54] intramolecular esterification gave the macrocycle **87**, which was eventually converted to the enantiomer of Kigoshi's intermediate *ent*-**55**. From this point, the final steps were carried out following Hoye's method[55] to afford haterumalide NA (**7**). In summary, the synthesis was completed in 24 steps from commercially available starting materials.

Scheme 2.13 Completion of Roulland's synthesis

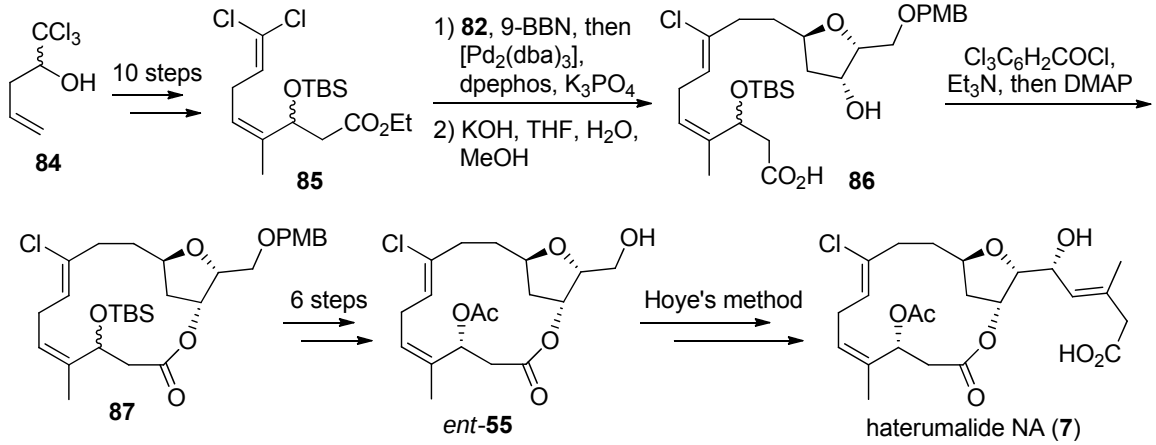

2.3.5. Kigoshi's 2008 Synthesis of Haterumalide NA

Also in early 2008, Kigoshi's research group reported their second-generation synthesis of haterumalide NA (**7**), which involves a key disconnection at C8-C9.[62] Like Roulland,[59] Kigoshi also utilized a Suzuki-Miyaura[61] coupling reaction to form the C8-C9 connection. The synthesis began with D-mannose, which was converted to the α,β-unsaturated methyl ester **88** in 5 steps (Scheme 2.14). The tetrahydrofuran **89** was then formed via an intramolecular oxy-Michael cyclization of **88** using Triton B in MeOH.[63] Tetrahydrofuran **89** was further converted to the terminal olefin **90** in 3 steps. Hydroboration of **90** with 9-BBN dimer followed by *B*-alkyl Suzuki-Miyaura coupling with vinyl iodide **91**[64] gave the desired vinyl silane **92** in quantitative yield. Chlorination of the vinyl silane **92** with NCS and K_2CO_3 gave vinyl chloride **93** with the correct alkene geometry in 58% yield. A series of functional group transformations followed, eventually

affording the seco-acid **94**. Macrocyclization of **94** using Yamaguchi conditions[54] formed the corresponding macrolactone, which was subsequently treated with TBAF for silyl group removal, and the resulting hydroxyl diastereomers were separated by flash chromatography. Acetylation of alcohol **95** followed by removal of the trityl group afforded the Kigoshi intermediate *ent*-**55**, which was transformed to haterumalide NA (**7**) following Hoye's method,[55] albeit with a minor variation. The synthesis was achieved in 33 steps (1.2% overall yield) from commercially available starting materials. As well, in a separate publication in 2009,[65] Kigoshi also completed the total synthesis of haterumalide B (**43**), which only differs from haterumalide NA (**7**) by the coupling partner used for the late-stage Nozaki-Hiyama-Kishi coupling[47,48] step.

Scheme 2.14 Kigoshi's second-generation synthesis of haterumalide NA

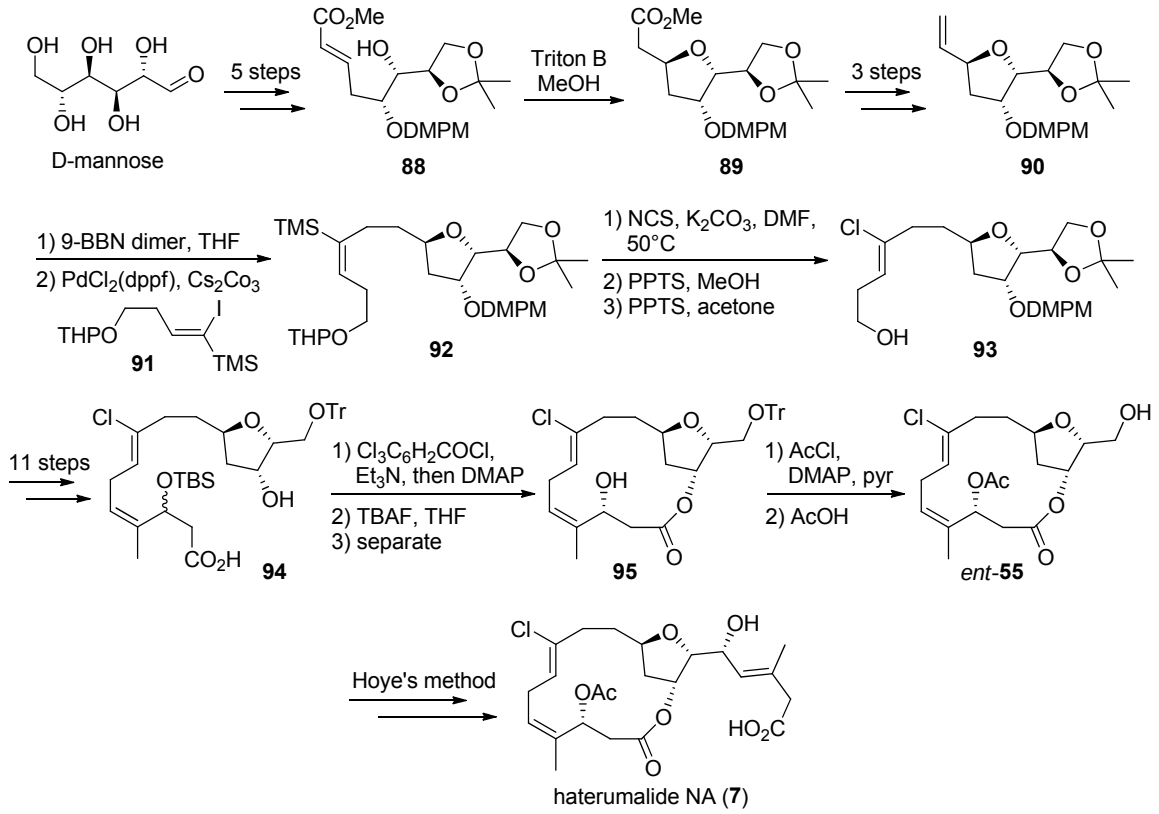

2.3.6. Borhan's 2008 Synthesis of Haterumalide NC

In mid-2008, Borhan and Schomaker reported the first total synthesis of haterumalide NC (**40**), as well as the formal synthesis of haterumalide NA (**7**).[66] They

utilized an intramolecular Falck-Mioskowski[67,68] chlorovinylidene chromium carbenoid reaction to furnish the C8-C9 bond while functionalizing C9. The key aldehyde substrate **101** for the Falck-Mioskowski reaction was obtained from the Mitsunobu esterification of tetrahydrofuran **99** and trichloroalkane **98** (Scheme 2.15). The tetrahydrofuran intermediate **99** was obtained in 5 steps from 2-deoxy-D-ribose, while trichloroalkane **98** was obtained in 7 steps from oxetane **96** via a key asymmetric Mukaiyama aldol step.[51] Mitsunobu esterification gave the terminal alkene **100**, which was transformed to the aldehyde **101** in 4 steps. Next, intramolecular Falck-Mioskowski reaction of **101** afforded the macrocycle **102** with the hydroxyl group at C9 (4:1 dr). Further transformations led to aldehyde **103**, which was subjected to the usual Nozaki-Hiyama-Kishi[47,48] conditions but with *n*-butyl ester **104**, followed by acid desilylation, to afford haterumalide NC (**40**). The synthesis was completed in 19 steps (longest linear sequence). Additionally, the Falck-Mioskowski adduct **102** could be subjected to a Barton-McCombie deoxygenation[69] to afford the C9-deoxy intermediate *ent*-**73**, which was found in Snider's synthesis of *ent*-haterumalide NA methyl ester (**44b**).[49]

Scheme 2.15 Borhan's synthesis of haterumalide NC

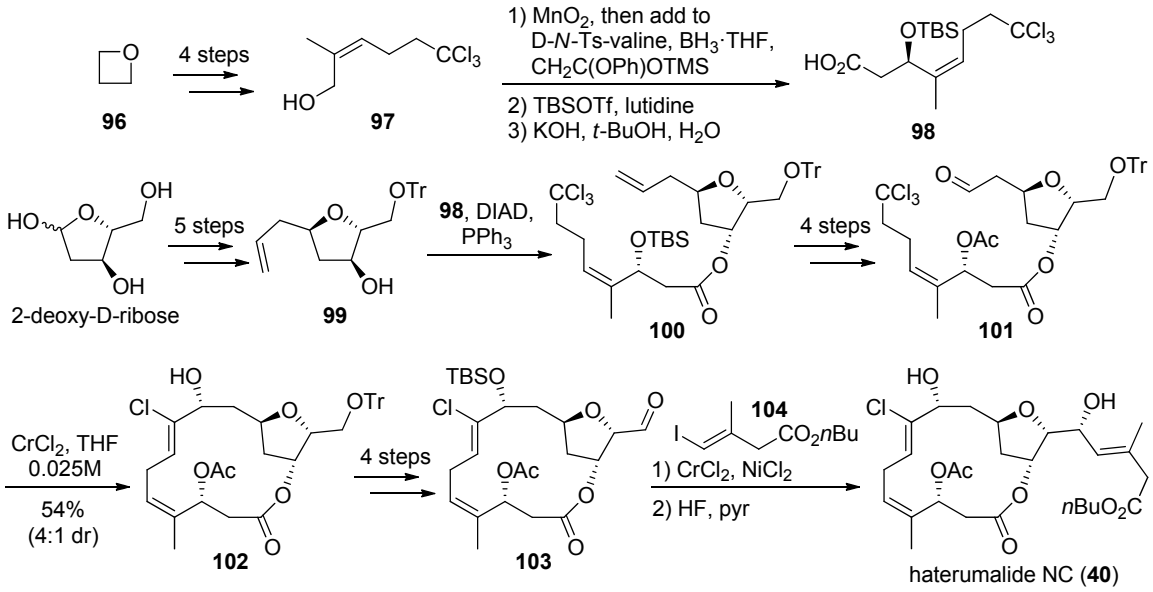

2.3.7. Kigoshi's Synthetic Studies toward Biselides

In 2012, Kigoshi's group published preliminary results, in two parts, from their studies toward the first total synthesis of biselides, although the synthesis itself was not completed.[43,70] In Part 1,[43] starting with common intermediate **93** from Kigoshi's previous synthesis of haterumalide NA (**7**), the alcohol was converted to the corresponding aldehyde, followed by coupling with an iodo Wittig reagent[71] to give the C20-oxygenated iodo olefin **105** (Scheme 2.16). Following reduction with DIBAL-H, the desired *Z*-isomer **106** was isolated by flash chromatography, and subsequently silylated with TBDPSCl to give vinyl iodide **107**. The authors attempted to install a one-carbon unit (CX; X = heteroatom) in place of the iodine at C4, but their various efforts were unsuccessful. Instead, conjugated diene **108** was made via Stille coupling[53] and then dihydroxylated to give the desired diol **109** in 30% yield over the two steps. Oxidative cleavage of the diol with $NaIO_4$ gave an aldehyde, which was alkylated with the enolate derived from *i*-propyl acetate in a non-selective aldol reaction, to give **110**. Intermediate **110** possesses the C1-C15 carbon framework of biselides A (**34**), B (**35**), and C (**36**). The authors stopped here, however, citing the poor yield and regioselectivity of the dihydroxylation step as the major detriment.[70]

Scheme 2.16 Kigoshi's synthesis of the biselide core using Stille coupling

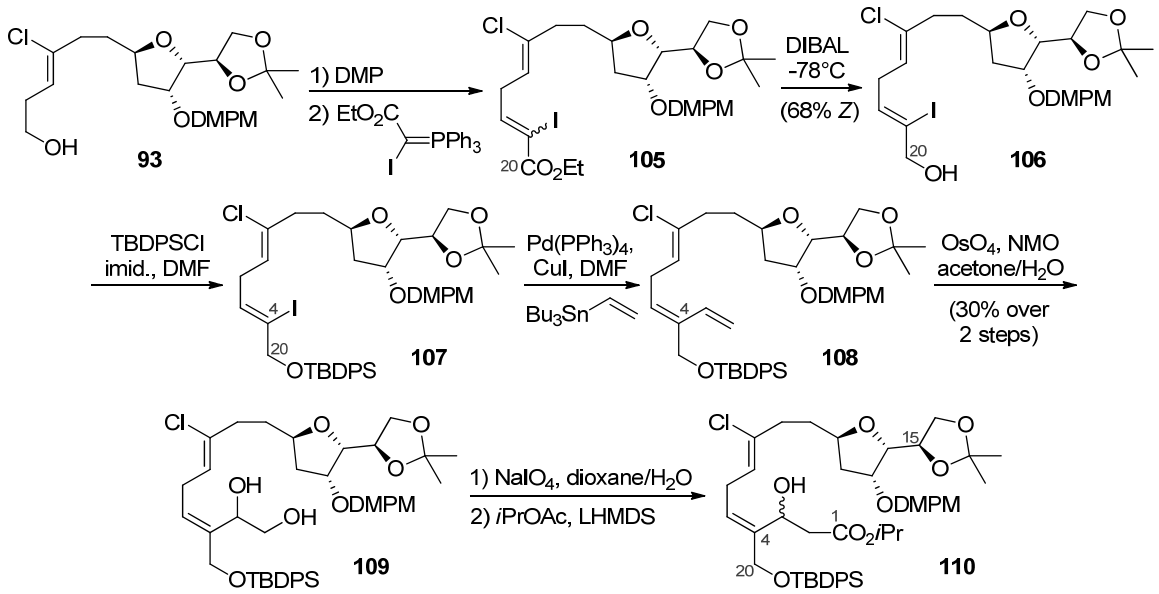

In Part 2, Kigoshi's group illustrated an alternative route to synthesize the C1-C15 carbon framework, using allylic oxidation to functionalize C20.[70] Beginning once again with the same alcohol intermediate **93**, several transformations were performed to afford the *p*-nitrobenzoyl allyl ether **111**, which was subjected to allylic oxidation with SeO_2 to give allyl alcohol **112** in 35% yield (Scheme 2.17). Further transformations once again gave the C1-C15 carbon framework intermediate **110**, which was subjected to a similar sequence as in Kigoshi's synthesis of haterumalide NA (**7**), to yield the macrocycle **113**. The synthesis stopped at this point, however, and the authors did not cite any reasons for failure to progress this material to the natural product. It is possible that they were unable to selectively remove the trityl group in the presence of the primary acetate.

Scheme 2.17 Kigoshi's synthesis of the biselide core using allylic oxidation

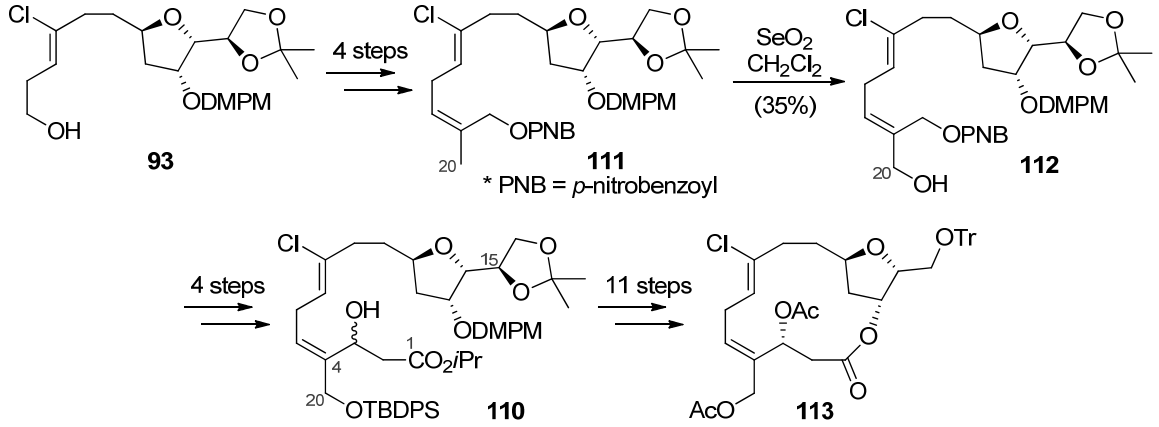

2.4. Initial Proposal for the Total Synthesis of Biselide A: Ring-Closing Metathesis Strategy

The challenging structural motifs and lack of a previous synthesis led our attention to the biselides, and a former member of our group, Dr. Bal Kang, first took on this challenge.[72] We intended to apply our chloropolyol cyclization methodology mentioned earlier in this chapter[27,31,32] to construct the key tetrahydrofuran component in the biselides. This strategy would allow us to easily access the 2,5-disubstituted-3-oxygenated tetrahydrofuran core starting with simple commercially-available materials, avoiding the complex chiral pool starting materials employed in previous syntheses. In

addition, we also envisioned the use of Hoye's endgame strategy[55] to install the carboxylic acid component towards the end of the proposed synthesis, as a result converging with previous syntheses at the C20-oxygenated Kigoshi intermediate **114** (Scheme 2.18). We planned to access the C20-oxygenated Kigoshi intermediate **114** via ring-closing metathesis (RCM) from the triene **115**, which could be made by esterification of tetrahydrofuranol **116** and carboxylic acid **117**. The tetrahydrofuranol **116** could be produced by the chlorohydrin cyclization methodology mentioned previously (Section 2.1.1), beginning with the aldol reaction of ketone **119** and enantiomerically-enriched α-chloroaldehyde **120**.[32]

Scheme 2.18 Initial retrosynthetic proposal involving key RCM step

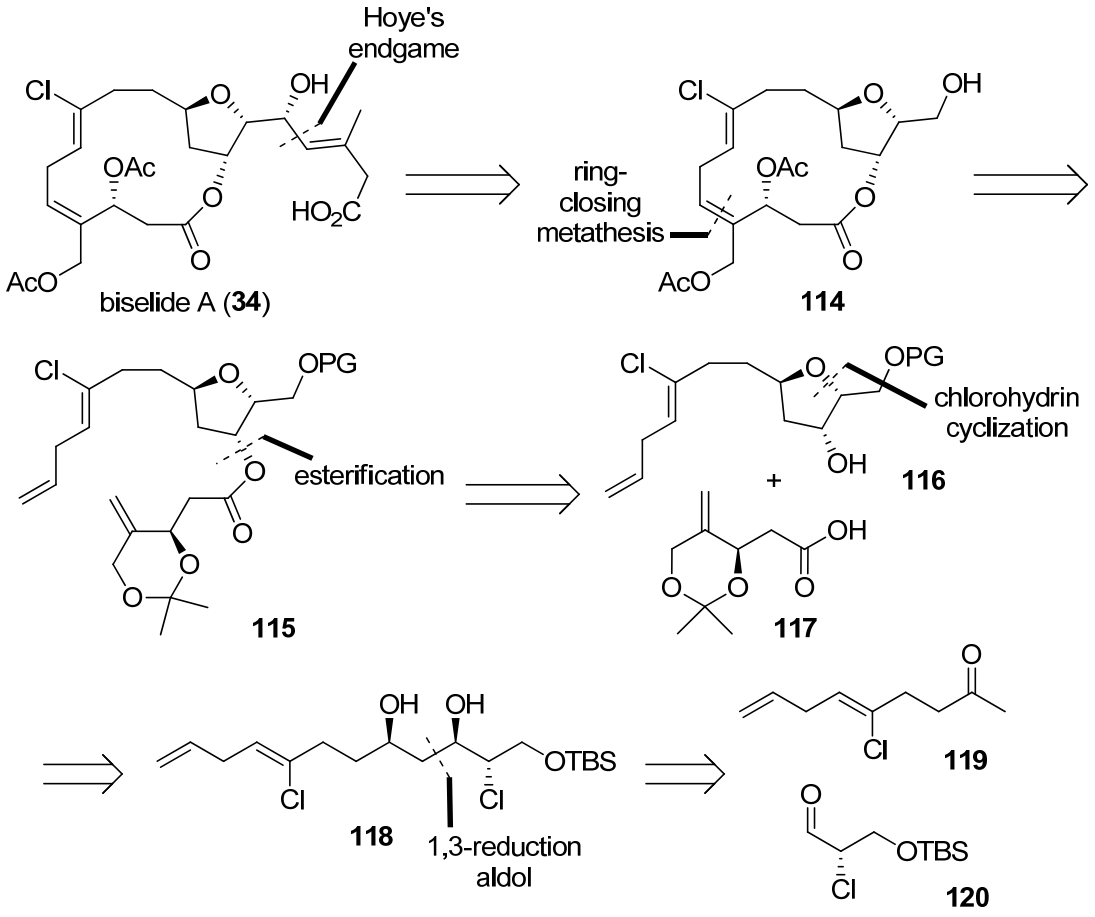

Towards the end of his Ph.D. studies, Kang carried out the initial synthesis of tetrahydrofuranol **125**[32] (Scheme 2.19) and further advanced this material to the RCM

substrate **130** (Scheme 2.20).[72] As proof-of-concept studies, the synthesis was carried out with the racemic α-chloroaldehyde (±)-**120**, which was made from the known aldehyde **172**[73] via chlorination with NCS and L-proline.[28] Notably, the enantioselective α-chlorination method previously mentioned, using L-prolinamide as an organocatalyst,[27,28,30,31,74] did not give the desired enantiomerically enriched α-chloroaldehyde but rather led to the elimination of the β-silyloxy group. Meanwhile, Kaneda chloroallylation[57] of propargyl bromide **121** with allyl chloride produced vinyl chloride **122**, which was engaged in an alkylation reaction with ethyl acetoacetate followed by decarboxylation[75] to give ketone **119**. Aldol reaction between ketone **119** and α-chloroaldehyde (±)-**120** gave the racemic *anti*-chlorohydrin (±)-**123** in good diastereoselectivity.[32] A 1,3-*syn*-reduction[27] of chlorohydrin (±)-**123** followed by microwave cyclization in H_2O[31] afforded the diol (±)-**124**, which was then selectively re-silylated to give tetrahydrofuranol (±)-**125**.

Scheme 2.19 Kang's synthesis of racemic tetrahydrofuranol 125

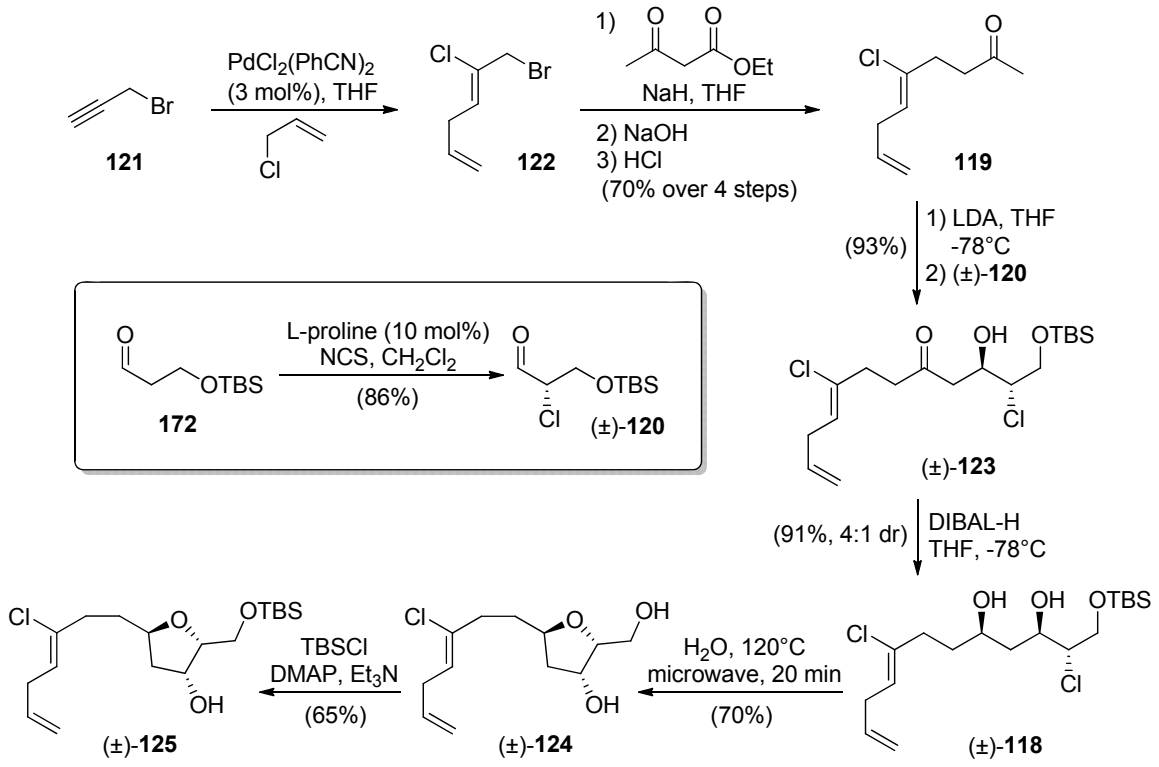

Synthesis of the acid fragment **117** began with the aldol reaction of ethyl acetate with methacrolein, affording a racemic mixture of the β-hydroxyester **126** (Scheme 2.20). Sharpless epoxidation[19] of the racemate gave epoxide **127** and unreacted (*R*)-enantiomer **128**, which could be separated. The desired (*R*)-enantiomer **128** was subjected to allylic oxidation[76] to afford the diol **129**, which was then transformed into the acetonide followed by hydrolysis to give the carboxylic acid **117**. Finally, DCC-coupling of acid **117** with tetrahydrofuranol (±)-**125** gave the RCM substrate **130**.

Scheme 2.20 Kang's synthesis of the RCM substrate 130

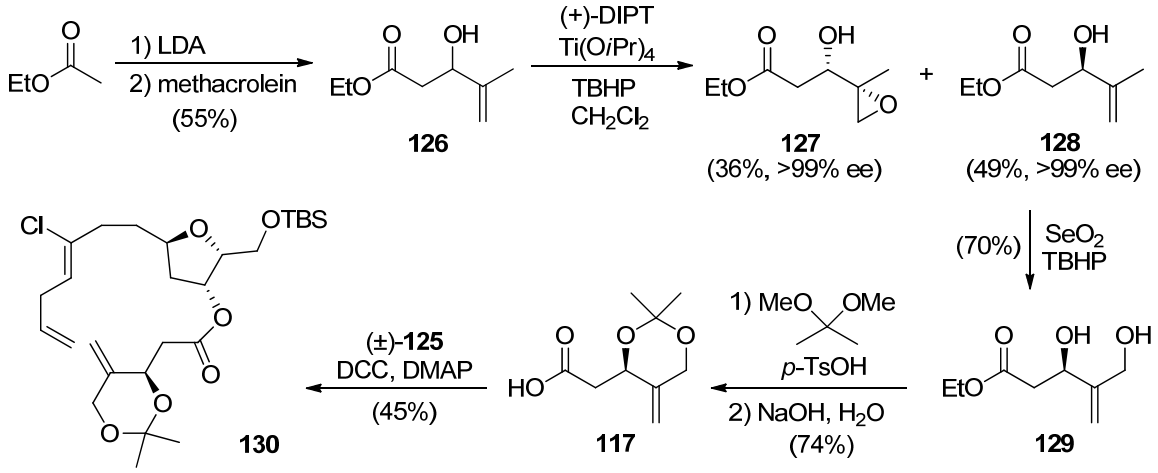

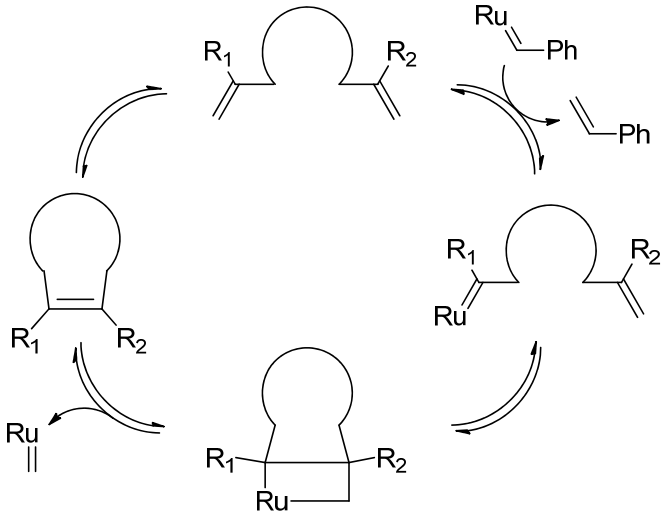

Figure 2.5 Simplified catalytic cycle for ring-closing metathesis

With the substrate **130** in hand, Kang attempted a number of RCM reactions (Figure 2.5) with various Ru-containing metathesis catalysts and under varied conditions.[72] In all cases, the desired macrocyclic product was not observed.

Kang observed the formation of metathesis dimers and truncation side products, but no desired RCM product (Scheme 2.21).[72] He attributed the failure of this reaction to the inherent reactivity difference between the monosubstituted terminal alkene and the 1,1-disubstituted alkene, as well the *trans*-relationship of the two side chains in **130**.

Scheme 2.21 Attempted RCM of 130 led to dimerization

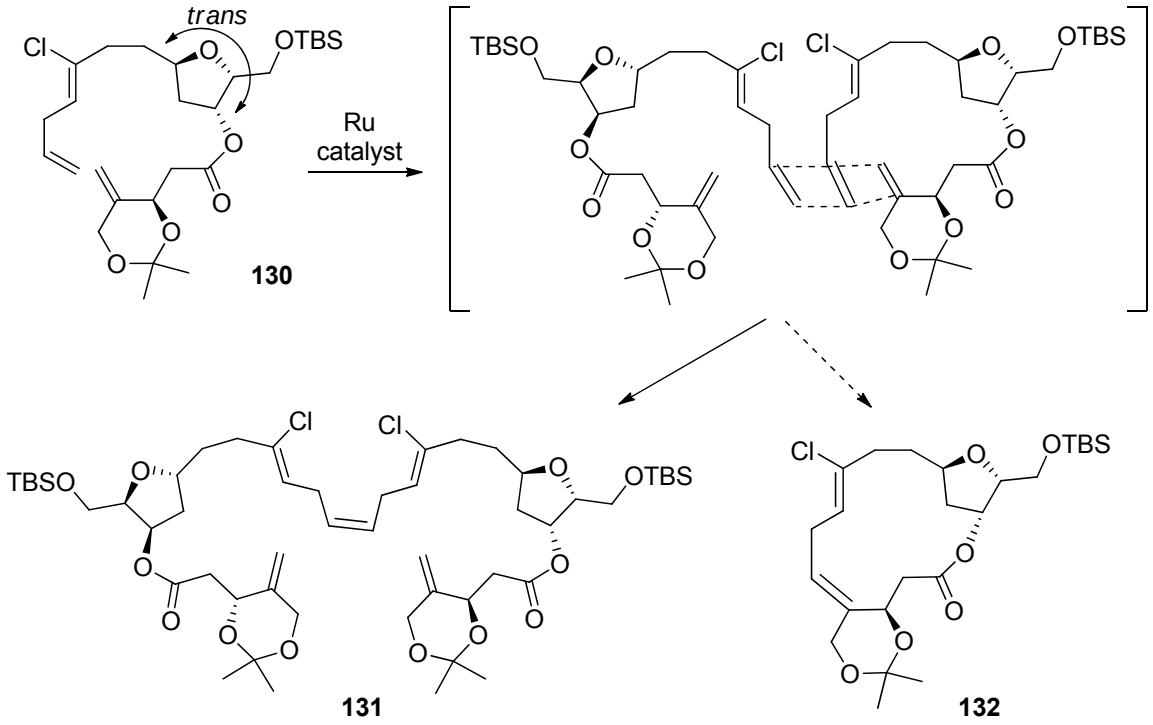

To further assess the validity of the purported challenges to this reaction, Kang synthesized the RCM substrate **134** (Scheme 2.22), and subjected it to RCM conditions. The result was the same – no desired RCM product was observed. With the Grubbs Second-Generation catalyst, no reaction was observed at all, while using the Hoveyda-Grubbs Second-Generation catalyst led to a small amount of dimer being formed.[72] The RCM reaction with **134** failed despite it possessing two sterically unhindered monosubstituted terminal alkenes, and from this observation, Kang concluded that the

difference in reactivity between the monosubstituted terminal alkene and the 1,1-disubstituted alkene is likely not a significant factor. Rather, the *trans*-relationship between the two side chains is the major reason for the failure of RCM, precluding the two alkenes from coming within proximity of each other.

Scheme 2.22 Synthesis of less hindered RCM substrate 134

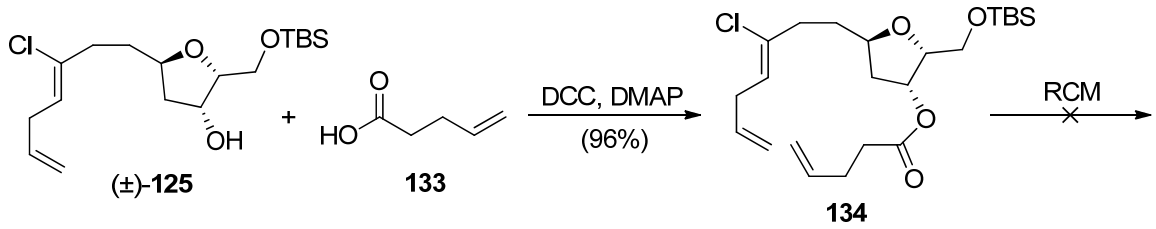

Scheme 2.23 Hoye's studies on the macrocyclization ring strain hypothesis

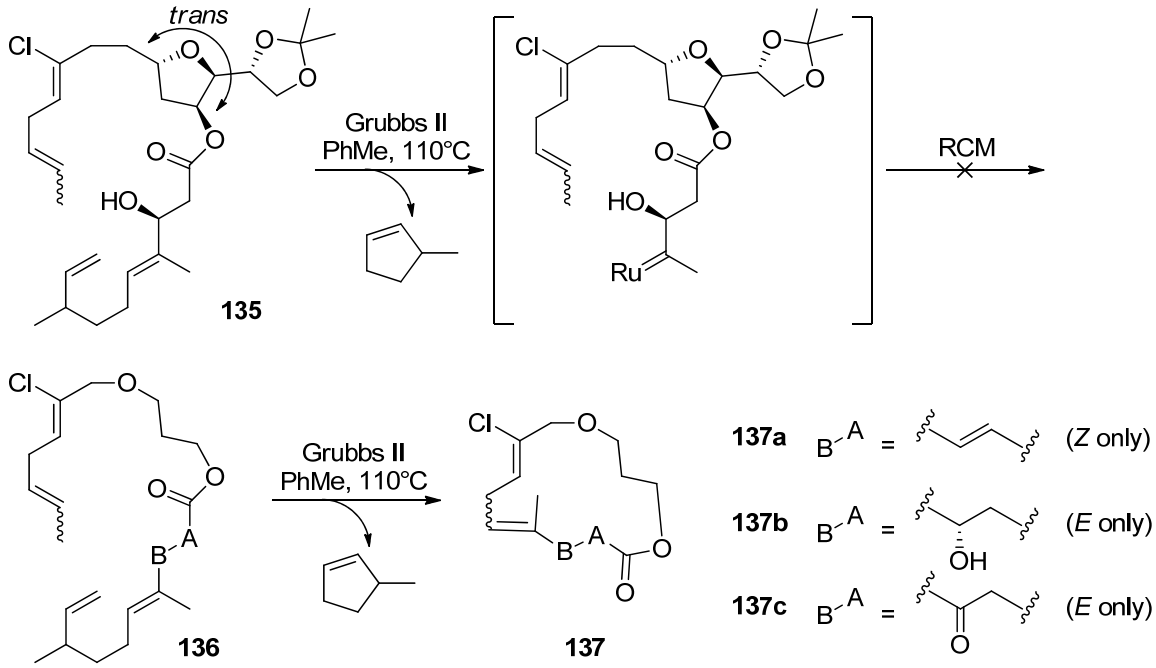

In related studies by Hoye examining metathesis as an alternative method for their synthesis of haterumalide NA,[55] the strain associated with attempting to macrocyclize the *trans* side chains was also evident in a relay ring-closing metathesis (RRCM) process.[77] Hoye performed RRCM on two substrates, one with the

tetrahydrofuran ring in place (**135**) and one without (**136**). The RRCM reaction with low-strain linear substrate **136** proceeded to give the desired macrocycle **137**, while the strained THF-containing substrate **135** did not lead to any macrocyclization product (Scheme 2.23).

2.4.1. Further Studies on RCM

Picking up where Kang had left off, and with Hoye's work proving that the removal of THF to release strain does allow their RRCM reaction to work as desired, we decided to further investigate the effects of removing ring strain on RCM, as well as the possible effects of ring size on the reaction. For proof-of-concept studies, we sought the synthesis of two linear RCM substrates that would lead to 8- and 12-membered ring macrolides (Scheme 2.24). Starting with previously described racemic β-hydroxyester **126**, the hydroxyl group was silylated with TBSOTf and lutidine to give silyl ether **138**, which was subsequently hydrolyzed in base to afford the carboxylic acid **139**. Meanwhile, ketone **119** was reduced to its corresponding alcohol **140**. DIC coupling of acid **139** and alcohol **140** gave the RCM substrate **142**, while the same reaction between acid **139** and 3-buten-1-ol (**141**) gave the RCM substrate **143**.

Scheme 2.24 Synthesis of RCM substrates for proof-of-concept studies

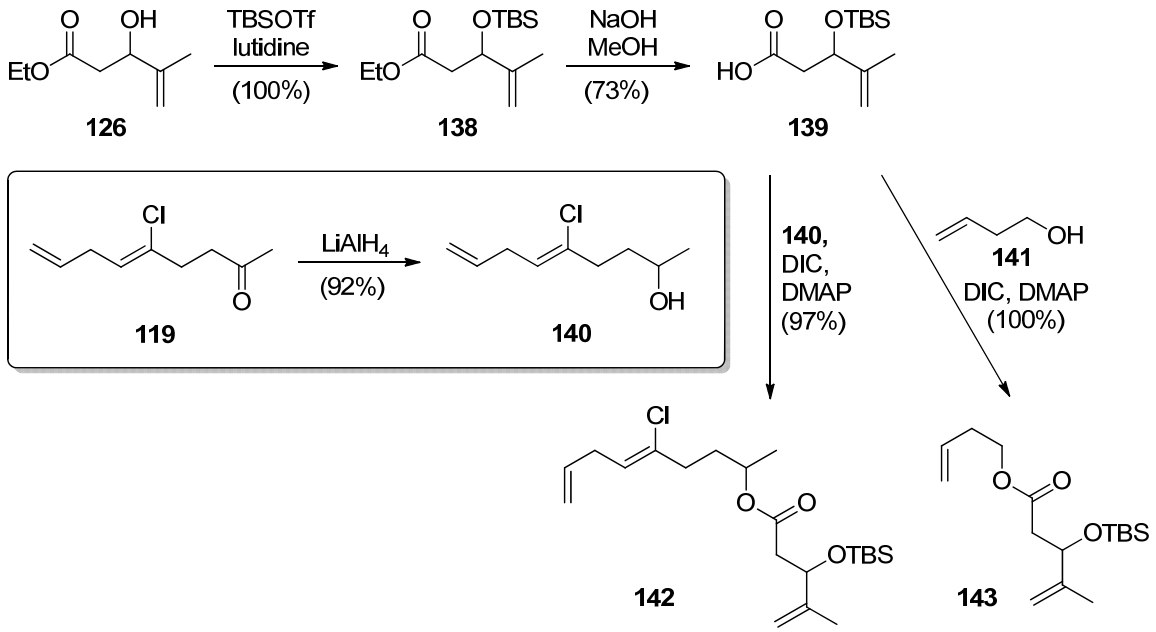

Should RCM proceed successfully, substrate **142** would give the 12-membered macrocycle **144**, whereas substrate **143** would give the 8-membered macrocycle **145a** (Scheme 2.25). Unfortunately, the reactions failed to produce the desired products. Substrate **142** remained mostly unreacted, while substrate **143** led to small amounts of dimerization product **145b**, characterized by the 2:1 ^{1}H NMR integration ratio between the 1,1-disubstituted alkene protons (4.97, s, 2H; 4.81, s, 2H) and the vinylic proton at the newly metathesized 1,2-disubstituted alkene (5.52, m, 2H). Varying reaction concentration, solvent, and catalyst did not did improve this result. With the failure of these proof-of-concept experiments, we decided not to pursue the testing of a 14-membered system as would be found in biselides.

Scheme 2.25 Attempted RCM reactions for proof-of-concept studies

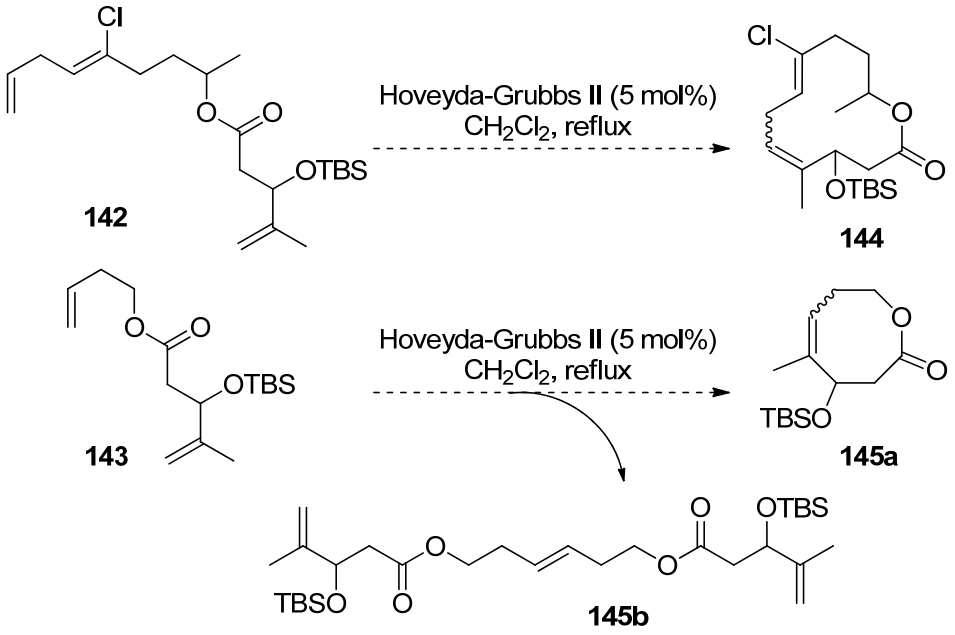

These observations prove that the inherent reactivity difference between the monosubstituted terminal alkene and the 1,1-disubstituted alkene does indeed play a significant role in preventing macrocyclization. Hoye's successful macrocyclization with a linear substrate via RRCM[77] further supports these conclusions, since the relay process helps to activate the hindered alkene to improve its reactivity. In conclusion, the problems facing the metathesis macrocyclization procedure were more complex than

initially expected, with alkene reactivity and structural strain both being significant and detrimental factors.

2.5. Revised Proposal: Relay Ring-Closing Metathesis Strategy

Following the observation discussed above, we abandoned the RCM strategy. However, inspired by the successful relay examples demonstrated by the likes of Hoye[55,77] (Scheme 2.23) and Porco[78] (Scheme 2.26), we decided to examine the RRCM approach as an alternative strategy for macrocyclization towards our total synthesis targets.

Scheme 2.26 Porco's application of RRCM in oximidine III synthesis

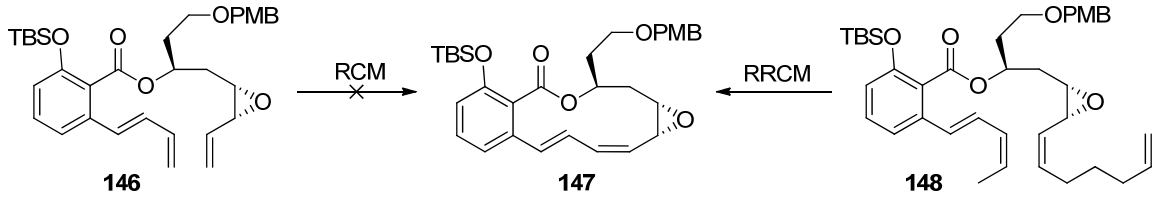

Relay ring-closing metathesis (Figure 2.6) would allow us to circumvent a major issue encountered in our RCM approach – the reactivity difference between the two terminal alkenes. As well, the use of a low-strain linear RRCM substrate would allow us to complementarily eliminate the physical challenge of having the two alkenes to come into contact.

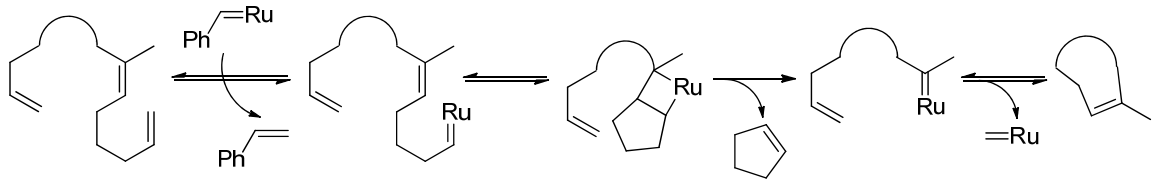

Figure 2.6 Relay ring-closing metathesis mechanism

We envisioned using a linear RRCM substrate such as **151**, with a 6-carbon relay chain attached to the 1,1-disubstituted alkene to improve its reactivity (Scheme 2.27).

As well, we needed the necessary functionalities in place that would allow us to perform our tetrahydrofuran-forming step[31,32] after macrocyclization. We could achieve this by synthesizing chlorohydrin fragment **152** via an aldol reaction, as in our previous example (Scheme 2.19). We were especially optimistic about this approach because our unique tetrahydrofuran-forming method would potentially allow us flexibility in installing the THF ring at a late stage in our synthesis, something that previous synthetic routes have been unable to achieve. Based on Hoye's results (Scheme 2.23),[77] we were fairly confident that RRCM of our substrate **151** would also proceed successfully. However, a major question relating to the resulting geometry of the RRCM olefin product remained, which, as was well-documented by Hoye, can be highly unpredictable and appears to be strictly substrate-dependent.

Scheme 2.27 Revised retrosynthetic plan involving RRCM

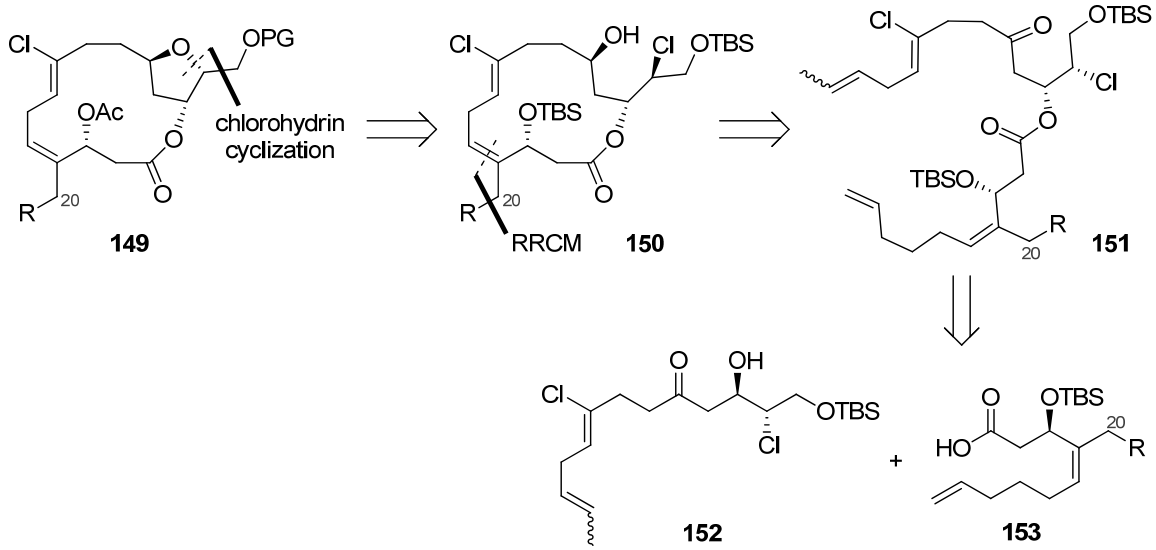

2.5.1. Results and Discussion

To access the materials required for our RRCM studies, we developed a synthesis of the modified carboxylic acid **160**, with the 6-carbon relay chain in place (Scheme 2.28). Since this was a proof-of-concept study for RRCM, we opted for the quickest route to the substrates we needed – simply using the β-hydroxyester **128** directly without performing allylic oxidation on what would become C-20 in the natural

product (which, if completed, would give haterumalide NA rather than biselide A). First, a Finkelstein reaction of 1-bromo-5-hexene (**154**) with NaI in refluxing acetone gave the corresponding alkyliodide **155**,[79] which was then treated with PPh_3 in CH_3NO_2 to form the known iodophosphonium salt **156**.[80] Direct transformation of the bromide **154** to its corresponding bromophosphonium salt was troublesome because it required high reaction temperatures (reflux in toluene) that also effected isomerization of the double bond. Meanwhile, the previously mentioned β-hydroxyester **128** was treated with TBSOTf and lutidine for silylation of the hydroxyl group, furnishing silyl ether **157**. Silyl ether **157** was then subjected to ozone followed by reductive workup with PPh_3 to give the corresponding ketone **158**. This latter material was then treated with the ylid derived from **156** in a Wittig reaction to give the *Z*-alkene **159**, albeit at in a modest yield (maximum yield = 61%). Stereochemistry of the (*Z*)-alkene was confirmed based on the 1D nOe correlation between the single vinylic proton at 5.14 (t, 1H, *J* = 7.1 Hz) and the methyl protons at 1.67 (s, 3H). Also, competing elimination of the -OTBS group was likely the cause for the poor and variable yield of this reaction. Finally, the ester moiety on *Z*-alkene **159** was hydrolyzed to afford the desired carboxylic acid fragment **160**.

Scheme 2.28 Synthesis of RRCM carboxylic acid precursor 160

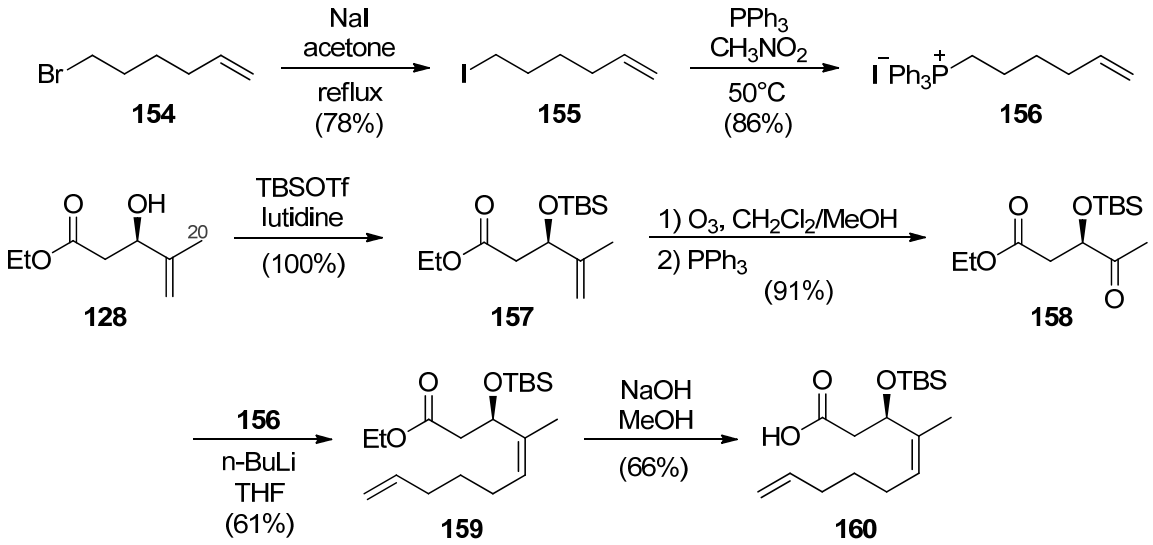

Before proceeding to synthesize the required coupling partner for carboxylic acid **160**, a sample of alcohol **140** was coupled with this material to form ester **161** (Scheme

2.29). With the ester **161** in hand, we investigated the proposed RRCM and were surprised that none of the desired 12-membered macrocyclization product (**162**) was produced. Instead, only the truncation (**163**) and the 14-membered macrocyclization (**164**) products were obtained. The truncation product **163** was easily identified by the obvious ^{1}H NMR signals of the vinylic protons of the 1,1-disubstituted alkene that resulted from truncation (4.97, s, 1H; 4.82, s, 1H). Meanwhile, the 14-membered macrocyclization product **164** was identified by ^{1}H NMR signals of the two only vinylic protons in the molecule (5.56, dd, 1H, *J* = 6.1, 9.7 Hz; 5.14, m, 1H) and their respective ^{1}H-^{1}H COSY correlations, as well as by the disappearance of the 1,4-diene methylene protons in substrate **161**. This confirmed that, aside from the relay chain required to activate the hindered alkene, it is also crucial to have an alkyl (e.g. methyl) group attached to the end of the monosubstituted terminal alkene in order to reduce reactivity of this alkene function. This fine-tuning of alkene reactivity is key for the success of the relay process, as Hoye[77] and Porco[78] have both previously confirmed with their respective systems (Schemes 2.23 and 2.26).

Scheme 2.29 Attempted RRCM with monosubstituted terminal alkene substrate 161

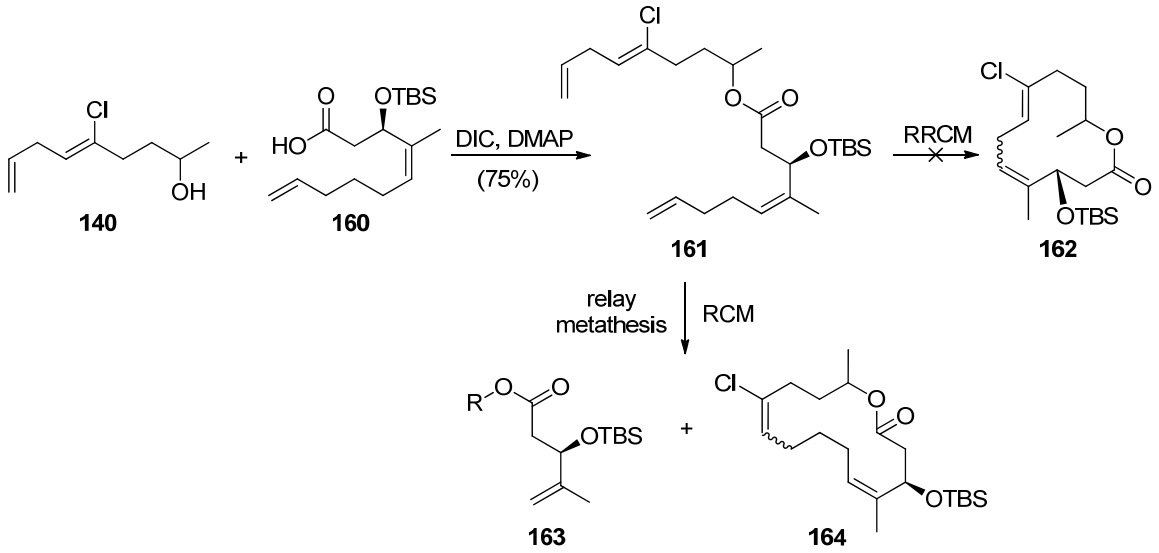

Bearing this result in mind, we modified our synthesis[32] of the ketone fragment in order to install the extra methyl group on the terminal alkene. Instead of using allyl chloride as in our previous example, 3-chlorobutene (**165**) was used for the Kaneda[57]

chloroallylation reaction (Scheme 2.30). The resulting allyl bromide **166** was obtained as an isomeric mixture, which was of no concern to us since the terminal $CHCH_3$ fragment would eventually be cleaved in the RRCM reaction. Alkylation of ethyl acetoacetate with allyl bromide **166** followed by hydrolysis and decarboxylation afforded ketone **167** in 27% yield over the four steps.

Scheme 2.30 Synthesis of modified ketone 167

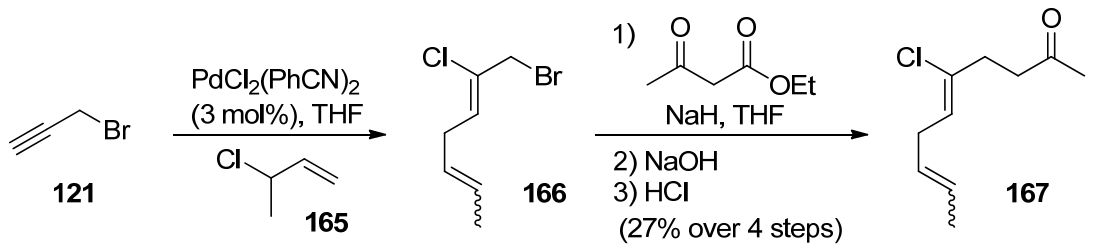

With the ketone **167** in hand, enantiomerically enriched α-chloroaldehyde **120** was synthesized following Kang's "work-around" procedure,[72] which was inspired by the work of de Kimpe.[81] This modified route to the enantiomerically enriched α-chloroaldehyde **120** was required since, as mentioned earlier, direct asymmetric chlorination of aldehyde **172** led to elimination of the β-silyloxy group (Section 2.4). Specifically, L-serine was converted into the corresponding diazonium species with $NaNO_2$ in 6N HCl, neighbouring group assistance and subsequent chloride addition gave α-chloroacid **168**, retaining the stereochemistry of the starting material (Scheme 2.31). It was noted that in order to retain high enantiomeric excess, the reaction must be kept between -15 and -20°C.[72] Esterification of α-chloroacid **168** with MeOH gave α-chloroester **169**, which was then subjected to silylation with TBSCl and imidazole. The TBS-protected α-chloroester **170** was then reduced with $NaBH_4$ to give α-chloroalcohol **171** in high yield. Finally, PCC oxidation of α-chloroalcohol **171** afforded the desired α-chloroaldehyde **120**.

Scheme 2.31 Synthesis of enantiomerically enriched α-chloroaldehyde 120

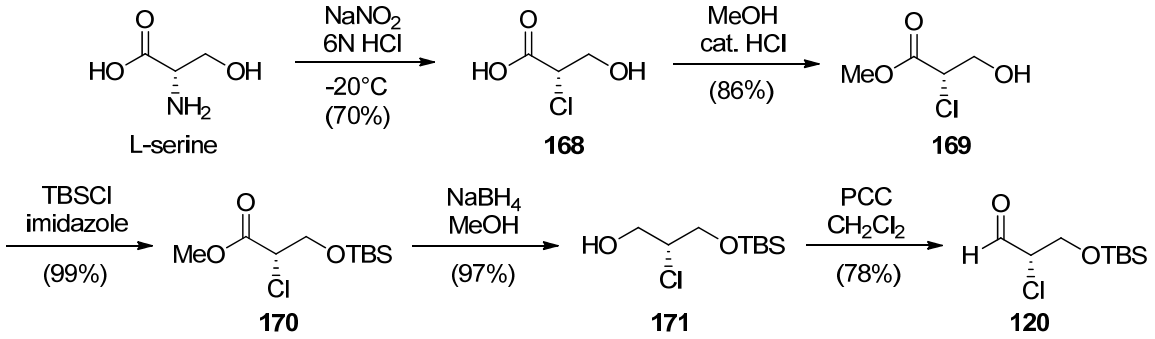

Surprisingly, following this sequence of reactions, chiral GC analysis of α-chloroaldehyde **120** indicated that our material was in fact racemic, and not enantiomerically enriched as expected. We hypothesized that racemization most likely occurred in the diazotization/chlorination step or in the PCC oxidation step, since all the other steps are unlikely to effect enol formation. To probe this issue further, α-chloroalcohol **171** was subjected to chiral GC analysis. Unfortunately, this material decomposed during analysis. To overcome this problem, a racemic mixture of α-chloroalcohol (±)-**171** was synthesized using a 50-50 mixture of L- and D-serine. This racemic α-chloroalcohol (±)-**171** as well as the purportedly chiral α-chloroalcohol **171** (synthesized from L-serine only) were both acetylated with Ac_2O, and the resulting esters (±)-**173** and **173** were analyzed by chiral GC (Scheme 2.32).

Scheme 2.32 Analyzing the enantiomeric excess of α-chloroalcohol 171

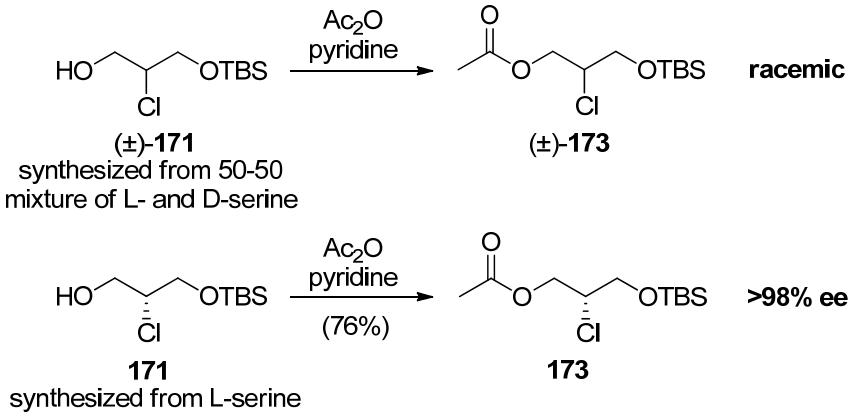

Chiral GC analysis showed the enantiomeric excess of chiral α-chloroester **173** to be >98%, thus confirming the PCC oxidation step to be responsible for the racemization of material. As a result, alternative oxidation methods were investigated. Following several experiments including oxidation with Swern's method,[82] Dess-Martin periodinane proved to be best, transforming α-chloroalcohol **171** to α-chloroaldehyde **120** at 74% yield and maintaining an ee of >92% (Scheme 2.33).

Scheme 2.33 Optimized synthesis of chiral α-chloroaldehyde 120

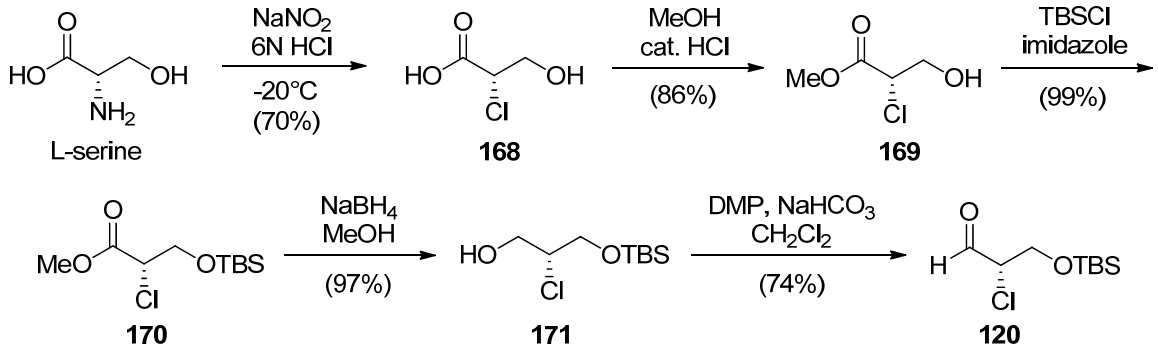

Finally, with the optically enriched α-chloroaldehyde **120** in hand, we were able to complete the synthesis of the RRCM substrate **174** (Scheme 2.34). Specifically, aldol reaction of ketone **167** with α-chloroaldehyde **120** gave the desired *anti*-chlorohydrin **152** in 53% yield and 4:1 dr (*anti*:*syn*). The diastereomeric aldol adducts could not be separated and were progressed together. Thus, the 4:1 diastereomeric mixture of chlorohydrins **152** was esterified with enantiomerically enriched carboxylic acid **160** under standard DIC-coupling conditions[83] to afford the RRCM substrate **174** as the major diastereomer.

Scheme 2.34 Completion of the synthesis of RRCM substrate 174

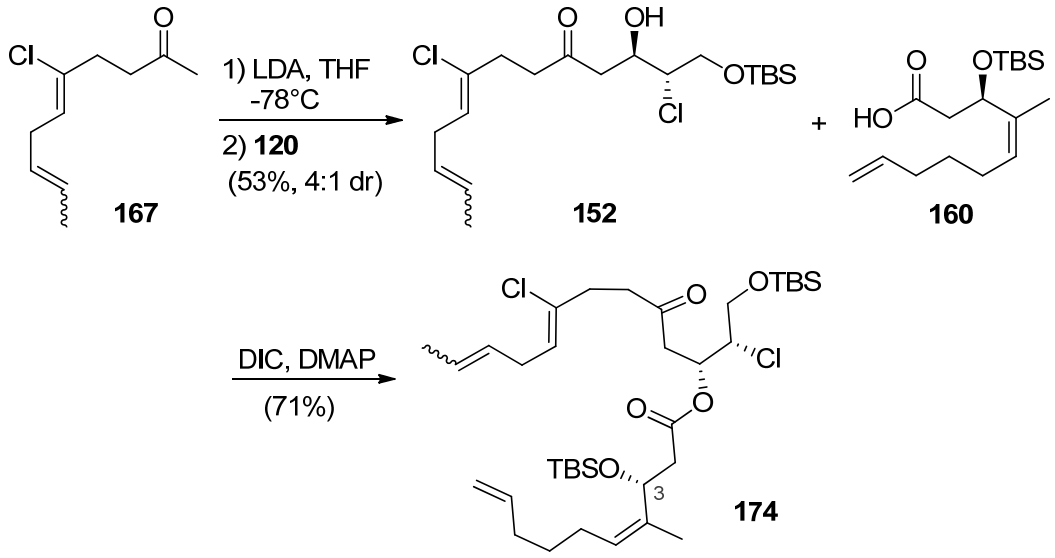

Next, we subjected the enantiomerically enriched RRCM substrate **174** to the standard RRCM conditions reported by Hoye[77,83] (10 mol% Grubbs II catalyst, 0.002M reaction concentration, sparge with N_2, then reflux in toluene, 1-5 minutes). Following purification by flash chromatography, two truncation products (**175** and **176**) along with two cyclization products (**177** and **178**) were isolated (Scheme 2.35), much to our delight. The truncation products were inseparable and presumably corresponded to the major and minor diastereomers of the RRCM substrate. The cyclization products, meanwhile, were separable and obtained in a ratio of roughly 4:1. They possessed slightly different R_f on TLC (10:1 hexanes/ethyl acetate) and more importantly, distinctive ^{1}H NMR spectra.

Scheme 2.35 Products obtained from RRCM of substrate 174

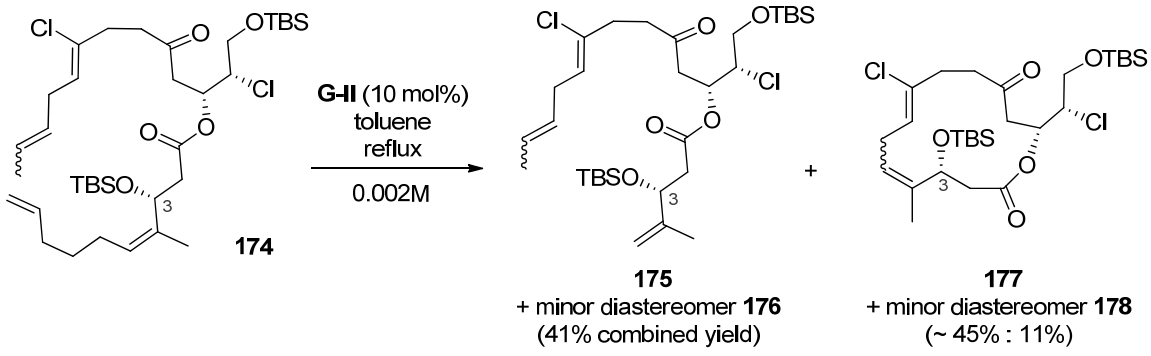

Before further analyzing these results, we sought to optimize the RRCM reaction conditions. We tested various reaction temperatures, concentration, catalysts, order of reagent addition, and solvents (Table 2.2). As well, inspired by Grubbs' report,[84] we tested the use of additives (Table 2.2, entries 13-14). Despite these efforts, the results described above were not improved and, moving forward, we opted to employ the standard RRCM conditions.

Table 2.2 Efforts to optimize RRCM reaction

Entry	Reaction Conditions	Time	Truncation:Cyclization*
Standard	SM [0.002M] in toluene, add 10 mol% Grubbs-II, N_2 sparge, immediately reflux (110°C) in preheated sand bath	1-5 min	0.73:1†
1	Same as standard, but [0.005M]	1-5 min	0.83:1†
2	Same as standard, but Hoveyda-Grubbs-II catalyst	1-5 min	More truncation than cyclization
3	Same as standard, but Grubbs-I catalyst	1-5 min	Decomposition
4	SM [0.005M] in toluene, add 10 mol% Grubbs-II, N_2 sparge, immediately heat to 50°C	2 hours	SM & truncation
5	SM [0.005M] in toluene, add 10 mol% Grubbs-II, N_2 sparge, immediately heat to 80°C	2 hours	SM & truncation
6	Same as standard, but [0.001M]	1-5 min	Not better than standard
7	25 mol% Grubbs-II in toluene, N_2 sparge, immediately reflux (110°C), then add SM [0.001M] at 110°C	1-5 min	Truncation & decomposition
8	SM [0.001M] in toluene, N_2 sparge, immediately reflux (110°C), drop-wise addition of 10 mol% Grubbs-II at 110°C	3-5 min	More truncation than cyclization
9	SM [0.002M] in CH_2Cl_2, add 10 mol% Grubbs-II, N_2 sparge, immediately reflux (>40°C)	18 hours	SM & truncation
10	Same as standard, but 50 mol% catalyst	1-5 min	Similar to standard
11	SM [0.002M] in hexanes, add 10 mol% Grubbs-II, N_2 sparge, immediately reflux (>70°C)	2 hours	SM & truncation
12	Toluene, N_2 sparge, heat to reflux, simultaneous drop-wise addition of SM [0.002M] and 10 mol% Grubbs-II at 110°C	3-5 min	Not better than standard
13	Same as standard, but 10 mol% DDQ as additive	1-5 min	No cyclization products
14	Same as standard, but 10 mol% benzoquinone as additive	1-5 min	More truncation than cyclization

* results analyzed from crude reaction ^{1}H NMR

† ratio based on isolated yields

Having failed in our attempts to optimize the RRCM reaction conditions, we returned to the structural analysis of our cyclization products (Scheme 2.35). The ^{1}H NMR spectrum of major cyclization product **177** displays two resonances corresponding to its vinylic protons – a triplet at δ 5.40 for the proton at position **c**, and a multiplet at δ 5.22 for the proton at position **a** (Figure 2.7). Another key resonance in the spectrum is a doublet of doublets at δ 4.38, corresponding to the proton at position **b**. We performed 1D nOe experiments on **177**, and were able to observe nOe correlations between protons **a** and **c**, as well as between **a** and **b** (Figure 2.8). The nOe correlation between protons **a** and **c** is expected regardless of alkene geometry. More crucially, the nOe correlation between protons **a** and **b** indicates the major cyclization product **177** to in fact be an (*E*)-alkene as depicted (**177a**). This unfortunate result indicated that the RRCM strategy would not provide the desired (*Z*)-alkene as the major product.

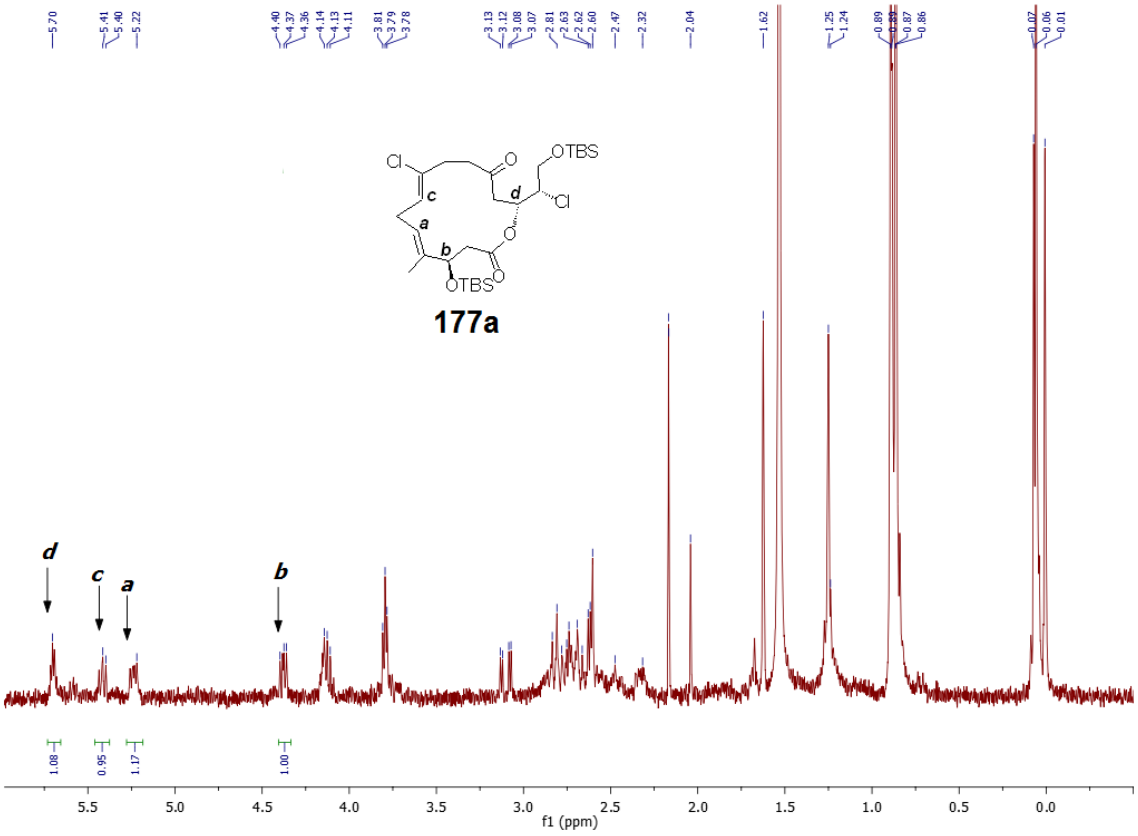

Figure 2.7 ^{1}H NMR spectrum of RRCM major cyclization product 177a

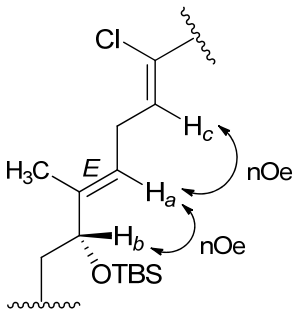

Figure 2.8 Key nOe correlations in RRCM major cyclization product 177a

In addition to the concerns regarding alkene geometry, we also lacked sufficient material to carry out reliable structural analysis of the minor cyclization product **178**, presumably the desired (*Z*)-alkene. Regardless, of pressing concern was the fact that the RRCM reaction gave the undesired (*E*)-alkene as the major product. This was most worrisome because the alkene geometry appeared to be strictly substrate-dependent. Our studies in Scheme 2.36 further supported this hypothesis – a racemic synthesis of RRCM substrate **174** (from racemic β-hydroxy ester **126**) gave a 1:1 mixture of two cyclization products whose R_f and ^1H NMR spectra matched those of the major and minor diastereomers mentioned above. Clearly, the cyclization products are specific for each diastereomeric RRCM substrate, and the optically enriched RRCM substrate **174** could only lead to the undesired (*E*)-alkene **177a**. The 1:1 ratio of RRCM products obtained from the racemic synthesis led us to believe that the substrate stereochemistry at C3 controls the outcome of the RRCM reaction. Thus, the C3-epimer of optically enriched RRCM substrate **174** should give the previously minor cyclization product **178** as the major product. If this is indeed to be the case and the corresponding cyclization product **178** is indeed the (*Z*)-alkene, the stereochemistry of C3 could always be rectified later on with a Mitsunobu inversion.[85]

Scheme 2.36 Non-optically enriched RRCM substrate 174 gave 1:1 mixture of products

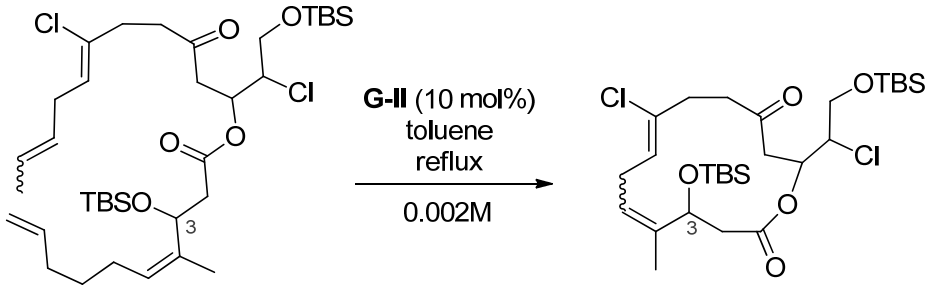

174, even mixture of diastereomers

177/**178**
1:1 mixture of two physically separable sets of compounds

To investigate this hypothesis, we synthesized the C3-epimer of the RRCM substrate **174**. Towards this end, we returned to the Sharpless epoxidation reaction of β-hydroxyester **126** (Scheme 2.20) and used (-)-DIPT as the chiral ligand, instead of (+)-DIPT (Scheme 2.37). This left the (*S*)-enantiomer **180** unreacted (>98% ee by chiral GC), which was processed following a series of reactions previously described for the (*R*)-enantiomer (see Scheme 2.28), to eventually arrive at the optically enriched RRCM substrate **181**, with the configuration at C3 now being (*S*). When this RRCM substrate **181** was subjected to the standard RRCM conditions, the resulting products were the major cyclization product **178a** and the minor diastereomer **177b** (once again 4:1 ratio). Compared to the products from the previous RRCM of epimeric substrate **174** (Scheme 2.35), product **178a** had the same R_f as previous minor product **178**, while minor product **177b** had the same R_f as previous major product **177a**.

Scheme 2.37 Synthesis and reaction of C3-epimeric RRCM substrate 181

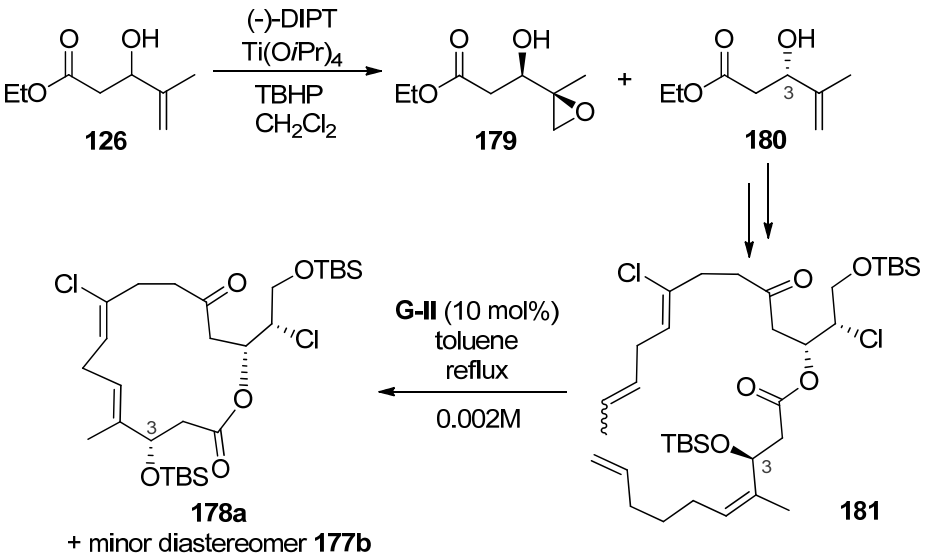

Furthermore, the major and minor cyclization products were analyzed by ^{1}H NMR spectroscopy, and the major product **178a** had an identical spectrum (Figure 2.9) to that recorded on the previously minor product **178**, with signals **h**, **g**, **e**, and **f** appearing at δ 5.63, 5.44, 5.33, and 4.43 respectively. On the other hand, minor product **177b** displayed the same spectrum to that recorded on the previously major product **177a** (Figure 2.7). Also, with enough material in hand for 1D nOe experiments this time, we were able to determine the alkene geometry of both the major and minor products to be (*E*), with the same nOe correlations as illustrated in Figure 2.8.

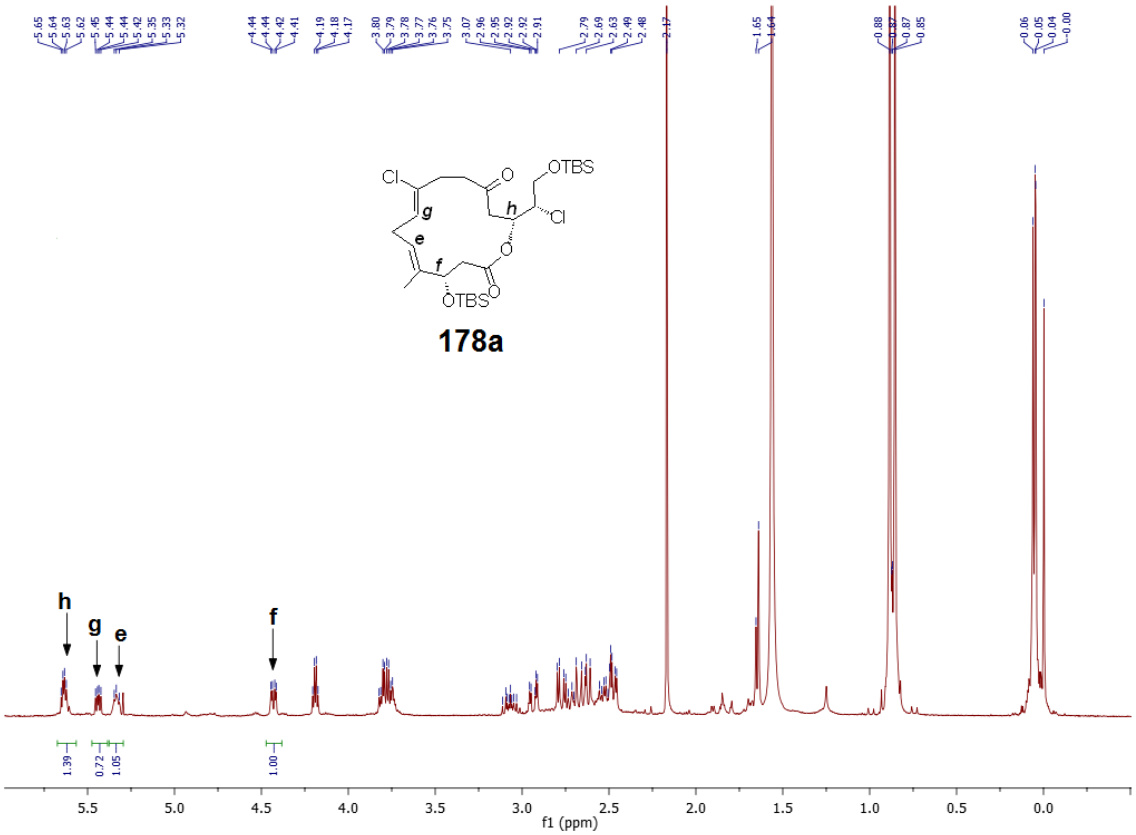

Figure 2.9 ***^{1}H NMR spectrum of RRCM major cyclization product 178a***

In summary (Scheme 2.38), these findings mean that both C3-epimers of the RRCM substrate led to the same two sets of separable cyclization products (**177** and **178**), with both sets possession (*E*) geometry at the newly formed alkene. These two sets of separable cyclization products were in fact not geometric isomers as originally suspected, but rather diastereoisomers as a result of the varying configurations of the substrates' stereocenters. Ignoring the influence of the C14 stereocenter on the RRCM reaction, which ends up outside of the ring (and should be negligible), the stereochemistry at C3 and C13 are in fact enantiomeric within each set of cyclization products. This enantiomeric relationship between each set of macrocycles provides rationale for the identical R_f and spectral data observed – the enantiomeric pair (3*R*, 13*R*) (**174**) and (3*S*, 13*S*) (**183**) both led to cyclization product **177** (**A**), while the enantiomeric pair (*3*S, 13*R*) (**181**) and (3*R*, 13*S*) (**182**) both led to cyclization product **178** (**B**). The presence of the minor RRCM substrate diastereomers **182** and **183** in

each case was a direct result of the 4:1 diastereomeric ratio of the aldol adducts (Scheme 2.34).

Scheme 2.38 Summary of RRCM findings

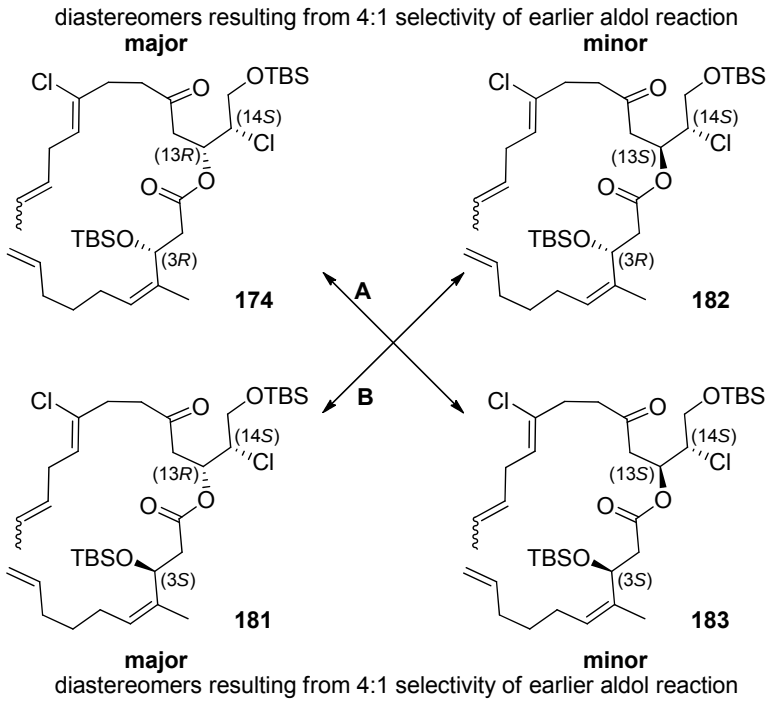

A
Both the (3*R*,13*R*,14*S*) and the (3*S*,13*S*,14*S*) compound leads to the cyclization product **177**, with the same R_f and ^{1}H NMR

B
Both the (3*S*,13*R*,14*S*) and the (3*R*,13*S*,14*S*) compound leads to the cyclization product **178**, with the same R_f and ^{1}H NMR

In the end, despite considerable effort, the alkene geometry of each cyclization product was (*E*), the opposite of what we desired. As a result, it was decided to not pursue the RRCM approach further as this would not provide a viable route to the biselides.

2.6. Final Proposal: Cross Metathesis Strategy

Having abandoned the RRCM approach to the haterumalide/biselide skeleton, a small positive result brought to our attention the potential of a cross metathesis strategy. A cross metathesis reaction of known dioxane **184**[86] with ketone **167** rather surprisingly gave the desired 1,4-diene **185** as the dominant product (Scheme 2.39). As well, unlike the previous RRCM reactions, the cross metathesis could be effected under mild reaction conditions, simply refluxing with Grubbs-II catalyst in CH_2Cl_2 at 40°C.

Scheme 2.39 A cross metathesis reaction to assemble a 1,4-diene

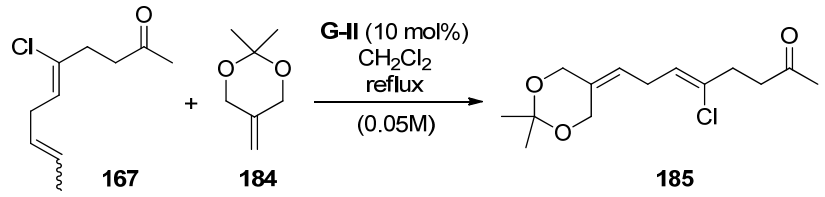

Scheme 2.40 Retrosynthetic plan involving cross metathesis

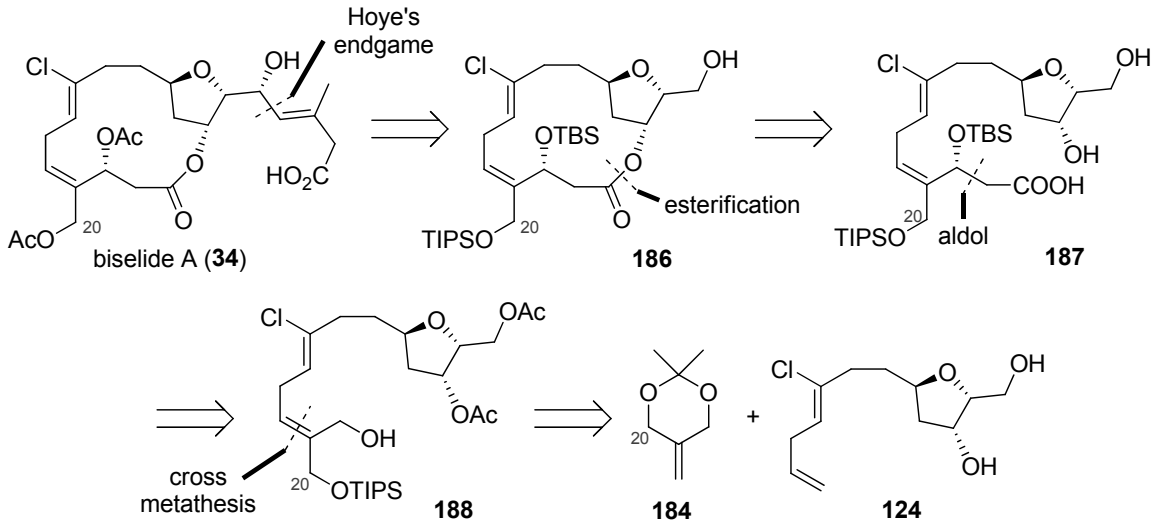

We envisioned the application of a similar cross metathesis reaction to assemble the challenging 1,4-diene component of biselide A, by starting with previously mentioned tetrahydrofuranol **124** and dioxane **184** (Scheme 2.40). We could subsequently remove the acetonide and selectively silylate the (*E*)-hydroxyl group with a bulky reagent such as TIPSCl to access an intermediate such as **188**. Oxidation of the free alcohol in **188** followed by aldol addition with an ethyl acetate derivative would lead to an intermediate such as **187**. Subsequent macrolactonization via Yamaguchi esterification[54] would afford intermediate **186**, which could be converted to biselide A (**34**) following Hoye's endgame strategy.[55]

2.6.1. Results and Discussion

We first sought to confirm the validity of our cross metathesis step by performing the same reaction using ketone **119**, without the methyl group attached to the monosubstituted terminal alkene (Scheme 2.41). To our delight, the desired product was obtained in 61% yield, despite the theoretically large difference in reactivity between the two alkenes. Optimization work performed by a colleague, Matthew Taron, showed that executing the reaction using the Hoveyda-Grubbs II catalyst in toluene at 60°C gave the best result.

Scheme 2.41 Cross metathesis reaction of terminal alkene 119 with dioxane 184

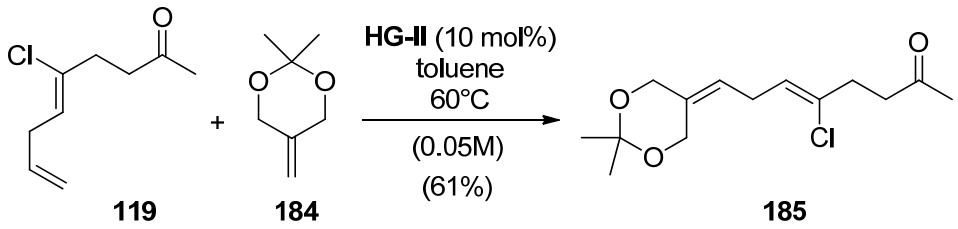

119 **184** **185**

With the validity of the cross metathesis confirmed, the previously prepared tetrahydrofuranol **124** was selectively silylated at the primary alcohol position to give silyl ether **125**, albeit in a modest yield of 54% (Scheme 2.42). Silyl ether **125** was then acetylated with Ac_2O to afford diene **189**, which was subsequently coupled with dioxane **184** in a cross metathesis reaction to give adduct **190**. Acid-catalyzed removal of the acetonide using PPTS then afforded diol **191** in 28% yield over the 4 steps.

Scheme 2.42 Synthesis of diol 191 from tetrahydrofuranol 124

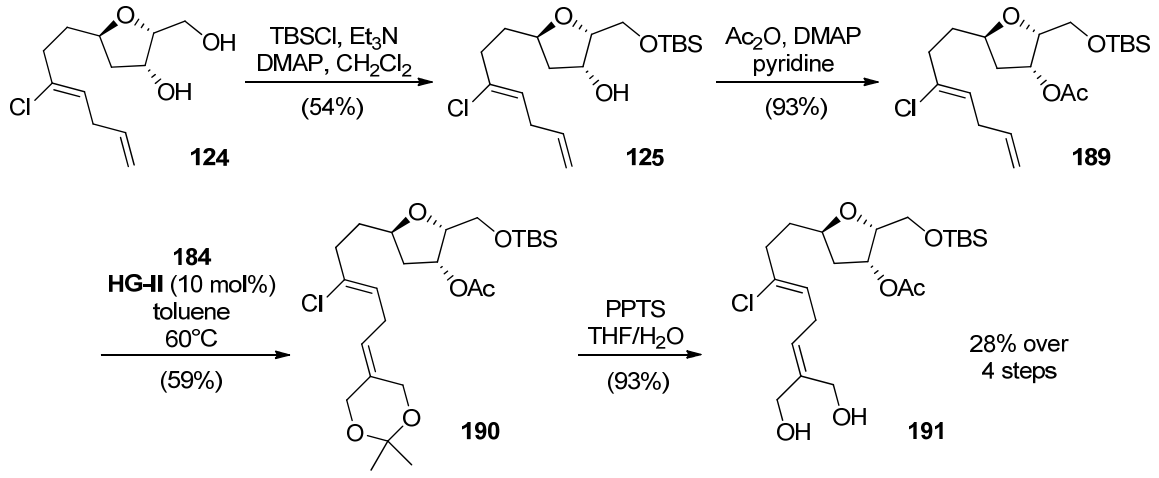

Alternatively, diol **194** was also synthesized from tetrahydrofuranol **124**, with two acetate groups rather than one acetate and one TBS group (Scheme 2.43). This synthesis required one less step – avoiding the low yielding selective silylation step. Surprisingly, the yield for the cross metathesis between **192** and the alkene **184** was particularly low. In the end, the synthesis of diol **194** from tetrahydrofuranol **124** was accomplished in 32% yield over the 3 steps.

Scheme 2.43 Synthesis of diol 194 from tetrahydrofuranol 124

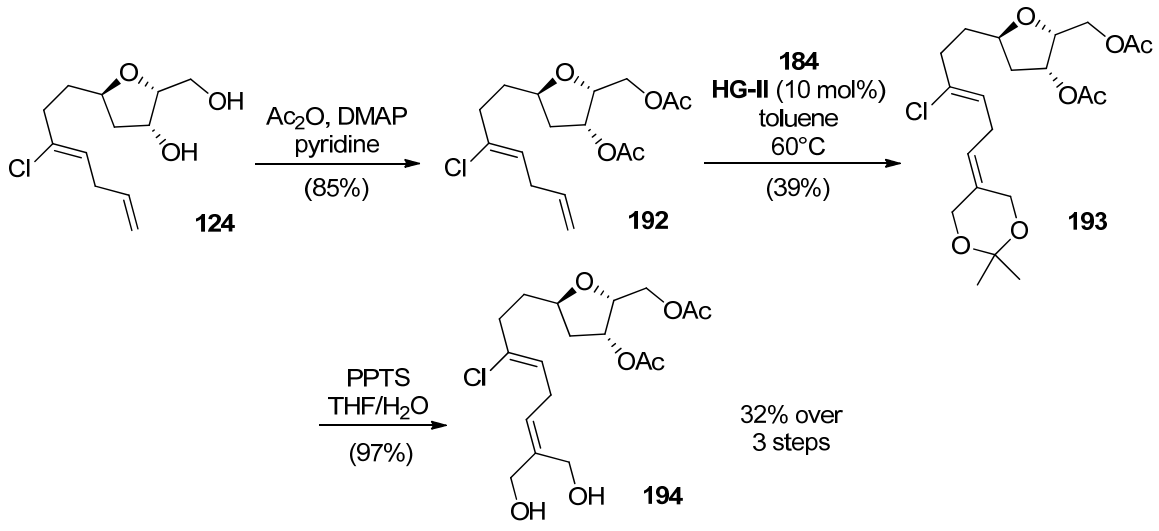

Finally, we subjected diol **194** to a silylation reaction with the sterically bulky silylating agent TIPSCl, in the presence of Et_3N and catalytic DMAP (Scheme 2.44). It was expected[87] that the steric bulk of the TIPS group would lead to selective silylation of the more accessible (*E*)-hydroxyl group. However, the result was a mixture of products, with the desired (*E*)-isomer (**195b**) obtained in a mere 21% yield, while the bis-silylated product (**196**) was the major product (31%), and a small amount of (*Z*)-isomer (**195a**) was obtained in 7% yield. The remainder of the crude product (~40%) was unreacted starting material, suggesting a slow silylation process, with little difference in reactivity between the two free alcohol functions. The geometry of the resulting products were determined by 1D nOe analysis of the acetylation product (**197**) derived from the (*E*)-isomer (Scheme 2.45). Acetylation was necessary to distinguish the ^1H NMR signals of the α-oxy methylene protons.

Scheme 2.44 Silylation of diol 194 with TIPSCl

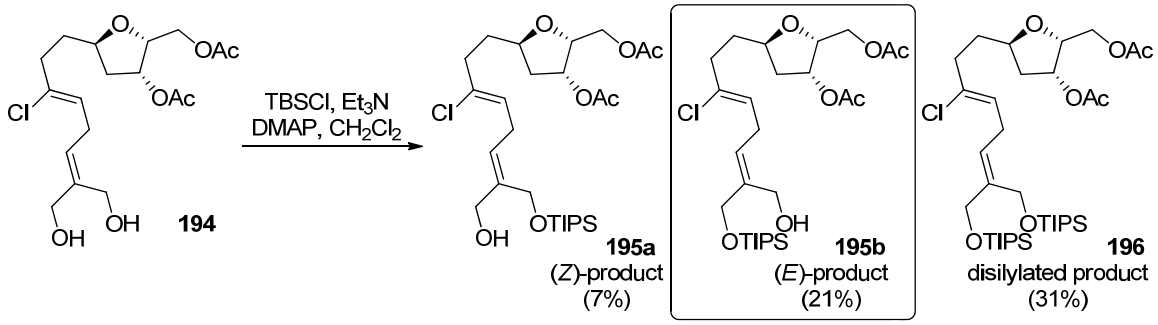

Scheme 2.45 Determination of alkene geometry of silylation product 195b

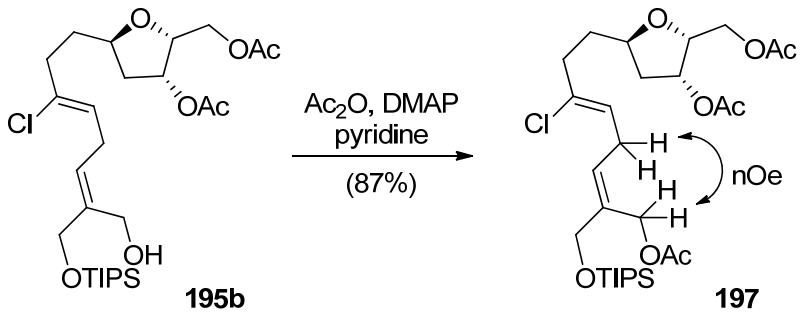

At this point in the synthesis, the small amount of remaining **195** (5 mg, *E*/*Z* mixture) was oxidized with Dess-Martin periodinane to afford the corresponding enal **198** (3 mg, ~60% yield) (Scheme 2.46) as a proof-of-concept in support of the proposed synthetic strategy outlined earlier.

Scheme 2.46 Formation of aldehyde 198

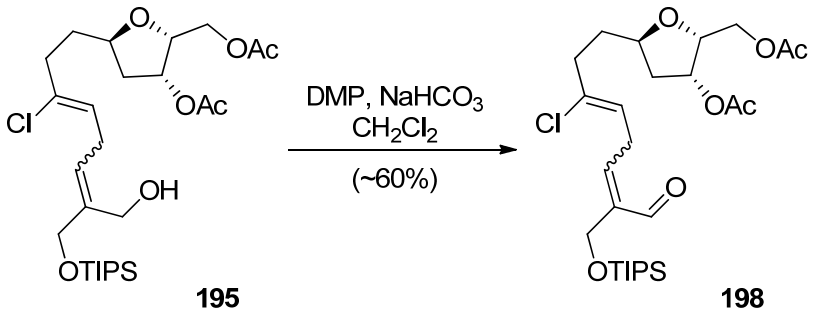

195 **198**

2.7. Future Direction

While these results represent our first success in constructing the (*Z*,*Z*)-1,4-diene functionality towards biselides, poor selectivity and yields remain significant obstacles. Further optimization work is required to improve the yields of the cross metathesis and selective silylation steps. Potential alternative conditions for the silylation step may include the use of NaH rather than a weak organic base such as Et_3N (Scheme 2.47). A reaction involving a sodium alkoxide intermediate should eliminate the formation of bis-silylated product **196**. However, it is not clear whether silyl migration may complicate the results of this reaction. Regardless, the undesired (*Z*)-isomer **195a** could be recycled to the desired (*E*)-isomer **199** (albeit with a different protecting group) via simple manipulations (Scheme 2.47).

Scheme 2.47 Alternative conditions for selective protection to obtain (E)-isomer

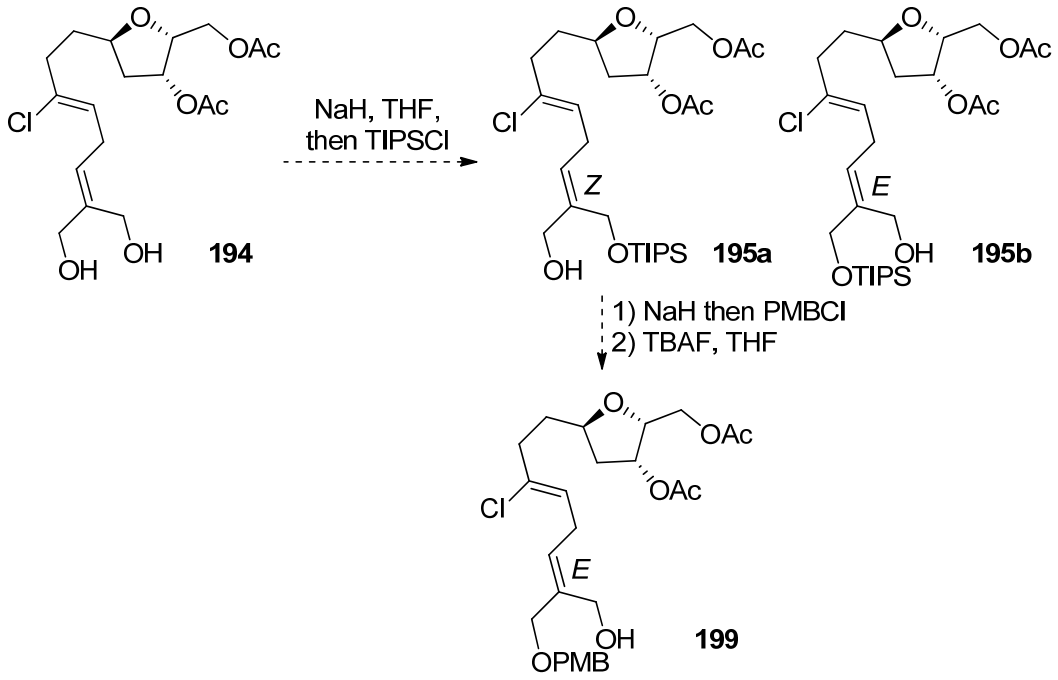

Alternatively, we can explore a slightly different synthetic sequence, by carrying out a mono-silylation of the diol **200** first (with a readily removed protecting group such as TES) before performing a cross metathesis between **201** and **192** (Scheme 2.48). The use of these different metathesis substrates may produce significantly different results. As well, should there not be any selectivity towards the desired (*E*)-isomer **202** in the cross metathesis, the undesired (*Z*)-isomer **203** could once again be recycled via protecting group manipulations (Scheme 2.48).

Scheme 2.48 Alternative sequence for obtaining (E)-isomer

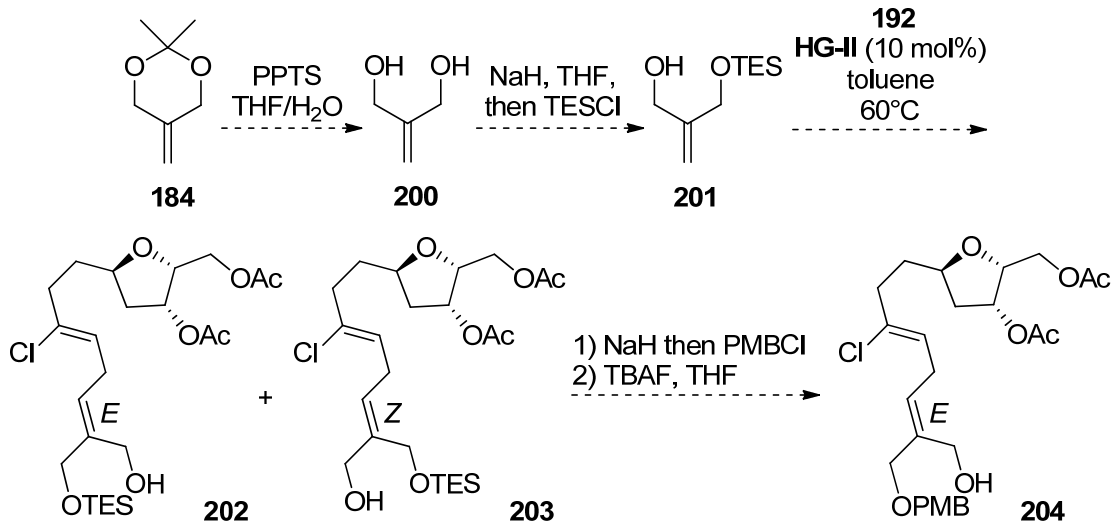

Once the *E*/*Z* selectivity issues are addressed, multiple members of the biselide family can be accessed from the common aldehyde intermediate **198**. Following Kigoshi's method,[62,70] non-selective aldol addition of isopropyl acetate to aldehyde **198** would give β-hydroxy ester **205**, which, following a series of protecting group manipulations, can be transformed to carboxylic acid **206** (Scheme 2.49). Intramolecular Yamaguchi esterification would then generate the macrolactone, followed by further deprotection and protection to give a diastereomeric mixture of the free alcohol **207**, which can be easily separated, according to Kigoshi. Further transformations from alcohol **207** followed by Hoye's endgame[55] would afford biselide A (**34**). Biselide B (**35**) could also be obtained by carrying out the NHK coupling step of Hoye's endgame with a different coupling partner, as evident in Borhan's synthesis.[66]

Scheme 2.49 Future steps to complete the synthesis of biselide A or B

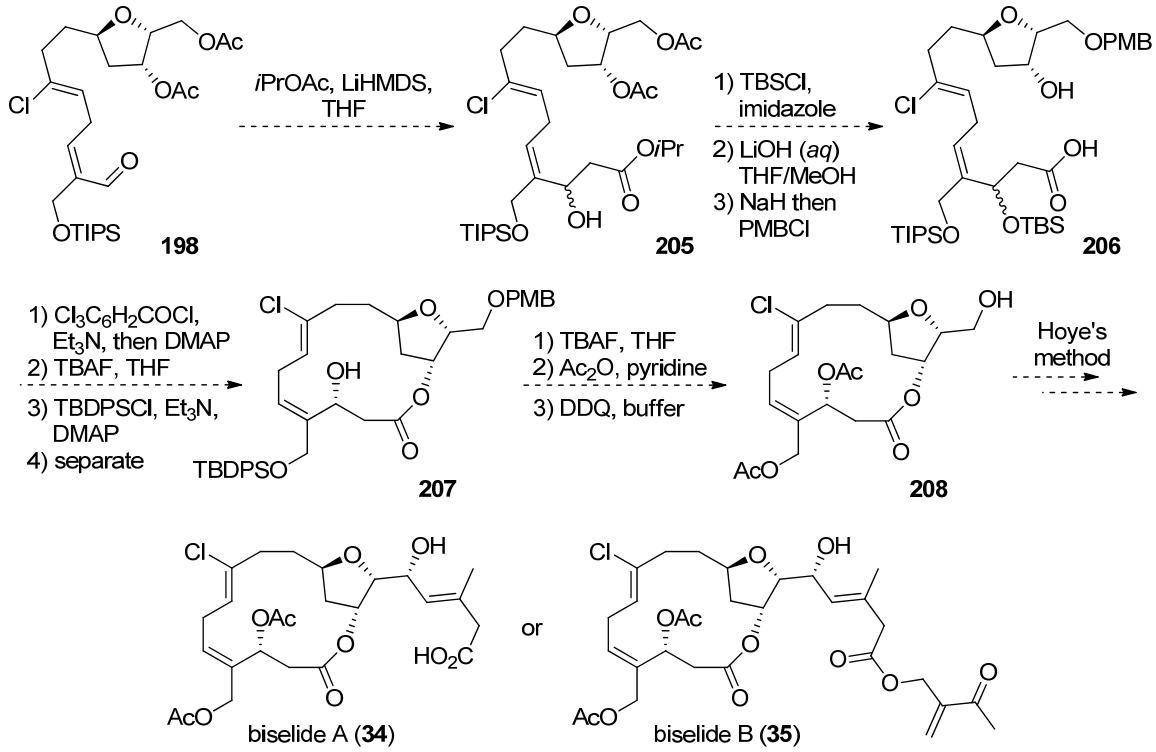

As well, biselide C (**36**) can be accessed from the common alcohol intermediate **207**, by retaining the TBDPS protecting group at C20 until after Hoye's endgame (Scheme 2.50). Likewise, biselide E (**38**), the non-macrocyclic member of the family, can be accessed once again from common aldehyde intermediate **198** (Scheme 2.51). Still-Gennari reaction[45] of aldehyde **198** with phosphonate **209** would give the (*Z*)-ene-ester **210**. Protecting group manipulations followed by intramolecular DCC coupling would then generate the six-membered lactone **211**. Further protecting group manipulations followed by Hoye's endgame and lastly, removal of the PMB group, would afford biselide E (**38**).

Scheme 2.50 Future steps to complete the synthesis of biselide C

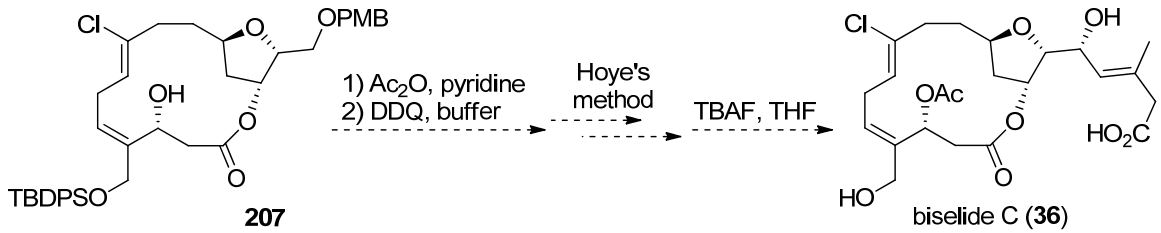

Scheme 2.51 Future steps to complete the synthesis of biselide E

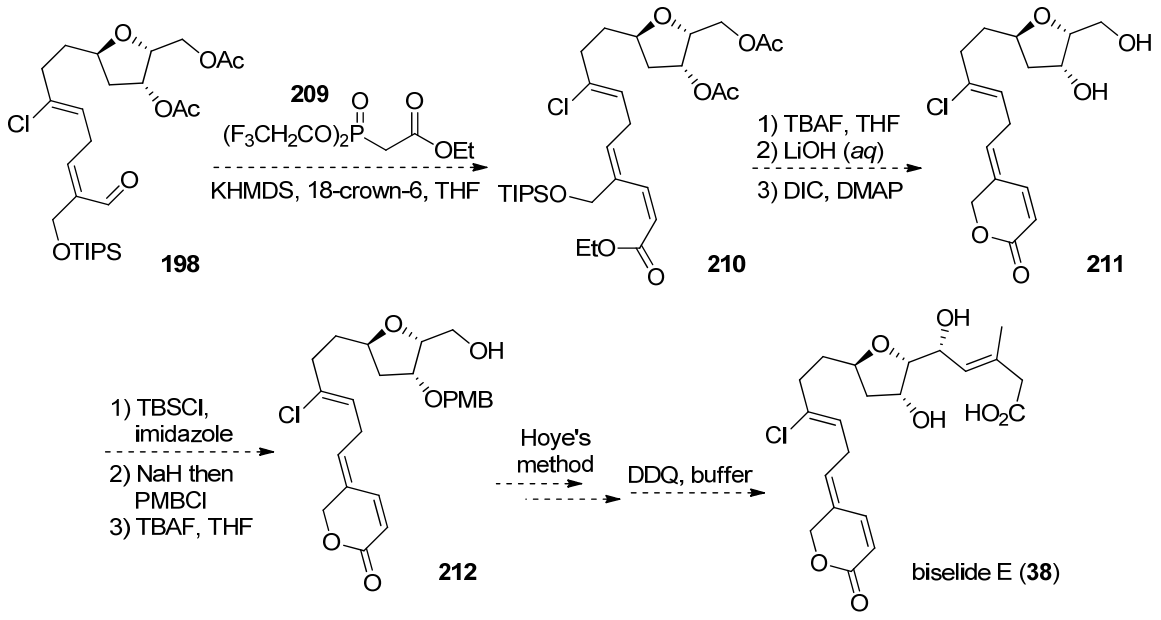

2.8. Conclusion

In this chapter, an overview of our efforts toward the total synthesis of the biselide family of natural products was presented. We have successfully applied our tetrahydrofuranol cyclization methodology to access the tetrahydrofuran core of the biselides in an enantioselective fashion in 8 steps, starting from simple and cheap commercial materials. This is in great contrast to previous syntheses of haterumalides, which often require complex chiral pool materials to access the tetrahydrofuran core. As well, through much experimentation, we made major advances towards construction of

the (*Z*,*Z*)-1,4-diene functionality, eventually utilizing a cross metathesis reaction. However, future work is still needed to improve the yield and selectivity of certain steps in our synthesis. Following our plan, completion of the synthesis of biselide A (**34**) would require a total of 26 steps (longest linear sequence), potentially making it the first reported total synthesis of biselide A (**34**). As well, our synthetic strategy provides flexibility which should allow us to easily access other members of the biselide family.

2.9. Experimental

All reactions described were performed under an atmosphere of dry argon or nitrogen using oven dried glassware unless otherwise specified. Tetrahydrofuran was distilled over Na/benzophenone and dichloromethane was dried by distillation over CaH_2. All other solvents were used directly from EMD drysolv septum sealed bottles unless otherwise specified. Flash chromatography was carried out with 230-400 mesh silica gel (E. Merck, Silica Gel 60). Thin layer chromatography was carried out on commercial aluminium backed silica gel 60 plates (E. Merck, type 5554, thickness 0.2 mm). Concentration and removal of trace solvents was performed on a Büchi rotary evaporator using dry ice/acetone condenser and vacuum from water or air aspirator.

All reagents and starting materials were purchased from Sigma Aldrich, Alfa Aesar, and/or TCI America and were used without further purification. All solvents were purchased from Sigma Aldrich, EMD, Anachemia or Caledon and used without further purification.

Nuclear magnetic resonance (NMR) spectra were recorded using deuterochloroform ($CDCl_3$) as the solvent. Signal positions (δ) are given in parts per million from tetramethylsilane (δ 0) and were measured relative to the signal of the solvent (δ 7.26, ^{1}H NMR; δ 77.00, ^{13}C NMR). Coupling constants (*J* values) are given in Hertz (Hz) and are reported to the nearest 0.1 Hz. ^{1}H NMR spectral data are tabulated in the order: multiplicity (s, singlet; d, doublet; t, triplet; m, multiplet), number of protons, coupling constants, assignment (where possible). NMR spectra were recorded on a Bruker Avance 600 equipped with a QNP or TCI cryoprobe (600 MHz), Bruker 500 (500 MHz),

or Bruker 400 (400 MHz). Assignments of ^{1}H and ^{13}C NMR spectra are based on analysis of ^{1}H-^{1}H COSY, HSQC, HMBC, TOCSY and 1D NOESY spectra.

High resolution mass spectra were performed on an Agilent 6210 TOF LC/MS or Bruker micrOTOF-II LC mass spectrometer.

Diastereomeric ratios were determined by analysis of ^{1}H NMR spectra recorded on crude reaction products.

2.9.1. Preparation of 3-[(*tert*-butyldimethylsilyl)oxy]-4-methylpent-4-enoic acid (139)

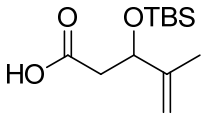

To a stirring solution of ethyl 3-[(tert-butyldimethylsilyl)oxy]-4-methylpent-4-enoate (**138**)[72] (200 mg, 0.73 mmol) in MeOH (7 mL) was added 2 M NaOH (1.4 mL) at room temperature. The turbid white mixture was stirred at room temperature for 18 hours, gradually turning clear. After this time, the reaction mixture was acidified to pH ~2 with 1 M HCl. The resulting mixture was partitioned between Et_2O (10 mL) and H_2O (10 mL), and the layers were separated. The aqueous layer was extracted with Et_2O (2 x 5 mL), and the combined organic layers were washed with brine then dried with anhydrous $MgSO_4$. Concentration in *vacuo* afforded carboxylic acid **139** as a viscous, colourless oil (130 mg, 73%).

^{1}H NMR (500 MHz, $CDCl_3$) δ: 4.99 (s, 1H), 4.84 (s, 1H), 4.54 (dd, 1H, *J* = 4.4, 8.2 Hz), 2.60 (dd, 1H, *J* = 8.2, 14.8 Hz), 2.51 (dd, 1H, *J* = 4.4, 14.8 Hz), 1.72 (s, 3H), 0.88 (s, 9H), 0.07 (s, 3H), 0.04 (s, 3H)

^{13}C NMR (125 MHz, $CDCl_3$) δ: 176.1, 146.0, 112.2, 73.6, 42.0, 25.8, 18.2, 17.3, -4.7, -5.3

Exact mass calcd. for $C_{12}H_{24}O_3Si$: 245.1573 $(M+H)^+$; found: 245.1596 $(M+H)^+$

2.9.2. Preparation of (*Z*)-5-chloronona-5,8-dien-2-ol (140)

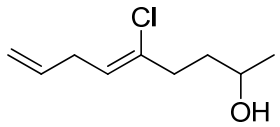

To a cold (0°C), stirring suspension of $LiAlH_4$ (45 mg, 1.13 mmol) in anhydrous Et_2O (3 mL) was added drop-wise a solution of (*Z*)-5-chloronona-5,8-dien-2-one (**119**)[32] (150 mg, 0.87 mmol) in Et_2O (0.5 mL). The reaction mixture was stirred for 3 hours while gradually warming to room temperature, after which it was cooled again to 0°C and diluted with 5 mL of Et_2O. The reaction was quenched with H_2O (50 µL) and then 2 M NaOH (50 µL), followed by the addition of another 0.15 mL of H_2O. The mixture was removed from ice bath and stirred for 5 minutes at room temperature, by which point a white precipitate has formed. Anhydrous $MgSO_4$ was added and the mixture was stirred for a further 5 minutes, before being filtered, rinsing with Et_2O. The filtrate was concentrated in *vacuo*, followed by purification by flash chromatography (silica gel, 6:1 hexanes:ethyl acetate) to afford alcohol **140** as a colourless oil (160 mg, 92%).

^{1}H NMR (500 MHz, $CDCl_3$) δ: 5.79 (m, 1H), 5.54 (t, 1H, *J* = 7.0 Hz), 5.08 (dm, 1H, *J* = 17.1 Hz), 5.03 (dm, 1H, *J* = 10.2 Hz), 3.82 (m, 1H), 2.93 (t, 2H, *J* = 6.7 Hz), 2.45 (m, 2H), 1.70 (m, 2H), 1.40 (br s, 1H), 1.22 (d, 3H, *J* = 6.3 Hz)

^{13}C NMR (125 MHz, $CDCl_3$) δ: 135.5, 135.4, 123.1, 115.5, 67.2, 37.1, 36.0, 32.9, 23.8

Exact mass calcd. for $C_9H_{15}ClO$: 175.0890 $(M+H)^+$; found: 175.0909 $(M+H)^+$

2.9.3. Preparation of (*Z*)-5-chloronona-5,8-dien-2-yl 3-[(tert-butyldimethylsilyl)oxy]-4-methylpent-4-enoate (142)

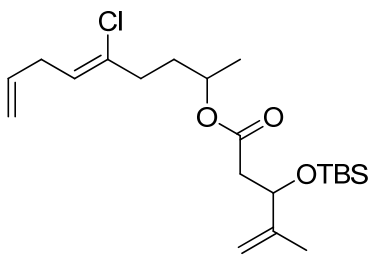

To a room-temperature solution of 3-[(tert-butyldimethylsilyl)oxy]-4-methylpent-4-enoic acid (**139**) (65 mg, 0.27 mmol) in CH_2Cl_2 (1.5 mL) was added (*Z*)-5-chlorononа-5,8-dien-2-ol (**140**) (31 mg, 0.18 mmol), followed by DMAP (4 mg, 0.035 mmol). The mixture was stirred at room temperature until dissolution of DMAP, and then treated with DIC (44 µL, 0.28 mmol). The clear solution gradually turned cloudy, and was stirred at room temperature for 16 hours. After this time, the reaction mixture was partitioned between CH_2Cl_2 (1 mL) and saturated aqueous $NaHCO_3$ (1 mL), and the layers were separated. The aqueous layer was extracted with CH_2Cl_2 (1 mL), and the combined organic layers were washed with brine, dried with anhydrous $MgSO_4$, and concentrated in *vacuo*. Purification of the crude mixture by flash chromatography (silica gel, 20:1 hexanes:ethyl acetate) afforded ester **142** as a colourless oil (70 mg, 97%).

^{1}H NMR (500 MHz, $CDCl_3$) δ: 5.78 (m, 1H), 5.49 (m, 1H), 5.07 (dm, 1H, *J* = 17.2 Hz), 5.02 (dm, 1H, *J* = 10.1 Hz), 4.94 (s, 1H), 4.89 (m, 1H), 4.79 (s, 1H), 4.55 (dd, 1H, *J* = 5.4, 8.2 Hz), 2.92 (m, 2H), 2.53 (dd, 1H, *J* = 8.2, 14.6 Hz), 2.42 (dd, 1H, *J* = 5.1, 14.6 Hz), 2.36 (m, 2H), 1.80 (m, 2H), 1.71 (s, 3H), 1.23 (t, 3H, *J* = 6.2 Hz), 0.87 (s, 9H), 0.06 (s, 3H), 0.02 (s, 3H)

^{13}C NMR (125 MHz, $CDCl_3$) δ: 170.9, 146.7, 135.3, 135.0, 123.3, 115.6, 112.4, 111.9, 73.9, 73.8, 70.3, 70.1, 43.5, 42.7, 35.8, 34.1, 32.9, 25.9, 20.2, 18.3, 17.0, -4.6, -5.0

Exact mass calcd. for $C_{21}H_{37}ClO_3Si$: 401.2279 $(M+H)^+$; found: 401.2300 $(M+H)^+$

2.9.4. Preparation of but-3-en-1-yl 3-[(tert-butyldimethylsilyl)oxy]-4-methylpent-4-enoate (143)

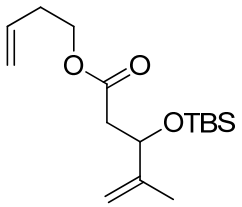

To a room-temperature solution of 3-[(tert-butyldimethylsilyl)oxy]-4-methylpent-4-enoic acid (**139**) (60 mg, 0.245 mmol) in CH_2Cl_2 (1.5 mL) was added 3-buten-1-ol (**141**) (18 µL, 0.205 mmol), followed by DMAP (5 mg, 0.041 mmol). The mixture was stirred at room temperature until dissolution of DMAP, and then treated with DIC (41 µL, 0.266 mmol).

The clear solution gradually turned cloudy, and was stirred at room temperature for 16 hours. After this time, the reaction mixture was partitioned between CH_2Cl_2 (1 mL) and saturated aqueous $NaHCO_3$ (1 mL), and the layers were separated. The aqueous layer was extracted with CH_2Cl_2 (1 mL), and the combined organic layer was washed with brine, dried with anhydrous $MgSO_4$, and concentrated in *vacuo*. Purification of the crude mixture by flash chromatography (silica gel, 20:1 hexanes:ethyl acetate) afforded ester **143** as a colourless oil (74 mg, 100%).

^{1}H NMR (500 MHz, $CDCl_3$) δ: 5.79 (m, 1H), 5.10 (dm, 1H, *J* = 17.1 Hz), 5.05 (dm, 1H, *J* = 10.3 Hz), 4.95 (s, 1H), 4.79 (s, 1H), 4.55 (dd, 1H, *J* = 4.6, 8.7 Hz), 4.11 (t, 2H, *J* = 6.9 Hz), 2.55 (dd, 1H, *J* = 8.7, 14.2 Hz), 2.42 (dd, 1H, *J* = 4.6, 14.2 Hz), 2.38 (m, 2H), 1.71 (s, 3H), 0.86 (s, 9H), 0.04 (s, 3H), 0.01 (s, 3H)

^{13}C NMR (125 MHz, $CDCl_3$) δ: 171.5, 146.7, 134.1, 117.3, 111.8, 73.9, 63.7, 42.6, 33.2, 25.8, 18.2, 17.0, -4.7, -5.2

Exact mass calcd. for $C_{16}H_{30}O_3Si$: 299.2042 $(M+H)^+$; found: 299.2060 $(M+H)^+$

2.9.5. Preparation of (*R*)-ethyl 3-[(*tert*-butyldimethylsilyl)oxy]-4-oxopentanoate (158)

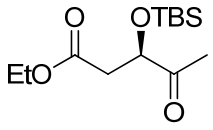

Optically enriched (*R*)-ethyl 3-[(*tert*-butyldimethylsilyl)oxy]-4-methylpent-4-enoate (**157**)[72] (0.40 g, 1.47 mmol) was solubilized in a 2:1 solution of CH_2Cl_2/MeOH (14 mL : 7 mL) and cooled to -78°C. The clear solution was bubbled with ozone at -78°C until it turned dark blue (~10 minutes), after which time it was bubbled with N_2 at -78°C until it turned back to clear (~5 minutes). PPh_3 (0.42 g, 1.62 mmol) was then added to the stirring clear solution in one portion at -78°C, and the mixture was stirred at room temperature for 1 hour. After this time, the reaction mixture was concentrated in *vacuo* to afford a crude white solid, which was extracted with hexanes (5 x 10 mL). The hexanes solution was cooled to -78°C to allow the byproduct to precipitate as a white solid, after which it was filtered off. This freeze-filter step was repeated two more times. Finally, the

remaining hexanes solution was concentrated in *vacuo* to afford the ketone **158** as a colourless oil (0.37 g, 91%).

^{1}H NMR (500 MHz, $CDCl_3$) δ: 4.35 (dd, 1H, *J* = 5.3, 5.8 Hz), 4.13 (m, 2H), 2.74 (dd, 1H, *J* = 5.8, 15.3 Hz), 2.63 (dd, 1H, *J* = 5.3, 15.3 Hz), 2.25 (s, 3H), 1.25 (t, 3H), 0.91 (s, 9H), 0.10 (s, 3H), 0.08 (s, 3H)

^{13}C NMR (125 MHz, $CDCl_3$) δ: 211.1, 170.3, 75.4, 60.9, 40.2, 26.2, 25.8, 18.1, 14.3, -4.8, -4.9

Exact mass calcd. for $C_{13}H_{26}O_4Si$: 297.1493 $(M+Na)^+$; found: 297.1508 $(M+Na)^+$

2.9.6. Preparation of (*R*,*Z*)-ethyl 3-[(*tert*-butyldimethylsilyl)oxy]-4-methyldeca-4,9-dienoate (159)

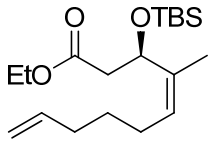

A suspension of hex-5-ene-triphenylphosphonium iodide (**156**)[80] (0.47 g, 1.00 mmol) in freshly distilled THF (8 mL) was cooled to -78°C, and 2.52 M *n*-butyl lithium (0.40 mL, 1.00 mmol) was added drop-wise. The resulting bright orange mixture was transferred to a 0°C bath and stirred for 1 hour. After this time, the reaction mixture was cooled to -20°C and a solution of (*R*)-ethyl 3-[(*tert*-butyldimethylsilyl)oxy]-4-oxopentanoate (**158**) (0.25 g, 0.911 mmol) in THF (1 mL) was added. The reaction mixture was then allowed to stir for 16 hours, gradually warming to room temperature. After this time, the resulting brown mixture was filtered, and the clear yellow filtrate was concentrated in *vacuo*. Purification of the crude mixture by flash chromatography (silica gel, 20:1 hexanes:ethyl acetate) afforded diene **159** as a colourless oil (0.19 g, 61%).

^{1}H NMR (500 MHz, $CDCl_3$) δ: 5.81 (m, 1H), 5.14 (t, 1H, *J* = 7.1 Hz), 5.04-4.94 (m, 3H), 4.11 (q, 2H, *J* = 7.2 Hz), 2.63 (dd, 1H, *J* = 9.2, 14.2 Hz), 2.28 (dd, 1H, *J* = 4.4, 14.2 Hz), 2.13-2.01 (m, 4H), 1.67 (s, 3H), 1.44 (m, 2H), 1.26 (t, 3H, *J* = 7.2 Hz), 0.85 (s, 9H), 0.04 (s, 3H), 0.00 (s, 3H)

^{13}C NMR (125 MHz, $CDCl_3$) δ: 171.5, 138.8, 136.7, 126.5, 114.7, 67.6, 60.5, 42.2, 33.6, 29.3, 27.0, 25.8, 18.2, 17.7, 14.4, -4.8, -5.1

Exact mass calcd. for $C_{19}H_{36}O_3Si$: 341.2512 $(M+H)^+$; found: 341.2506 $(M+H)^+$

2.9.7. Preparation of (*R*,*Z*)-3-[(*tert*-butyldimethylsilyl)oxy]-4-methyldeca-4,9-dienoic acid (160)

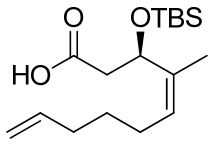

To a stirring solution of (*R*,*Z*)-ethyl 3-[(*tert*-butyldimethylsilyl)oxy]-4-methyldeca-4,9-dienoate (**159**) (185 mg, 0.54 mmol) in MeOH (5 mL) was added 2 M NaOH (2 mL) at room temperature. The turbid white mixture was stirred at room temperature for 18 hours, gradually turning clear. After this time, the reaction mixture was acidified to pH ~2 with 1 M HCl. The resulting mixture was partitioned between Et_2O (10 mL) and H_2O (10 mL), and the layers were separated. The aqueous layer was extracted with Et_2O (2 x 5 mL), and the combined organic layers were washed with brine, dried with anhydrous $MgSO_4$, and concentrated *in vacuo*. Purification of the crude mixture by flash chromatography (silica gel, 10:1 hexanes:ethyl acetate) afforded carboxylic acid **160** as a viscous, colourless oil (113 mg, 66%).

^{1}H NMR (500 MHz, $CDCl_3$) δ: 5.80 (m, 1H), 5.17 (t, 1H, *J* = 7.2 Hz), 5.04-4.94 (m, 3H), 2.65 (dd, 1H, *J* = 8.9, 14.7 Hz), 2.37 (dd, 1H, *J* = 4.4, 14.7 Hz), 2.09-2.02 (m, 4H), 1.44 (m, 2H), 0.87 (s, 9H), 0.07 (s, 3H), 0.03 (s, 3H)

^{13}C NMR (125 MHz, $CDCl_3$) δ: 175.1, 138.7, 136.1, 127.2, 114.8, 67.5, 41.4, 33.5, 29.2, 27.0, 25.8, 18.2, 17.7, -4.8, -5.1

Exact mass calcd. for $C_{17}H_{32}O_3Si$: 335.2013 $(M+Na)^+$; found: 335.2041 $(M+Na)^+$

2.9.8. Preparation of (3*R*,*Z*)-(*Z*)-5-chloronona-5,8-dien-2-yl 3-[(*tert*-butyldimethylsilyl)oxy]-4-methylnona-4,8-dienoate (161)

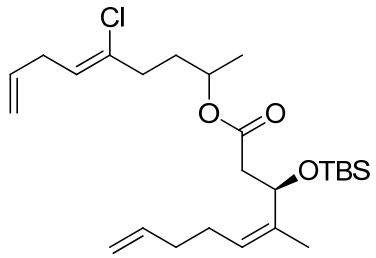

To a room-temperature solution of (*R*,*Z*)-3-[(*tert*-butyldimethylsilyl)oxy]-4-methyldeca-4,9-dienoic acid (**160**) (38 mg, 0.122 mmol) in CH_2Cl_2 (1.2 mL) was added (*Z*)-5-chloronona-5,8-dien-2-ol (**140**) (16 mg, 0.094 mmol), followed by DMAP (2.3 mg, 0.019 mmol). The mixture was stirred at room temperature until dissolution of DMAP, and then treated with DIC (19 µL, 0.122 mmol). The clear solution gradually turned cloudy, and was stirred at room temperature for 16 hours. After this time, the reaction mixture was partitioned between CH_2Cl_2 (1 mL) and saturated aqueous $NaHCO_3$ (1 mL), and the layers were separated. The aqueous layer was extracted with CH_2Cl_2 (1 mL), and the combined organic layers were washed with brine, dried with anhydrous $MgSO_4$, and concentrated in *vacuo*. Purification of the crude mixture by flash chromatography (silica gel, 12:1 hexanes:ethyl acetate) afforded ester **161** as a colourless oil (43 mg, 75%).

^{1}H NMR (500 MHz, $CDCl_3$) δ: 5.84-5.77 (m, 2H), 5.49 (dt, 1H, *J* = 7.0, 8.2 Hz), 5.13 (t, 1H, *J* = 7.2 Hz), 5.08-4.96 (m, 4H), 4.94 (m, 1H), 3.56 (m, 1H), 2.92 (t, 2H, *J* = 6.6 Hz), 2.61 (dd, 1H, *J* = 8.8, 14.6 Hz), 2.36-2.26 (m, 3H), 2.11-2.03 (m, 4H), 1.82 (m, 2H), 1.68 (s, 3H), 1.43 (m, 2H), 0.85 (s, 9H), 0.05 (s, 3H), 0.01 (s, 3H)

^{13}C NMR (125 MHz, $CDCl_3$) δ: 171.0, 138.8, 136.7, 135.3, 135.0, 126.5, 123.3, 115.6, 114.7, 70.2, 70.1, 67.5, 67.3, 49.1, 42.3, 35.8, 34.0, 33.6, 33.0, 29.3, 27.1, 25.9, 20.2, 17.7, -4.8, -5.0

Exact mass calcd. for $C_{25}H_{43}ClO_3Si$: 455.2748 $(M+H)^+$; found: 455.2732 $(M+H)^+$

2.9.9. Preparation of (5*Z*)-5-chlorodeca-5,8-dien-2-one (167)

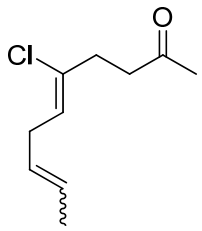

Following Kaneda's procedure,[32,57] propargyl bromide (**121**) (1.85 mL, 15.0 mmol) and 3-chlorobutene (**165**) (4.53 mL, 45.0 mmol) were reacted in the presence of $PdCl_2(PhCN)_2$ (0.17 g, 0.45 mmol) to form (2*Z*)-1-bromo-2-chlorohepta-2,5-diene (**166**). **166** was not isolated, but filtered through a plug of Celite™ and concentrated *in vacuo*. Meanwhile, to a stirring suspension of NaH (0.72 g, 18.0 mmol) in freshly distilled THF (30 mL) at -10°C was added ethyl acetate (2.29 mL, 18.0 mmol) drop-wise over 15 minutes. The reaction mixture turned almost clear after completion of the addition and cessation of bubbling. At this point, the crude mixture of **166** was added in one portion at -10°C, and resulting mixture was stirred for 16 hours while gradually warming to room temperature. After this time, the cloudy brown reaction mixture was quenched with 1 M HCl (10 mL) and turned clear red. The layers were separated, and the aqueous layer was extracted with Et_2O (3 x 10 mL). The combined organic layer was washed with brine, dried with anhydrous $MgSO_4$, and concentrated *in vacuo*. The crude mixture was subsequently solubilized in MeOH (80 mL), and 2 M NaOH (64 mL) was added. The resulting turbid mixture was stirred at room temperature for 40 hours, gradually turning clear. After this time, the reaction mixture was acidified to pH ~2 with 1 M HCl. The resulting mixture was partitioned between Et_2O (80 mL) and H_2O (80 mL), and the layers were separated. The aqueous layer was extracted with Et_2O (3 x 20 mL), and the combined organic layers were washed with brine, dried with anhydrous $MgSO_4$, and concentrated *in vacuo*. Purification of the crude mixture by flash chromatography (silica gel, 15:1 hexanes:ethyl acetate) afforded ketone **167** as a light yellow liquid (0.74 g, 1:1 *E*/*Z*, 27% over 4 steps).

^{1}H NMR (500 MHz, $CDCl_3$) δ: 5.70 (dt, 0.5H, *J* = 6.9, 9.4 Hz), 5.53-5.36 (m, 2.5H), 2.92-2.80 (m, 2H), 2.72-7.58 (m, 4H), 2.16 (s, 3H), 1.65 (m, 3H)

^{13}C NMR (125 MHz, $CDCl_3$) δ: 207.4, 207.3, 128.3, 127.6, 127.3, 126.9, 126.6, 126.4, 125.6, 125.1, 42.5, 41.7, 35.8, 34.7, 33.7, 31.9, 30.3, 29.7, 18.0

Exact mass calcd. for $C_{10}H_{15}ClO$: 209.0704 $(M+Na)^+$; found: 209.0703 $(M+Na)^+$

2.9.10. Preparation of 3-[(*tert*-butyldimethylsilyl)oxy]-2-chloropropyl acetate (173)

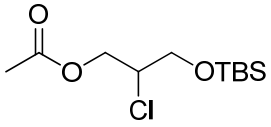

To a stirring solution of 3-[(*tert*-butyldimethylsilyl)oxy]-2-chloropropan-1-ol (**171**) (20 mg, 0.089 mmol) in anhydrous pyridine (0.3 mL) was added Ac_2O (0.3 mL) at room temperature. The resulting mixture was stirred at room temperature for 16 hours. After this time, the reaction mixture was partitioned between Et_2O (1 mL) and H_2O (1 mL). The layers were separated, and the organic layer was washed with 1 M HCl (0.5 mL), H_2O (0.5 mL), saturated $NaHCO_3$ solution (0.5 mL), and brine (0.5 mL). It was then dried with anhydrous $MgSO_4$ and concentrated *in vacuo* to afford ester **173** as a colourless oil (18 mg, 76%).

^{1}H NMR (500 MHz, $CDCl_3$) δ: 4.40 (dd, 1H, *J* = 4.4, 11.8 Hz), 4.25 (dd, 1H, *J* = 6.3, 11.8 Hz), 4.06 (m, 1H), 3.86-3.76 (m, 2H), 2.10 (s, 1H), 0.90 (s, 9H), 0.08 (s, 6H)

^{13}C NMR (125 MHz, $CDCl_3$) δ: 170.7, 64.8, 64.2, 58.2, 25.9, 20.9, 18.4, -5.3

Exact mass calcd. for $C_{11}H_{23}ClO_3Si$: 289.0997 $(M+Na)^+$; found: 289.1004 $(M+Na)^+$

2.9.11. Preparation of (2*S*,3*R*,8*Z*)-1-[(*tert*-butyldimethylsilyl)oxy]-2,8-dichloro-3-hydroxytrideca-8,11-dien-5-one (152)

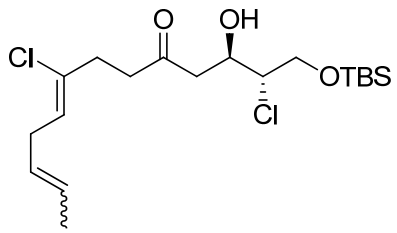

To a cold (-78°C), stirring solution of DIPA (0.25 mL, 1.80 mmol) in freshly distilled THF (15 mL) was slowly added *n*-BuLi (2.66 M in hexanes, 0.62 mL, 1.65 mmol). The resulting solution was stirred at -78°C for 30 minutes, then warmed to 0°C and stirred for an additional 15 minutes. After this time, the slightly yellow solution was again cooled to -78°C and (5*Z*)-5-chlorodeca-5,8-dien-2-one (**167**) (0.28 g, 1.50 mmol) was added in one portion. The reaction mixture was stirred for 30 minutes. A solution of (*S*)-3-[(tert-butyldimethylsilyl)oxy]-2-chloropropanal (**120**) (0.40 g, 1.80 mmol) in THF (2 mL) was then added drop-wise over 5 minutes at -78°C, and the resulting mixture was stirred for an additional 30 minutes. Saturated aqueous NH_4Cl (10 mL) was added to quench the reaction, and the mixture was diluted with EtOAc (20 mL). The phases were separated, and the aqueous phase was extracted with EtOAc (3 x 10 mL). The combined organic layers were washed with brine (15 mL), dried with anhydrous $MgSO_4$, and concentrated *in vacuo*. Purification of the crude mixture by flash chromatography (silica gel, 8:1 pentane:ethyl acetate) afforded chlorohydrin **152** as a yellow oil (0.32 g, 53%, 4:1 dr).

^{1}H NMR (500 MHz, $CDCl_3$) δ: 5.71 (m, 0.5H), 5.54-5.45 (m, 1.5H), 5.38 (m, 1H), 4.34 (m, 1H), 3.98-3.79 (m, 3H), 3.45 (d, 1H, *J* = 3.8 Hz), 2.92-2.60 (m, 8H), 1.65 (m, 3H), 0.90 (s, 9H), 0.10 (s, 6H)

^{13}C NMR (125 MHz, $CDCl_3$) δ: 209.3, 133.2, 127.6, 126.4, 125.3, 69.6, 65.2, 63.2, 46.0, 41.8, 33.4, 31.9, 25.9, 18.0, 14.4, -5.3

Exact mass calcd. for $C_{19}H_{34}Cl_2O_3Si$: 433.1703 $(M+Na+2H)^+$; found: 433.1696 $(M+Na+2H)^+$

2.9.12. Preparation of (*R*,4*Z*)-(2*S*,3*R*,8*Z*)-1-[(*tert*-butyldimethylsilyl)oxy]-2,8-dichloro-5-oxotrideca-8,11-dien-3-yl 3-[(*tert*-butyldimethylsilyl)oxy]-4-methyldeca-4,9-dienoate (174)

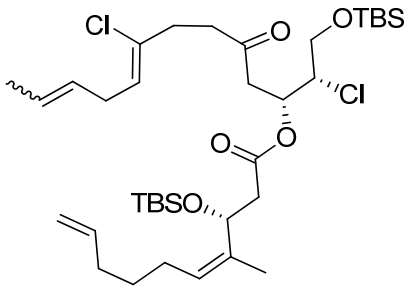

To a room-temperature solution of (2*S*,3*R*,8*Z*)-1-[(*tert*-butyldimethylsilyl)oxy]-2,8-dichloro-3-hydroxytrideca-8,11-dien-5-one (**152**) (90 mg, 0.22 mmol) in CH_2Cl_2 (1.3 mL) was added (*R*,*Z*)-3-[(*tert*-butyldimethylsilyl)oxy]-4-methyldeca-4,9-dienoic acid (**160**) (82 mg, 0.26 mmol), followed by DMAP (5 mg, 0.044 mmol). The mixture was stirred at room temperature until dissolution of DMAP, and then treated with DIC (51 µL, 0.33 mmol). The clear solution gradually turned cloudy, and was stirred at room temperature for 16 hours. After this time, the reaction mixture was partitioned between CH_2Cl_2 (1 mL) and saturated aqueous $NaHCO_3$ (1 mL), and the layers were separated. The aqueous layer was extracted with CH_2Cl_2 (1 mL), and the combined organic layers were washed with brine, dried with anhydrous $MgSO_4$, and concentrated in *vacuo*. Purification of the crude mixture by flash chromatography (silica gel, 15:1 hexanes:ethyl acetate) afforded ester **174** as a viscous colourless oil (110 mg, 71%).

^{1}H NMR (500 MHz, $CDCl_3$) δ: 5.81 (m, 1H), 5.70 (m, 0.5H), 5.59-5.36 (m, 3.5H), 5.14 (dt, 1H, *J* = 7.0, 7.4 Hz), 5.03-4.94 (m, 3H), 4.21 (m, 1H), 3.79 (m, 2H), 2.90-2.81 (m, 4H), 2.69-2.59 (m, 5H), 2.35 (dd, 0.5H, *J* = 5.5, 15.0 Hz), 2.29 (dd, 0.5H, *J* = 5.5, 15.0 Hz), 2.12-2.01 (m, 4H), 1.67-1.63 (m, 6H), 1.43 (m, 2H), 0.89 (s, 9H), 0.85 (s, 9H), 0.08-0.01 (m, 12H)

^{13}C NMR (125 MHz, $CDCl_3$) δ: 205.1, 170.2, 138.8, 136.4, 128.2, 126.9, 126.8, 114.7, 70.0, 67.1, 64.5, 62.5, 43.3, 41.7, 41.6, 35.5, 34.7, 33.6, 31.9, 29.3, 27.1, 25.9, 18.4, 18.2, 18.0, 17.6, -4.8, -4.9, -5.3, -5.4

Exact mass calcd. for $C_{36}H_{64}Cl_2O_5Si_2$: 725.3562 $(M+Na)^+$; found: 725.3591 $(M+Na)^+$

2.9.13. Preparation of (*Z*)-5-chloro-8-(2,2-dimethyl-1,3-dioxan-5-ylidene)oct-5-en-2-one (185)

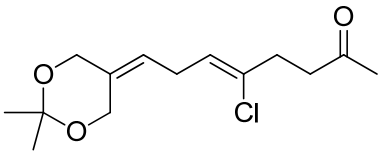

To a glass vial containing a solution of (5*Z*)-5-chlorodeca-5,8-dien-2-one (**167**) (10 mg, 0.054 mmol) in freshly distilled CH_2Cl_2 (1.1 mL) was added 2,2-dimethyl-5-methylene-1,3-dioxane (**184**) (34 mg, 0.27 mmol), followed by Grubbs 2nd Generation catalyst (4.5 mg, 0.005 mmol). The mixture was gently bubbled with N_2 for 2 minutes at room temperature, and the glass vial was sealed. The reaction mixture was then stirred at reflux (~40°C) for 2 hours. After this time, the yellow-brown solution was concentrated *in vacuo*, and the resulting crude mixture was purified by flash chromatography (silica gel, 5:1 hexanes/ethyl acetate) to afford acetonide **185** as a light yellow liquid (5.5 mg, 38%).

^{1}H NMR (500 MHz, $CDCl_3$) δ: 5.47 (t, 1H, *J* = 7.0 Hz), 5.20 (m, 1H), 4.42 (s, 2H), 4.22 (s, 2H), 2.84-2.56 (m, 6H), 2.16 (s, 3H), 1.42 (s, 6H)

^{13}C NMR (125 MHz, $CDCl_3$) δ: 207.2, 126.8, 124.5, 124.0, 119.6, 67.4, 64.5, 60.1, 41.5, 33.6, 30.3, 29.9, 24.2

Exact mass calcd. for $C_{14}H_{21}ClO_3$: 273.1252 $(M+H)^+$; found: 273.1257 $(M+H)^+$

2.9.14. Preparation of (2*R*,3*R*,5*R*)-2-[((*tert*-butyldimethylsilyl)oxy)methyl]-5-((*Z*)-3-chlorohepta-3,6-dien-1-yl)tetrahydrofuran-3-yl acetate (189)

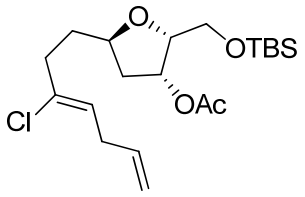

To a stirring solution of (2*R*,3*R*,5*R*)-2-[((*tert*-butyldimethylsilyl)oxy)methyl]-5-((*Z*)-3-chlorohepta-3,6-dien-1-yl)tetrahydrofuran-3-ol (**125**)[32] (25 mg, 0.069 mmol) in anhydrous pyridine (0.14 mL) was added Ac_2O (13 µL, 0.139 mmol) at room temperature. The

resulting mixture was stirred at room temperature for 16 hours. After this time, the reaction mixture was partitioned between Et_2O (1 mL) and H_2O (1 mL). The layers were separated, and the organic layer was washed with 1 M HCl (0.5 mL), H_2O (0.5 mL), saturated $NaHCO_3$ solution (0.5 mL), and brine (0.5 mL). It was then dried with anhydrous $MgSO_4$ and concentrated *in vacuo* to afford acetate **189** as a viscous colourless oil (26 mg, 93%).

^{1}H NMR (500 MHz, $CDCl_3$) δ: 5.79 (m, 1H), 5.53 (t, 1H, *J* = 7.2 Hz), 5.40 (t, 1H, *J* = 4.0 Hz), 5.03 (m, 2H), 4.14 (m, 1H), 4.05 (m, 1H), 3.91-3.71 (m, 2H), 2.92 (t, 1H, *J* = 6.6 Hz), 2.62-2.34 (m, 3H), 2.12 (dd, 1H, *J* = 6.1, 14.1 Hz), 2.06 (s, 3H), 1.88-1.74 (m, 3H), 0.87 (s, 9H), 0.05 (s, 3H), 0.04 (s, 3H)

^{13}C NMR (125 MHz, $CDCl_3$) δ: 170.7, 135.7, 126.7, 123.5, 115.9, 81.1, 77.2, 74.9, 61.6, 39.6, 36.7, 34.4, 33.3, 26.3, 21.6, 18.7, -4.8, -5.0

Exact mass calcd. for $C_{20}H_{35}ClO_4Si$: 403.2066 $(M+H)^+$; found: 403.2045 $(M+H)^+$

2.9.15. Preparation of acetonide 190

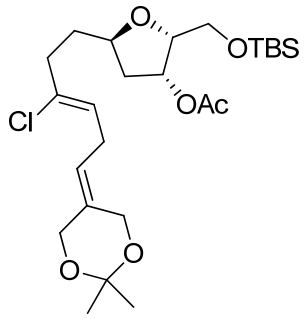

To a glass vial containing a solution of (2*R*,3*R*,5*R*)-2-(((*tert*-butyldimethylsilyl)oxy)methyl)-5-((*Z*)-3-chlorohepta-3,6-dien-1-yl)tetrahydrofuran-3-yl acetate (**189**) (8.5 mg, 0.021 mmol) in toluene (0.42 mL) was added 2,2-dimethyl-5-methylene-1,3-dioxane (**184**) (13 mg, 0.105 mmol), followed by Hoveyda-Grubbs 2nd Generation catalyst (1.3 mg, 0.002 mmol). The mixture was gently bubbled with N_2 for 2 minutes at room temperature, and the glass vial was sealed. The reaction mixture was then heated to 60°C and stirred for 16 hours. After this time, the brown solution was concentrated *in vacuo*, and the resulting crude mixture was purified by flash

chromatography (silica gel, 15:1 hexanes/ethyl acetate) to afford acetonide **190** as a viscous colourless oil (6.3 mg, 59%).

^{1}H NMR (500 MHz, $CDCl_3$) δ: 5.44 (t, 1H, *J* = 7 Hz), 5.43 (t, 1H, *J* = 3.7 Hz), 5.23 (t, 1H, *J* = 7.7 Hz), 4.43 (s, 2H), 4.23 (s, 2H), 4.18-4.02 (m, 3H), 3.92-3.77 (m, 1H), 2.83 (t, 2H, *J* = 7.1 Hz), 2.60-2.30 (m, 4H), 2.12 (dd, 1H, *J* = 6.1, 13.7 Hz), 2.06 (s, 3H), 1.88-1.72 (m, 3H), 1.43 (s, 6H), 0.87 (s, 9H), 0.05 (s, 3H), 0.04 (s, 3H)

Exact mass calcd. for $C_{25}H_{43}ClO_6Si$: 503.2596 $(M+H)^+$; found: 503.2589 $(M+H)^+$

2.9.16. Preparation of diol 191

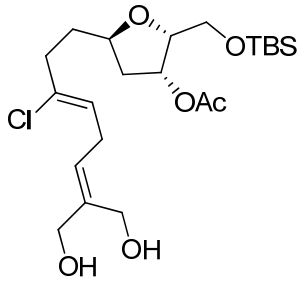

To a glass vial containing a solution of acetonide **190** (6 mg, 0.012 mmol) in a 1:1 mixture of THF and water (0.24 mL) was added PPTS (<1 mg). The reaction mixture was stirred for 16 hours at room temperature. After this time, the mixture was concentrated *in vacuo*, and then re-partitioned between EtOAc (1 mL) and saturated aqueous $NaHCO_3$ (1 mL). The layers were separated, and the aqueous layer was extracted with EtOAc (2 x 0.5 mL). The combined organic layers were washed with H_2O (0.5 mL), brine (0.5 mL), dried with anhydrous $MgSO_4$, and concentrated *in vacuo*. Purification of the crude mixture by flash chromatography (silica gel, 1:3 hexanes:ethyl acetate) afforded diol **191** as a viscous colourless oil (5.2 mg, 0.011 mmol).

^{1}H NMR (500 MHz, $CDCl_3$) δ: 5.53 (t, 1H, *J* = 7.7 Hz), 5.48 (t, 1H, *J* = 7.3 Hz), 5.39 (m, 1H), 4.36 (s, 2H), 4.23 (s, 2H), 4.17-4.01 (m, 2H), 3.91-3.74 (m, 2H), 2.97 (t, 2H, *J* = 7.3 Hz), 2.52-2.31 (m, 2H), 2.12 (dd, 1H, *J* = 6.0, 13.9 Hz), 2.06 (s, 3H), 1.88-1.74 (m, 2H), 0.88 (s, 9H), 0.05 (s, 3H), 0.04 (s, 3H)

^{13}C NMR (125 MHz, $CDCl_3$) δ: 170.9, 138.9, 135.8, 127.4, 123.7, 81.1, 75.1, 67.9, 61.6, 60.6, 39.6, 36.6, 34.3, 30.2, 27.6, 26.3, 21.6, 18.5, -4.9, -5.0

Exact mass calcd. for $C_{22}H_{39}ClO_6Si$: 463.2277 $(M+H)^+$; found: 463.2255 $(M+H)^+$

2.9.17. Preparation of diacetate 192

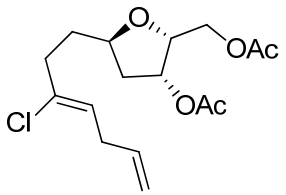

To a stirring solution of (2*R*,3*R*,5*R*)-5-((*Z*)-3-chlorohepta-3,6-dien-1-yl)-2-(hydroxymethyl)tetrahydrofuran-3-ol (**124**)[32] (63 mg, 0.255 mmol) in anhydrous pyridine (0.5 mL) was added Ac_2O (73 µL, 0.766 mmol) at room temperature. The resulting mixture was stirred at room temperature for 16 hours. After this time, the reaction mixture was partitioned between Et_2O (1 mL) and H_2O (1 mL). The layers were separated, and the organic layer was washed with 1 M HCl (0.5 mL), H_2O (0.5 mL), saturated aqueous $NaHCO_3$ (0.5 mL), and brine (0.5 mL). It was then dried with anhydrous $MgSO_4$ and concentrated *in vacuo*. Purification of the crude mixture by flash chromatography (silica gel, 5:1 hexanes:ethyl acetate) afforded diacetate **192** as a viscous colourless oil (72 mg, 85%).

^{1}H NMR (500 MHz, $CDCl_3$) δ: 5.79 (m, 1H), 5.54 (t, 1H, *J* = 6.9 Hz), 5.43 (t, 1H, *J* = 4.4 Hz), 5.03 (m, 2H), 4.31-4.00 (m, 4H), 2.92 (t, 2H, *J* = 6.4 Hz), 2.52-2.36 (m, 2H), 2.15-2.06 (m, 4H), 1.89-1.75 (m, 3H)

^{13}C NMR (125 MHz, $CDCl_3$) δ: 171.3, 170.7, 135.8, 126.9, 123.7, 115.9, 78.2, 77.4, 75.1, 63.2, 39.6, 36.6, 34.0, 33.3, 21.5, 21.4

Exact mass calcd. for $C_{16}H_{23}ClO_5$: 353.1126 $(M+Na)^+$; found: 353.1111 $(M+Na)^+$

2.9.18. Preparation of acetonide 193

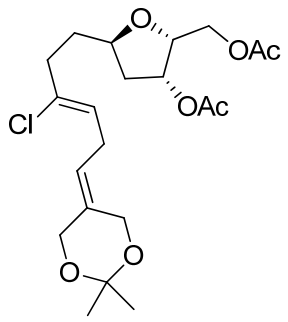

To a solution of diacetate **192** (70 mg, 0.212 mmol) in toluene (4.25 mL) was added 2,2-dimethyl-5-methylene-1,3-dioxane (**184**) (107 mg, 0.846 mmol), followed by Hoveyda-Grubbs 2nd Generation catalyst (13 mg, 0.021 mmol). Through the mixture was gently bubbled N_2 for 2 minutes at room temperature, and then the mixture was heated to 60°C and stirred at this temperature for 16 hours. After this time, the brown solution was concentrated *in vacuo*, and the resulting crude mixture was purified by flash chromatography (silica gel, 5:1 hexanes/ethyl acetate) to afford acetonide **193** as a viscous colourless oil (36 mg, 39%).

^{1}H NMR (500 MHz, $CDCl_3$) δ: 5.48-5.40 (m, 2H), 5.21 (m, 1H), 4.43 (s, 2H), 4.23 (s, 2H), 4.29-4.11 (m, 4H), 2.84 (t, 2H, *J* = 7.0 Hz), 2.51-2.31 (m, 2H), 2.16-2.05 (m, 7H), 1.92-1.75 (m, 3H), 1.43 (s, 6H)

^{13}C NMR (125 MHz, $CDCl_3$) δ: 171.4, 170.8, 139.0, 135.3, 127.2, 123.9, 82.4, 78.2, 77.4, 75.1, 67.7, 63.2, 60.4, 39.6, 36.4, 33.7, 31.4, 27.6, 21.5, 21.4

Exact mass calcd. for $C_{21}H_{31}ClO_7$: 431.1837 $(M+H)^+$; found: 431.1831 $(M+H)^+$

2.9.19. Preparation of diol 194

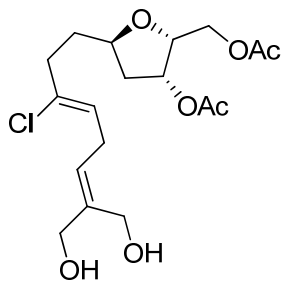

To a solution of acetonide **193** (33 mg, 0.077 mmol) in a 1:1 mixture of THF and water (1.5 mL) was added PPTS (2 mg, 0.008 mmol). The reaction mixture was stirred for 16 hours at room temperature. After this time, the mixture was concentrated *in vacuo*, and then re-partitioned between EtOAc (3 mL) and saturated aqueous $NaHCO_3$ (3 mL). The layers were separated, and the aqueous layer was extracted with EtOAc (2 x 2 mL). The combined organic layers were washed with H_2O (1 mL), brine (1 mL), dried with anhydrous $MgSO_4$, and concentrated *in vacuo*. The desired diol **194** was obtained without further purification, as a viscous colourless oil (29 mg, 97%).

^{1}H NMR (500 MHz, $CDCl_3$) δ: 5.51 (m, 2H), 5.42 (m, 1H), 4.36 (s, 2H), 4.23 (s, 2H), 4.28-4.16 (m, 4H), 2.97 (t, 2H, *J* = 7.7 Hz), 2.53-2.33 (m, 2H), 2.15-2.07 (m, 7H), 1.91-1.76 (m, 3H)

^{13}C NMR (125 MHz, $CDCl_3$) δ: 171.4, 170.8, 138.9, 135.3, 127.2, 123.8, 78.2, 77.4, 75.1, 67.8, 63.3, 60.5, 39.6, 36.5, 33.8, 27.6, 21.5, 21.4

Exact mass calcd. for $C_{18}H_{27}ClO_7$: 413.1338 $(M+Na)^+$; found: 413.1311 $(M+Na)^+$

2.9.20. Preparation of (*E*)-allyl silyl ether 195b

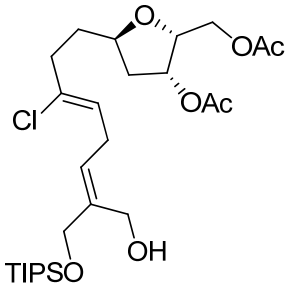

To a solution of diol **194** (25 mg, 0.064 mmol) in freshly distilled CH_2Cl_2 (0.26 mL) was added DMAP (<1 mg) and Et_3N (9 µL, 0.064 mmol). The mixture was cooled to 0°C, and TIPSCl (14 µL, 0.064 mmol) was added. The reaction mixture was stirred for 16 hours, while gradually warming to room temperature. After this time, the mixture was concentrated *in vacuo*, and then Et_2O was added to the crude mixture. The resulting precipitate was filtered off, and the filtrate was concentrated *in vacuo*. Purification of the resulting crude mixture by flash chromatography (2:1, hexanes:ethyl acetate) afforded TIPS ether **195b** as a viscous colourless oil (7.3 mg, 21%).

^{1}H NMR (500 MHz, $CDCl_3$) δ: 5.48 (t, 2H, *J* = 7.2 Hz), 5.43 (m, 1H), 4.32 (s, 2H), 4.29 (s, 2H), 4.27-4.02 (m, 4H), 2.98 (t, 2H, *J* = 7.2 Hz), 2.52-2.31 (m, 2H), 2.15-2.06 (m, 7H), 1.91-1.75 (m, 3H), 1.18-1.03 (m, 21H)

^{13}C NMR (125 MHz, $CDCl_3$) δ: 170.7, 167.1, 138.7, 135.3, 125.7, 124.0, 78.3, 77.4, 75.1, 68.7, 63.2, 60.5, 39.6, 36.5, 34.1, 27.5, 21.5, 21.4, 18.5, 12.3

Exact mass calcd. for $C_{27}H_{47}ClO_7Si$: 547.2852 $(M+H)^+$; found: 547.2874 $(M+H)^+$

2.9.21. Preparation of triacetate 197

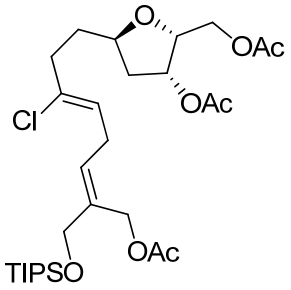

To a vial containing a solution of TIPS ether **195b** (4 mg, 0.007 mmol) in anhydrous pyridine (30 μL) was added Ac_2O (4 μL, 0.046 mmol) at room temperature. The resulting mixture was stirred at room temperature for 16 hours. After this time, the reaction mixture was partitioned between Et_2O (1 mL) and H_2O (0.5 mL). The layers were separated, and the organic layer was washed with 1 M HCl (0.2 mL), H_2O (0.2 mL), saturated aqueous $NaHCO_3$ (0.2 mL), and brine (0.2 mL). It was then dried with anhydrous $MgSO_4$ and concentrated *in vacuo* to afforded triacetate **197** as a viscous colourless oil (3.5 mg, 87%).

^{1}H NMR (500 MHz, $CDCl_3$) δ: 5.70 (t, 1H, *J* = 7.3 Hz), 5.48 (t, 1H, *J* = 6.9 Hz), 5.43 (m, 1H), 4.66 (s, 2H), 4.22 (s, 2H), 4.27-4.08 (m, 4H), 3.02 (t, 2H, *J* = 6.9 Hz), 2.51-2.43 (m, 1H), 2.40-2.32 (m, 1H), 2.12 (dd, 1H, *J* = 5.8, 13.8 Hz), 2.07 (s, 6H), 2.04 (s, 3H), 1.89-1.74 (m, 3H), 1.17-1.03 (m, 21H)

^{13}C NMR (125 MHz, $CDCl_3$) δ: 171.5, 171.3, 170.7, 135.3, 135.0, 127.6, 123.9, 78.3, 77.6, 75.0, 65.7, 63.2, 60.3, 39.5, 36.5, 34.1, 27.7, 21.5, 21.4, 21.4, 18.5, 12.5

Exact mass calcd. for $C_{29}H_{49}ClO_8Si$: 589.2958 $(M+H)^+$; found: 589.2951 $(M+H)^+$

3. Radical Fluorination of Aliphatic Compounds

3.1. Introduction

The strategic incorporation of a fluorine atom into an advanced drug candidate is common practice in medicinal chemistry.[14,88] Oftentimes, a single hydrogen-to-fluorine substitution improves drug-like properties by blocking undesired metabolism at a specific site in a drug lead, increasing lipophilicity or binding affinity, or altering drug absorption, distribution or excretion. In addition to the medicinal advantages often presented by fluorination, valuable pharmacokinetic information can be gleaned from non-invasive positron emission tomography (PET) imaging of ^{18}F labeled drugs in vivo.[89] The critical role fluorine plays in the drug discovery process is highlighted by the fact that one third of the so-called 'blockbuster drugs' are fluorinated in at least one position.[15]

Since Fried's observation that fluorination of cortisone leads to a more active drug[90] harbingered the era of fluoropharmaceuticals, advances in this field have necessarily relied on the discovery of mild fluorination reagents that can be handled safely and obviate the need for fluorine gas or its surrogates.[14,91] Presently, common fluorination methods involve displacement reactions by fluoride or addition of electrophilic fluorine to alkenes[91,92] or organometallics.[93,94] However, there is particular contemporary interest in the development of reactions that effect the direct fluorination of C-H bonds. In this regard, success has been realized in allylic[95] and benzylic[96] fluorination. However, the identification of reagent systems that effect selective fluorination of so called unactivated C(sp^3)-H bonds, or those that are not adjacent to sp^2 hybridized carbons or other functional groups that facilitate the formation of radicals or anions, remains a significant challenge.

Recently, Groves and coworkers disclosed a protocol fluorination of unactivated C(sp^3)-H bonds through a radical process that relies on a manganese porphyrin catalyst working in concert with an oxidant (iodosylbenzene), AgF, and a catalytic amount of

tetrabutylammonium fluoride (TBAF) (Scheme 3.1, **213** → **214**).[97] Lectka[98] and Inoue[99] have also demonstrated that *N*-oxyl radicals are capable of catalyzing the fluorination of C(sp^3)-H bonds in unfunctionalized cycloalkanes (e.g., cyclohexane, cyclooctane) using Selectfluor™ as the fluorine transfer reagent (Scheme 3.1, **216** → **217**). An earlier report by Sandford and Chambers also described a catalyst-free electrophilic fluorination reaction of saturated hydrocarbons using Selectfluor™ in refluxing MeCN.[100]

Scheme 3.1 Fluorination of unactivated C-H bonds using silver(I) fluoride or Selectfluor™ as the fluorine atom source

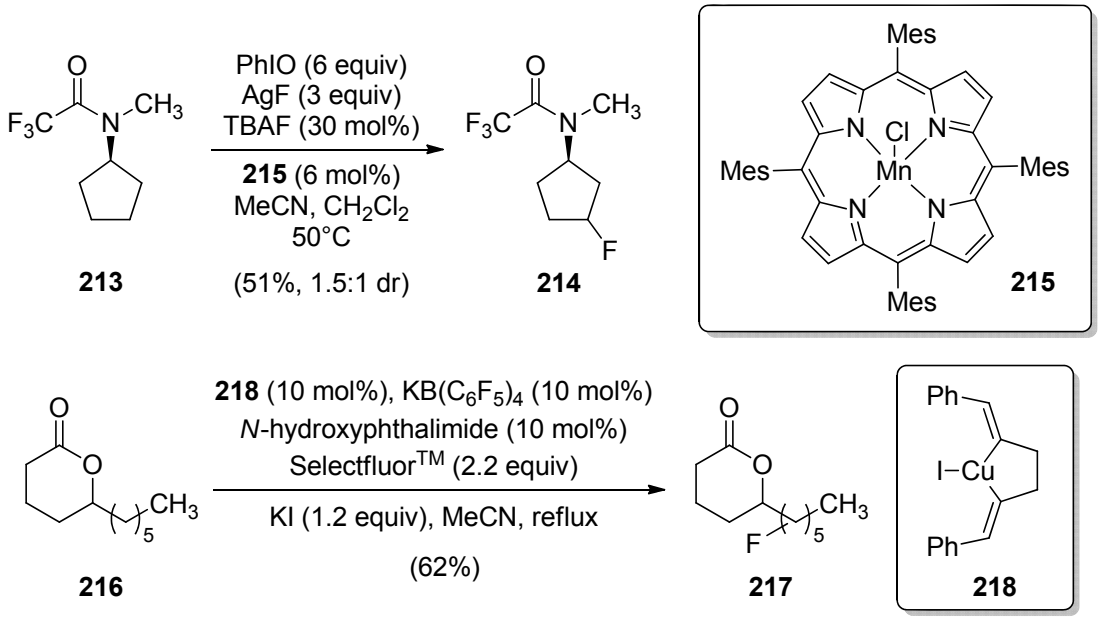

For the reasons discussed above, we have been interested in developing a simple protocol for the direct fluorination of unactivated C(sp^3)-H bonds and were particularly intrigued by a process that would involve the generation and trapping of alkyl radicals with fluorine transfer reagents. In this regard, Sammis has calculated[101] the homolytic N-F bond dissociation energy (BDE) for several electrophilic fluorinating reagents including *N*-fluorobenzenesulfonimide (NFSI) (BDE_{NF} = 63 kcal mol^{-1}) and demonstrated the utility of NFSI in fluorine transfer to alkyl radicals generated via decarboxylative processes.[102] Considering that [^{18}F]-NFSI (**220**) can be readily prepared from the reaction of [^{18}F]F_2 and $NaN(SO_2Ph)_2$ (**219**) (Scheme 3.2),[103] the development of an NFSI-based fluorination of unactivated C(sp^3)-H bonds could also serve as a platform

technology for the production of new radiotracers for PET imaging. Bearing this in mind, we conceptualized a reaction that combines the well-known hydrogen abstraction ability of the polyoxometalate decatungstate[104] with a fluorine transfer reagent such as NFSI to directly transform unactivated C(sp^3)-H bonds into C-F bonds. Considering both the steric bulk and redox potential of decatungstate catalysts,[105] this process may mimic *in vivo* oxidative metabolism by selecting for C(sp^3)-H bonds prone to metabolic degradation and replacing them with C-F bonds; a potentially transformative reaction for lead optimization in medicinal chemistry.

Scheme 3.2 Synthesis of [^{18}F]-NFSI

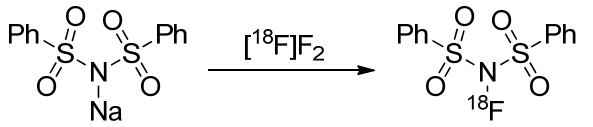

219 [^{18}F]-NFSI (**220**)

3.2. Results and Discussion

A variety of polyoxometalates have proven effective as photocatalysts in oxidative transformations.[106] For example, the decatungstate anion $W_{10}O_{32}^{4-}$ has been studied extensively for these purposes.[107,108] The tetrabutylammonium salt of decatungstate (TBADT (**224**)) is a well-characterized polyoxometalate catalyst that is particularly efficient at abstracting hydrogen atoms from saturated hydrocarbons.[107] For example, applications for TBADT catalysis include formation of carbon-carbon bonds[109] and oxidation of alcohols.[110] From a practical perspective, TBADT is readily prepared in one step from sodium tungstate[107] (<$50 USD kg^{-1}) and can be photoexcited with wavelengths of light that do not interact with common organic reagents (e.g., 350-400 nm). Photocatalysis with TBADT also involves mild reaction conditions (e.g. room temperature, non-distilled solvents) and is functional group tolerant. Herein we report the discovery of an operationally simple and economical photocatalytic system for the direct fluorination of unactivated C(sp^3)-H bonds that exploits the hydrogen abstraction ability of TBADT and fluorine transfer capacity of NFSI.

Table 3.1 Demonstration and optimization of the fluorination of bornyl acetate

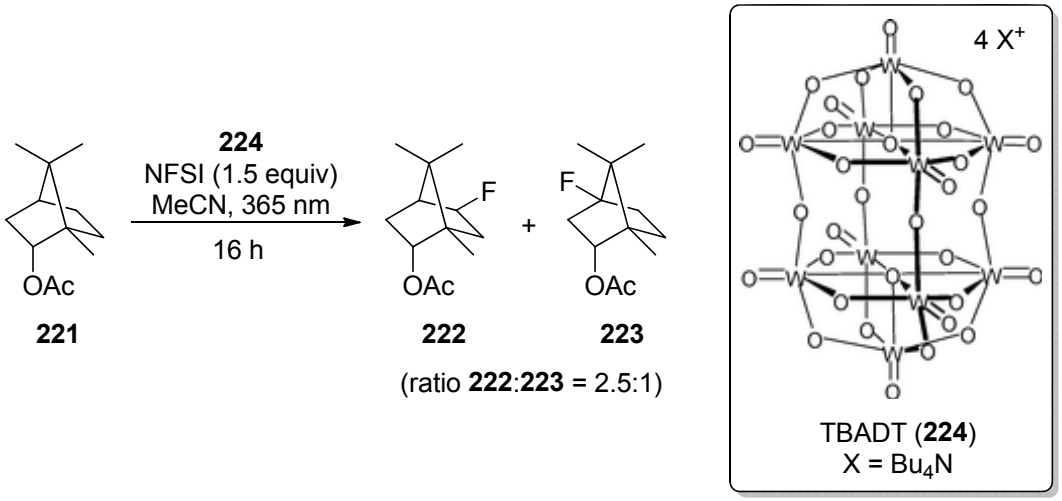

entry	TBADT (mol %)	conc. (M)	additive (0.1 equiv)	yield[a] (%)
1	2	0.2	-	32
2	1	0.2	-	12
3	0	0.2	-	0
4	5	0.2	-	20
5	2	1.0	-	43
6	2	2.0	-	46
7	2	2.0	Na_2CO_3	52
8	2	2.0	$NaHCO_3$	56 (70%)[b]

[a] combined isolated yield of 222 and 223; [b] conversion in parentheses

As depicted in Table 3.1, we initially investigated combinations of TBADT and NFSI in acetonitrile for the fluorination of bornyl acetate (**221**), which contains 16 unactivated C(sp^3)-H bonds. Photoexcitation was achieved by irradiating the reaction mixture with two 15-watt black light bulbs (centered at 365 nm). We were delighted to find that using 2 mol % of TBADT and a small excess of NFSI, bornyl acetate could in fact be converted into the fluoroacetates **222** and **223** in modest yield (32%). Increasing

the reaction time (up to 60 hours) had little effect on this result, while reduction in catalyst loading significantly impacted the yield of **222** and **223** (entries 3 and 4), and no product was observed in the absence of TBADT or light. We next examined the effect of reaction concentration and found that fluorination proceeded optimally at high concentration of bornyl acetate (e.g., 2 M, entry 4). Finally, as acetamide side products derived from acetonitrile displacement of fluoride were also observed, various inorganic bases (e.g., Na_2CO_3, $NaHCO_3$, K_2CO_3, $KHCO_3$, Li_2CO_3) were added in an effort to consume the small amounts of coincident hydrofluoric acid deemed deleterious to the desired process. Optimally, the addition of a catalytic amount of base (<20 mol%) substantially increased conversion, and when 10 mol% of $NaHCO_3$ was employed (entry 7), the fluoroacetates **222** and **223** were produced in a combined yield of 56% (~80% yield considering 30% of the starting material was also recovered).

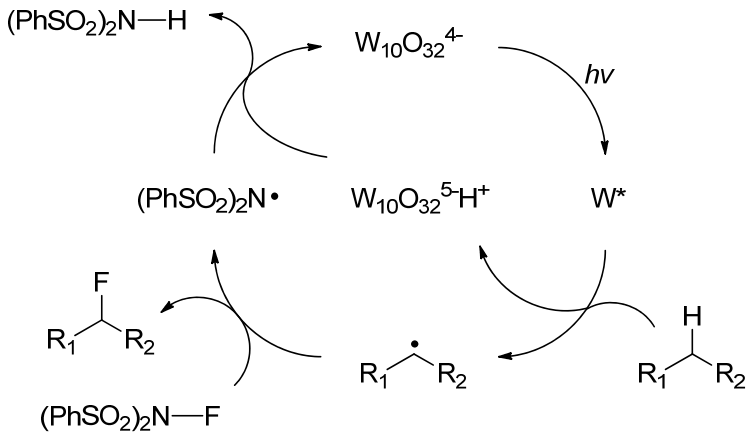

Figure 3.1 Proposed catalytic cycle for the TBADT/NFSI fluorination of unactivated C(sp^3)-H bonds

While a full mechanistic understanding of this reaction will require further experimentation, we suggest the mechanism depicted in Figure 3.1, which is consistent with both the photocatalytic reactivity of TBADT and fluorine transfer capacity of NFSI. Thus, photoexcitation of the decatungstate anion ($W_{10}O_{32}^{4-}$) produces a short-lived excited state (picoseconds) that rapidly decays to a reactive intermediate (denoted W*) capable of hydrogen atom abstraction.[111,112] Fluorine atom transfer from NFSI to the resulting carbon radical (or a single electron transfer from the radical species to NFSI to generate a carbocation, followed by fluoride transfer[101]) provides the fluorinated product. Acquisition of a hydrogen atom by the sulfonamide radical from the catalyst would then

regenerate the decatungstate anion ($W_{10}O_{32}^{4-}$). This proposal is further supported by the fact that reaction of bornyl acetate (Table 3.1, entry 7) in the presence of the radical scavenger TEMPO provided none of the fluorinated products **222** or **223**. Bearing in mind the size and electron density of the catalyst, the selectivity observed in the C-H fluorination of bornyl acetate is consistent with the avoidance of sterically congested C-H bonds and destabilizing electrostatic interactions.

Having demonstrated the direct C(sp^3)-H fluorination of bornyl acetate using a photocatalytic TBADT/NFSI system, without further optimization we explored the scope of this reaction through the fluorination of several small organic molecules, all of which possess multiple unactivated C(sp^3)-H bonds (Table 3.2). In general, the TBADT/NFSI fluorination reaction is functional group tolerant, and aliphatic ketones, esters, and lactones were all fluorinated to varying degrees. In line with observations summarized above, examination of the products depicted in Table 3.2 highlights the selectivity of this reaction for fluorination at sterically accessible branched methines or methylenes that are also remote from electron withdrawing groups. The influence of carbonyl groups on the efficiency of this reaction is further demonstrated when the fluorination of camphor (example 2), the corresponding lactone (example 3), and bornyl acetate **221** (Table 3.1) are compared. In all cases, fluorination occurs at positions most remote from the carbonyl function and the relative inefficiency of formation of the fluorocamphors **228** and **229**, and the lactone **230** correlates with their decreased electron density relative to bornyl acetate. Additionally, no difluoro compounds were detected in any of these reactions. These electronic gearing factors are also evidenced in the monofluorination of menthol acetate (example 3), which occurs equally at the most sterically accessible methine and the methylene most remote from the acetoxy group.

Table 3.2 Fluorination of aliphatic substrates

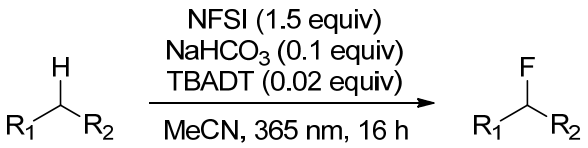

example	major product(s)	combined yield
1	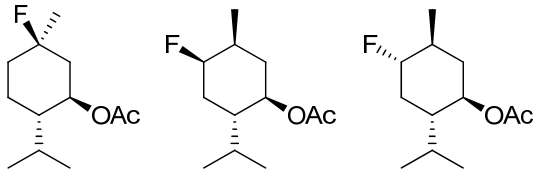 **225** (14%) **226** (10%) **227** (4%)	28%
2	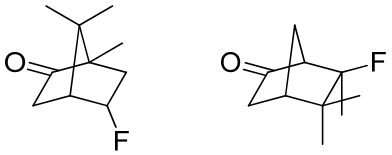 **228** (17%, β:α 2:1) **229** (14%)	31%
3	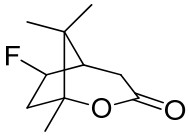 **230** (14%)	14%
4	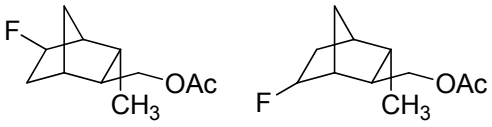 **231** (20%) **232** (20%)	40%
5	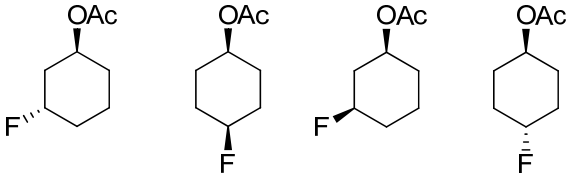 **233** (25%) **234** (11%) **235** (7%) **236** (7%)	49%

Note: in each case, a large quantity of unreacted starting material was recovered

As well, in order to compare the present catalyst system with that reported by Groves,[97] the fluorination of sclareolide (**237**) was also investigated. As depicted in Scheme 3.3, these unique catalyst/reagent systems are similar in producing (2*S*)-2-fluorosclareolide (**238**) as the major product.

Scheme 3.3 Fluorination of sclareolide

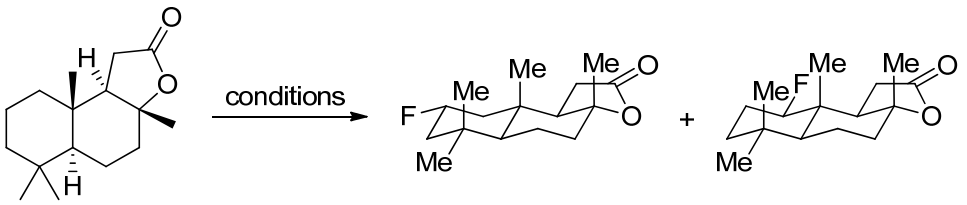

237 **238** (58%, α/β = 4:1) **239** (10%)

3.3. Conclusion & Future Direction

In conclusion, here we presented a novel methodology for the radical fluorination of unactivated C(sp^3)-H bonds using TBADT/NFSI. A number of small molecule aliphatic compounds were successfully fluorinated, with fluorination occurring at the most sterically and electronically favourable positions, as expected. In the meantime, related work by Shira (Halperin) Bogner in our group has been examining several other applications of our TBADT/NFSI fluorination methodology. For example, considering the relatively low BDE for acylhydrides (CO-H BDE ~ 89 kcal mol^{-1}),[113] the direct conversion of aldehydes into acylfluorides, which are a relatively stable but underutilized class of acyl halide, was explored (Scheme 3.4). Employing the optimized reaction conditions, benzaldehyde (**240**) was rapidly converted into benzoylfluoride (**241**), which was characterized by ^{1}H and ^{19}F NMR spectroscopy and transformed directly into *N*-benzylbenzamide (**242**) on reaction with benzylamine. This facile conversion of an aldehyde directly into an acyl fluoride is a rare example of this potentially useful reaction, which has previously been limited to the use of strongly electrophilic fluorinating reagents (e.g., BrF_3,[114] $CsSO_4F$[115]). Further investigations into this methodology will look to expand its utility towards potential fluoropharmaceuticals and amino acids.

Scheme 3.4 Direct conversion of benzaldehyde to N-benzylbenzamide via fluorination and acyl substitution

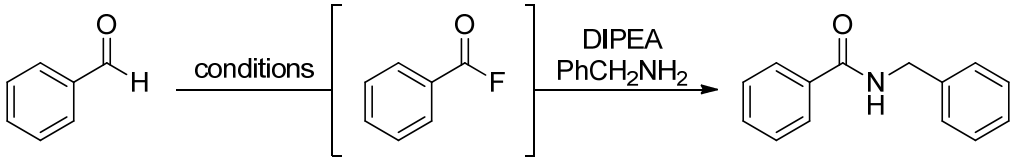

240 **241** **242**

3.4. Experimental

All reactions described were performed under an atmosphere of dry argon or nitrogen using oven dried glassware unless otherwise specified. Tetrahydrofuran was distilled over Na/benzophenone and dichloromethane was dried by distillation over CaH_2. All other solvents were used directly from EMD drysolv septum sealed bottles unless otherwise specified. Flash chromatography was carried out with 230-400 mesh silica gel (E. Merck, Silica Gel 60). Thin layer chromatography was carried out on commercial aluminium backed silica gel 60 plates (E. Merck, type 5554, thickness 0.2 mm). Concentration and removal of trace solvents was performed on a Büchi rotary evaporator using dry ice/acetone condenser and vacuum from water or air aspirator.

All reagents and starting materials were purchased from Sigma Aldrich, Alfa Aesar, and/or TCI America and were used without further purification. All solvents were purchased from Sigma Aldrich, EMD, Anachemia or Caledon and used without further purification.

Nuclear magnetic resonance (NMR) spectra were recorded using deuterochloroform ($CDCl_3$) as the solvent. Signal positions (δ) are given in parts per million from tetramethylsilane (δ 0) or trichlorofluoromethane (δ 0, for ^{19}F NMR) and were measured relative to the signal of the solvent (δ 7.26, ^{1}H NMR; δ 77.00, ^{13}C NMR). Coupling constants (*J* values) are given in Hertz (Hz) and are reported to the nearest 0.1 Hz. ^{1}H NMR spectral data are tabulated in the order: multiplicity (s, singlet; d, doublet; t, triplet; m, multiplet), number of protons, coupling constants, assignment (where possible). NMR spectra were recorded on a Bruker Avance 600 equipped with a QNP or TCI cryoprobe (600 MHz), Bruker 500 (500 MHz), or Bruker 400 (400 MHz). Assignments of ^{1}H, ^{13}C, and ^{19}F NMR spectra are based on analysis of ^{1}H-^{1}H COSY, HSQC, ^{13}C-^{19}F HSQC, HMBC, TOCSY and 1D NOESY spectra.

High resolution mass spectra were performed on an Agilent 6210 TOF LC/MS or Bruker micrOTOF-II LC mass spectrometer.

Diastereomeric ratios were determined by analysis of ^{1}H NMR spectra recorded on crude reaction products.

3.4.1. General Procedure for the Fluorination of Aliphatic Substrates

A 2 mL glass vial equipped with a magnetic stir bar was charged with the aliphatic substrate (0.300 mmol) in acetonitrile (0.15 mL). $NaHCO_3$ solid (2.5 mg, 0.030 mmol), TBADT (20 mg, 0.006 mmol), and NFSI (142 mg, 0.450 mmol) were then added. This resulting suspension was purged for 5 minutes by bubbling with N_2 through a 3.5'' septic needle. The vial was then quickly capped and sealed, and was allowed to stir under UV irradiation at room temperature for 16 hours. The resulting dark blue mixture was quenched with 1 mL of saturated $NaHCO_3$ solution, and extracted with CH_2Cl_2. The organic layer was dried with anhydrous $MgSO_4$ and concentrated in *vacuo* to give the crude product mixture, which was further purified by flash chromatography as indicated below.

3.4.2. Fluorination of (-)-bornyl acetate (221)

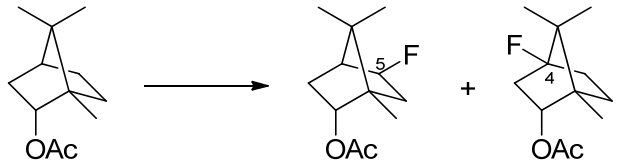

The reaction was performed according to the general procedure above using (-)-bornyl acetate (**221**) as substrate. Purification by flash chromatography (4% EtOAc/pentane) afforded the fluorination products in a combined yield of 56%. The major 5-*exo*-fluoro isomer was obtained as a colourless oil (26 mg, 40%). Experimental data matches previously reported literature values for the same compound.[97]

5-*exo*-fluoro-(-)-bornyl acetate:

^{1}H NMR (500 MHz, $CDCl_3$) δ: 4.79 (d, 1H, *J* = 9.7 Hz), 4.63 (ddd, 1H, *J* = 60.0, 7.6, 2.3 Hz), 2.40 (m, 2H), 2.06-1.99 (m, 1H), 2.04 (s, 3H), 1.69 (dd, 1H, *J* = 35.3, 15.4 Hz), 1.04 (s, 3H), 0.92 (s, 3H), 0.90 (s, 3H), 0.74 (dd, 1H, *J* = 14.5, 3.4 Hz)

^{13}C NMR (125 MHz, $CDCl_3$) δ: 171.2, 95.8 (d, $^1J_{C\text{-}F}$ = 186 Hz), 77.6, 50.5 (d, $^2J_{C\text{-}F}$ = 18.1 Hz), 49.5, 47.3, 37.5 (d, $^2J_{C\text{-}F}$ = 18.1 Hz), 32.2 (d, $^3J_{C\text{-}F}$ = 11.3 Hz), 21.2, 20.2 (d, $^4J_{C\text{-}F}$ = 5.5 Hz), 19.4, 12.6

^{19}F NMR (500 MHz, $CDCl_3$): -157.8 ppm

Exact mass calcd. for $C_{12}H_{19}FO_2$: 237.1267 $(M+Na)^+$; found: 237.1261 $(M+Na)^+$

3.4.3. Fluorination of L-menthyl acetate

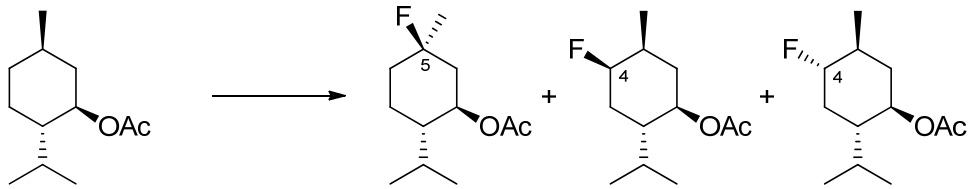

3.1 : 2.4 : 1.0

The reaction was performed according to the general procedure above using L-menthyl acetate[116] as substrate. Purification by flash chromatography (6% EtOAc/hexane) afforded the fluorination products [^{19}F NMR: -150.0 ppm (5β), -178.1 ppm (4α), -199.5 ppm (4β)] in an inseparable mixture, as a colourless oil (18 mg, 28% combined yield). The 5β-fluoro isomer was the major product. Regiochemical assignment for the 5β-fluoro compound was made on the basis of: (i) lack of a typical H-C-F ^{1}H signal in the δ4-5 range with a large $^2J_{H\text{-}F}$ value (40-50 Hz); (ii) the presence of an obvious vicinal methyl doublet signal with $^3J_{H\text{-}F}$ = 21 Hz. The stereochemical assignment was made on the basis of the weak through-space H-H COSY coupling between the axial H-COAc ^{1}H signal and the methyl doublet signal. Regiochemical assignment for the 4-fluoro compounds was made based on H-F splitting patterns and 2D-COSY. The stereochemical assignment was based on the lack of $^3J_{HH}$ splitting of the H-C-F ^{1}H signal (only $^2J_{H\text{-}F}$ was apparent, J = 50 Hz), which would only occur if the proton was in the equatorial position (see figure below). If the proton was axial, large trans-vicinal coupling would occur between adjacent hydrogens.

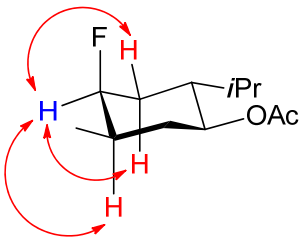

expect minimal $^{3}J_{Heq\text{-}Hax}$ coupling
(assigned as 4β)

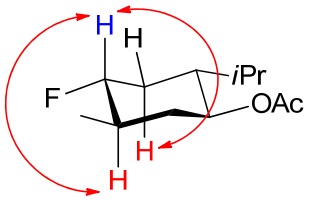

expect large $^{3}J_{Hax\text{-}Hax}$ coupling
(assigned as 4α)

5β-fluoro-L-menthyl acetate:

^{1}H NMR (500 MHz, $CDCl_3$) δ: 4.98 (ddd, 1H, *J* = 10.8, 10.8, 4.7 Hz), 2.30 (m, 1H), 1.93-1.79 (m, 4H), 1.46-1.30 (m, 6H), 1.35 (d, 3H, *J* = 21.1 Hz), 0.92 (d, 3H, *J* = 6.8 Hz), 0.80 (d, 3H, *J* = 6.8 Hz)

^{13}C NMR (125 MHz, $CDCl_3$) δ: 169.8, 94.6 (d, $^{1}J_{C\text{-}F}$ = 169 Hz), 70.6, 46.1, 41.9 (d, $^{2}J_{C\text{-}F}$ = 21 Hz), 39.5, 35.6 (d, $^{2}J_{C\text{-}F}$ = 22 Hz), 26.9 (d, $^{2}J_{C\text{-}F}$ = 24 Hz), 25.7, 25.3, 20.3, 15.6

^{19}F NMR (500 MHz, $CDCl_3$): -150.0 ppm

Exact mass calcd. for $C_{12}H_{21}FO_2$: 239.1423 $(M+Na)^+$; found: 239.1418 $(M+Na)^+$

3.4.4. Fluorination of D-camphor

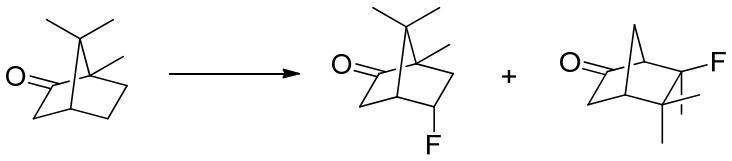

1 : 1

The reaction was performed according to the general procedure above using D-camphor as substrate. Purification by flash chromatography (8% EtOAc/hexane) afforded the major fluorination products in a 1:1 mixture [^{19}F NMR: -139.1 ppm (6-F rearranged product), -190.1 ppm (5-*endo*-F)] as a white solid (11.3 mg, 25%). The remaining material consisted of the 5-*exo*-F product (6%) and unreacted starting material.

5-*endo*-fluoro-D-camphor:

^{1}H NMR (500 MHz, $CDCl_3$) δ: 5.35 (dm, 1H, *J* = 56.6 Hz), 2.56 (d, 1H, *J* = 18.6 Hz), 2.43 (m, 1H), 2.26 (dd, 1H, *J* = 18.6, 4.5 Hz), 2.23 (m, 1H), 1.55 (ddd, 1H, *J* = 27.4, 14.8, 3.2 Hz), 1.16 (d, 3H, *J* = 6.6 Hz), 0.93 (s, 3H), 0.87 (s, 3H)

^{19}F NMR (500 MHz, $CDCl_3$): -190.1 ppm

6-fluoroisocamphanone:

^{1}H NMR (500 MHz, $CDCl_3$) δ: 2.69 (d, 1H, *J* = 7.5 Hz), 2.41 (dm, 1H, *J* = 10.9 Hz), 2.27 (m, 1H), 2.20 (m, 1H), 1.98 (dd, 1H, *J* = 18.8, 4.4 Hz), 1.66 (d, 1H, *J* = 10.9 Hz), 1.27 (d, 3H, *J* = 24.2 Hz), 0.98 (s, 3H), 0.89 (s, 3H)

^{19}F NMR (500 MHz, $CDCl_3$): -139.1 ppm

Exact mass calcd. for $C_{10}H_{15}FO$: 193.1005 $(M+Na)^+$; found: 193.0999 $(M+Na)^+$

3.4.5. Fluorination of (1*S*,5*R*)-1,8,8-trimethyl-2-oxabicyclo[3.2.1]octan-3-one

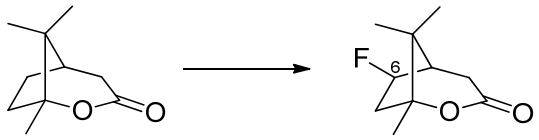

The reaction was performed according to the general procedure above using (1*S*,5*R*)-1,8,8-trimethyl-2-oxabicyclo[3.2.1]octan-3-one[117] as substrate. Purification by flash chromatography (16% EtOAc/hexane) afforded a single fluorination product as a white solid (7.6 mg, 14%), isolated with 7.5 mg of starting material. The stereochemistry assignment was made based on the lack of coupling between fluorine and the single hydrogen at C5 (doublet, $^{3}J_{H\text{-}H}$ = 16 Hz), it was deduced that the fluorine was therefore *trans* (close to 90°) to the proton, as this would significantly reduce its coupling constant.[118]

6-*exo*-fluoro-(1*S*,5*R*)-1,8,8-trimethyl-2-oxabicyclo[3.2.1]octan-3-one:

^{1}H NMR (500 MHz, $CDCl_3$) δ: 4.91(ddd, 1H, *J* = 54.3, 7.4, 2.3 Hz), 2.87 (dt, 1H, *J* = 19.3, 6.2 Hz), 2.70 (ddd, 1H, *J* = 16.2, 16.2, 7.4 Hz), 2.42 (d, 1H, *J* = 19.3 Hz), 2.30 (dd, 1H, *J* = 39.2, 16.8 Hz), 2.27 (d, 1H, *J* = 16.2 Hz), 1.34 (s, 3H), 1.18 (s, 3H), 1.07 (s, 3H)

^{13}C NMR (125 MHz, $CDCl_3$) δ: 169.6, 96.5 (d, $^{1}J_{C\text{-}F}$ = 183.8 Hz), 92.9 (d, $^{3}J_{C\text{-}F}$ = 3.4 Hz), 48.7 (d, $^{2}J_{C\text{-}F}$ = 20.9 Hz), 46.7 (d, $^{2}J_{C\text{-}F}$ = 20.9 Hz), 42.2 (d, $^{4}J_{C\text{-}F}$ = 1.8 Hz), 34.5 (d, $^{3}J_{C\text{-}F}$ = 11.5 Hz), 24.1 (d, $^{3}J_{C\text{-}F}$ = 4.4 Hz), 18.1, 18.0

^{19}F NMR (500 MHz, $CDCl_3$): -160.2 ppm

Exact mass calcd. for $C_{10}H_{15}FO_2$: 209.0954 $(M+Na)^+$; found: 209.0948 $(M+Na)^+$

3.4.6. Fluorination of 2-*endo*-methyl-3-*exo*-hydroxymethyl-bicyclo-[2.2.1]-heptanyl acetate

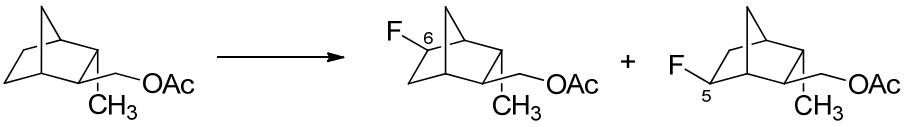

1 : 1

The reaction was performed according to the general procedure above using 2-*endo*-Methyl-3-*exo*-hydroxymethyl-bicyclo-[2.2.1]-heptanyl acetate as substrate. Purification by flash chromatography (4% EtOAc/hexane) afforded the fluorination products in an inseparable 1:1 mixture [^{19}F NMR: -160.6 (5-*exo*-F), -171.3 ppm (6-*exo*-F)] as a colourless oil (24 mg, 40% combined yield).

5-*exo*-fluoro-2-*endo*-Methyl-3-*exo*-hydroxymethyl-bicyclo-[2.2.1]-heptanyl acetate:

^{1}H NMR (500 MHz, $CDCl_3$) δ: 4.55 (dd, 1H, *J* = 55.9, 6.4 Hz), 3.98-3.88 (m, 2H), 2.28 (d, 1H, *J* = 8.6 Hz), 2.10 (m, 1H), 2.04 (s, 3H), 2.03 (m, 1H), 1.60 (d, 2H, *J* = 10.6 Hz), 1.49-1.41 (m, 2H), 0.92 (dt, 1H, *J* = 8.0, 6.6 Hz), 0.89 (d, 3H, *J* = 6.9 Hz)

^{19}F NMR (500 MHz, $CDCl_3$): -160.6 ppm

6-*exo*-fluoro-2-*endo*-Methyl-3-*exo*-hydroxymethyl-bicyclo-[2.2.1]-heptanyl acetate:

^{1}H NMR (500 MHz, $CDCl_3$) δ: 4.93 (dm, 1H, *J* = 55.2 Hz), 3.87 (m, 2H), 2.35 (m, 1H), 2.15 (m, 1H), 2.06 (s, 3H), 1.75 (m, 1H), 1.70 (m, 1H), 1.53 (m, 1H), 1.39 (t, 2H, *J* = 8.8 Hz), 1.11 (dt, 1H, *J* = 7.1, 6.7 Hz), 0.98 (d, 3H, *J* = 7.3 Hz)

^{19}F NMR (500 MHz, $CDCl_3$): -171.3 ppm

Exact mass calcd. for $C_{11}H_{17}FO_2$: 223.1110 $(M+Na)^+$; found: 223.1105 $(M+Na)^+$

3.4.7. Fluorination of cyclohexyl acetate

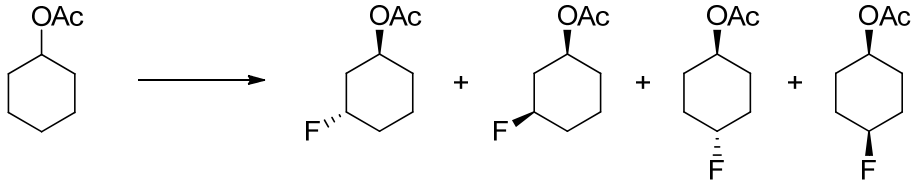

3.6 : 1 : 1 : 1.6

The reaction was performed according to the general procedure above using cyclohexyl acetate as substrate. Purification by flash chromatography (6% EtOAc/hexane) afforded the fluorination products [^{19}F NMR: -172.3 ppm (4-*cis*), -180.0 ppm (3-*trans*), -181.0 ppm (4-*trans*), -186.0 ppm (3-*cis*)] in a mixture as a volatile, colourless oil. The overall reaction yield was determined from crude ^{1}H NMR to be 49%, by using 1,3,5-trimethoxybenzene as internal standard. The 3-*trans*-fluoro isomer was the major product.

3-*trans*-fluorocyclohexyl acetate:

^{1}H NMR (500 MHz, $CDCl_3$) δ: 5.11 (tt, 1H, *J* = 8.4, 4.1 Hz), 4.89 (dtt, 1H, *J* = 48.2, 6.1, 2.9 Hz), 2.04 (m, 2H), 2.03 (s, 3H), 1.88-1.45 (m, 6H)

^{19}F NMR (500 MHz, $CDCl_3$): -180.0 ppm

Exact mass calcd. for $C_8H_{13}FO_2$: 183.0797 $(M+Na)^+$; found: 183.0792 $(M+Na)^+$

3.4.8. Fluorination of (3a*R*)-(+)-sclareolide (237)

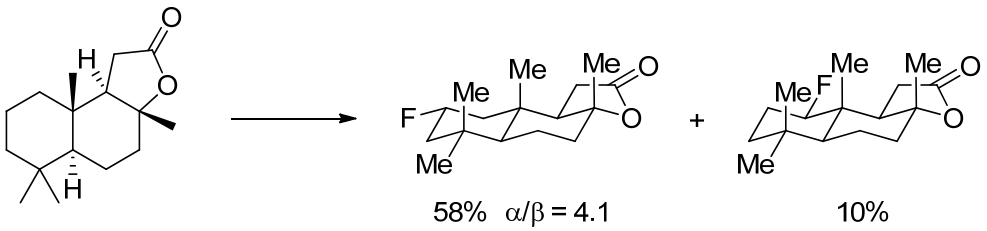

58% α/β = 4.1 10%

The reaction was performed according to the general procedure above using (3a*R*)-(+)-sclareolide (**237**) as substrate. Purification by flash chromatography (100% hexanes to 20% EtOAc/hexanes gradient) afforded the fluorination products [^{19}F NMR: -179.9 ppm (2α), -187.3 ppm (2β), -180.9 ppm (3β)] in a combined yield of 68%. The major 2α-fluoro isomer was obtained as a white solid, mixed with a small amount of the β-anomer (47 mg, 58%). Experimental data matches previously reported literature values for the same compound.[97]

2α-fluoro-(3a*R*)-(+)-sclareolide:

^{1}H NMR (500 MHz, $CDCl_3$) δ: 4.84 (dtt, 1H, *J* = 48.0, 11.3, 4.6 Hz), 2.46 (dd, 1H, *J* = 16.2, 14.7 Hz), 2.28 (dd, 1H, *J* = 15.8, 6.5 Hz), 2.13-1.86 (m, 6H), 1.71 (td, 1H, *J* = 12.6, 4.1 Hz), 1.44-1.31 (m, 6H), 1.00 (s, 3H), 0.96 (s, 3H), 0.90 (s, 3H)

^{19}F NMR (500 MHz, $CDCl_3$): -179.9 ppm

Exact mass calcd. for $C_{16}H_{25}FO_2$: 291.1736 $(M+Na)^+$; found: 291.1731 $(M+Na)^+$

4. Conclusions

In conclusion, we have directed our attention towards research areas that could positively impact the field of therapeutic agents and pharmaceuticals. Our efforts toward completing the first total synthesis of the biselide family of cytotoxic marine natural products relied on a concise synthesis of the 2,5-disubstituted-3-hydroxytetrahydrofuran core via the chloropolyol cyclization methodology previously developed in our group. Construction of the (*Z*,*Z*)-1,4-diene functionality in biselides proved to be a major challenge, with many of our efforts coming to no fruition. The RCM strategy was not viable due to the inherent reactivity difference between the alkenes required for metathesis, while the RRCM strategy also hit a dead-end due to the substrate's specific conformation leading to the undesired alkene geometry. Eventually, cross metathesis allowed successful construction of the (*Z*,*Z*)-1,4-diene, representing a major breakthrough in our efforts toward completing the total synthesis of biselides. On the other hand, we have also demonstrated a novel photocatalytic methodology which would allow for the direct displacement of a C(sp^3) hydrogen with fluorine. This mild process requires TBADT as a radical initiator and NFSI as the fluorine source, and represents one of the first methodologies which allow the direct installation of a fluorine atom at a non-benzylic C(sp^3) site. Further studies are currently ongoing in the Britton group both with regards to completing the total synthesis of biselides and to expanding the radical fluorination methodology towards medically relevant systems such as amino acids.

References

(1) Davis, A. *Medicines by Design*; National Institute of General Medical Sciences, 2006.

(2) Newman, D. J.; Cragg, G. M. *J. Nat. Prod.* **2007**, *70*, 461–477.

(3) Cragg, G. M.; Newman, D. J.; Snader, K. M. *J. Nat. Nroducts* **1997**, *60*, 52–60.

(4) Newman, D. J.; Cragg, G. M.; Snader, K. M. *J. Nat. Prod.* **2003**, *66*, 1022–1037.

(5) Baker, D. D.; Chu, M.; Oza, U.; Rajgarhia, V. *Nat. Prod. Rep.* **2007**, *24*, 1225–1244.

(6) Cragg, G. M.; Newman, D. J. *Expert Opin. Investig. Drugs* **2000**, *9*, 2783–2797.

(7) Blunt, J. W.; Copp, B. R.; Munro, M. H. G.; Northcote, T.; Michèle, R. *Nat. Prod. Rep.* **2004**, *21*, 1–49.

(8) Simmons, T. L.; Andrianasolo, E.; Mcphail, K.; Flatt, P.; Gerwick, W. H. *Mol. Cancer Ther.* **2005**, *4*, 333–342.

(9) Molinski, T. F.; Dalisay, D. S.; Lievens, S. L.; Saludes, J. P. *Nat. Rev. Drug Discov.* **2009**, *8*, 69–85.

(10) Koehn, F. E.; Carter, G. T. *Nat. Rev. Drug Discov.* **2005**, *4*, 206–220.

(11) Mowat, J. S. Ph.D. Thesis, Simon Fraser University, 2012.

(12) Drews, J. *Science* **2000**, *287*, 1960–1964.

(13) Schreiber, S. L. *Science* **2000**, *287*, 1964–1969.

(14) Hagmann, W. K. *J. Med. Chem.* **2008**, *51*, 4359–4369.

(15) O'Hagan, D. *J. Fluor. Chem.* **2010**, *131*, 1071–1081.

(16) Lorente, A.; Lamariano-Merketegi, J.; Albericio, F.; Álvarez, M. *Chem. Rev.* **2013**, *113*, 4567–4610.

(17) Peterson, A. C.; Harlin, H.; Karrison, T.; Vogelzang, N. J.; Knost, J. a; Kugler, J. W.; Lester, E.; Vokes, E.; Gajewski, T. F.; Stadler, W. M. *Invest. New Drugs* **2006**, *24*, 141–149.

(18) Quinoa, E.; Kakou, Y.; Crews, P. *J. Org. Chem.* **1988**, *53*, 3642–3644.

(19) Katsuki, T.; Sharpless, K. B. *J. Am. Chem. Soc.* **1980**, *102*, 5974–5976.

(20) Gollner, A.; Mulzer, J. *Org. Lett.* **2008**, *10*, 4701–4704.

(21) Tsuda, M.; Endo, T.; Kobayashi, J. *J. Org. Chem.* **2000**, *65*, 1349–1352.

(22) Kobayashi, J.; Kubota, T.; Endo, T.; Tsuda, M. *J. Org. Chem.* **2001**, *66*, 134–142.

(23) Yadav, J. S.; Reddy, C. S. *Org. Lett.* **2009**, *11*, 1705–1708.

(24) Li, H.; Wu, J.; Luo, J.; Dai, W.-M. *Chem. Eur. J.* **2010**, *16*, 11530–11534.

(25) Satoh, T.; Nanba, K.; Suzuki, S. *Chem. Pharm. Bull.* **1971**, *19*, 817–820.

(26) Takada, N.; Sato, H.; Suenaga, K.; Arimoto, H.; Yamada, K.; Ueda, K.; Uemura, D. *Tetrahedron Lett.* **1999**, *40*, 6309–6312.

(27) Kang, B.; Mowat, J.; Pinter, T.; Britton, R. *Org. Lett.* **2009**, *11*, 1717–20.

(28) Halland, N.; Braunton, A.; Bachmann, S.; Marigo, M.; Jørgensen, K. A. *J. Am. Chem. Soc.* **2004**, *126*, 4790–4791.

(29) Brochu, M. P.; Brown, S. P.; MacMillan, D. W. C. *J. Am. Chem. Soc.* **2004**, *126*, 4108–4109.

(30) Kang, B.; Britton, R. *Org. Lett.* **2007**, *9*, 5083–5086.

(31) Kang, B.; Chang, S.; Decker, S.; Britton, R. *Org. Lett.* **2010**, *12*, 1716–1719.

(32) Halperin, S.; Kang, B.; Britton, R. *Synthesis (Stuttg).* **2011**, 1946–1953.

(33) Cornforth, J. W.; Cornforth, R. H.; Mathew, K. K. *J. Chem. Soc.* **1959**, 112–127.

(34) Cee, V. J.; Cramer, C. J.; Evans, D. a *J. Am. Chem. Soc.* **2006**, *128*, 2920–2930.

(35) Evans, D. A.; Chapman, K. T.; Carreira, E. M. *J. Am. Chem. Soc.* **1988**, *110*, 3560–3578.

(36) Evans, D. A.; Hoveyda, A. H. *J. Org. Chem.* **1990**, *55*, 5190–5192.

(37) Cao, S. G.; Wu, X. H.; Sim, K. Y.; Tan, B. K. H.; Pereira, J. T.; Goh, S. H. *Tetrahedron* **1998**, *54*, 2143–2148.

(38) Kigoshi, H.; Hayakawa, I. *Chem. Rec.* **2007**, *7*, 254–264.

(39) Ueda, K.; Hu, Y. *Tetrahedron Lett.* **1999**, *40*, 6305–6308.

(40) Kigoshi, H.; Kita, M.; Ogawa, S.; Itoh, M.; Uemura, D. *Org. Lett.* **2003**, *5*, 957–960.

(41) Teruya, T.; Shimogawa, H.; Suenaga, K.; Kigoshi, H. *Chem. Lett.* **2004**, *33*, 1184–1185.

(42) Teruya, T.; Suenaga, K.; Maruyama, S.; Kurotaki, M.; Kigoshi, H. *Tetrahedron Lett.* **2005**, *61*, 6561–6567.

(43) Satoh, Y.; Kawamura, D.; Yamaura, M.; Ikeda, Y.; Ochiai, Y.; Hayakawa, I.; Kigoshi, H. *Tetrahedron Lett.* **2012**, *53*, 1390–1392.

(44) Tamao, K.; Akita, M.; Maeda, K.; Kumadat, M. *J. Org. Chem.* **1987**, *52*, 1100–1106.

(45) Still, W. C.; Gennari, C. *Tetrahedron Lett.* **1983**, *24*, 4405–4408.

(46) Kanai, K.; Wakabayashi, H.; Honda, T. *Org. Lett.* **2000**, *2*, 2549–2551.

(47) Takai, K.; Kimura, K.; Kuroda, T.; Hiyama, T.; Nozaki, H. *Tetrahedron Lett.* **1983**, *24*, 5281–5284.

(48) Jin, H.; Uenishi, J.; Christ, W. J.; Kishi, Y. *J. Am. Chem. Soc.* **1986**, *108*, 5644–5646.

(49) Gu, Y.; Snider, B. B. *Org. Lett.* **2003**, *5*, 4385–4388.

(50) Duboudin, J. G.; Jousseaume, B.; Bonakdar, A.; Saux, A. *J. Organomet. Chem.* **1979**, *168*, 227–232.

(51) Kiyooka, S.; Kaneko, Y.; Komura, M.; Matsuo, H.; Nakano, M. *J. Org. Chem.* **1991**, *56*, 2276–2278.

(52) Singer, R. A.; Carreira, E. M. *J. Am. Chem. Soc.* **1995**, *117*, 12360–12361.

(53) Sheffy, F. K.; Godschalx, J. P.; Stille, J. K. *J. Am. Chem. Soc.* **1984**, *106*, 4833–4840.

(54) Inanaga, J.; Hirata, K.; Saeki, H.; Katsuki, T.; Yamaguchi, M. *Bull. Chem. Soc. Jpn.* **1979**, *52*, 1989–1993.

(55) Hoye, T. R.; Wang, J. *J. Am. Chem. Soc.* **2005**, *127*, 6950–6951.

(56) Micalizio, G. C.; Roush, W. R. *Org. Lett.* **2001**, *3*, 1949–1952.

(57) Kaneda, K.; Uchiyama, T.; Fujiwara, Y.; Imanaka, T.; Teranishi, S. *J. Org. Chem.* **1979**, *44*, 55–63.

(58) Gemal, A. L.; Luche, J. L. *J. Am. Chem. Soc.* **1981**, *103*, 5454–5459.

(59) Roulland, E. *Angew. Chem. Int. Ed. Engl.* **2008**, *47*, 3762–5.

(60) Araki, S.; Ito, H.; Butsugan, Y. *J. Org. Chem.* **1988**, *53*, 1831–1833.

(61) Miyaura, N.; Suzuki, A. *Chem. Rev.* **1995**, *95*, 2457–2483.

(62) Hayakawa, I.; Ueda, M.; Yamaura, M.; Ikeda, Y.; Suzuki, Y.; Yoshizato, K.; Kigoshi, H. *Org. Lett.* **2008**, *10*, 1859–1862.

(63) Ko, S. S.; Klein, L. L.; Pfaff, K.-P.; Kishi, Y. *Tetrahedron Lett.* **1982**, *23*, 4415–4418.

(64) Miura, K.; Hondo, T.; Okajima, S.; Nakagawa, T.; Takahashi, T.; Hosomi, A. *J. Org. Chem.* **2002**, *67*, 6082–6090.

(65) Ueda, M.; Yamaura, M.; Ikeda, Y.; Suzuki, Y.; Yoshizato, K.; Hayakawa, I.; Kigoshi, H. *J. Org. Chem.* **2009**, *74*, 3370–3377.

(66) Schomaker, J. M.; Borhan, B. *J. Am. Chem. Soc.* **2008**, *130*, 12228–12229.

(67) Baati, R.; Barma, D. K.; Falck, J. R.; Mioskowski, C. *J. Am. Chem. Soc.* **2001**, *123*, 9196–9197.

(68) Baati, R.; Barma, D. K.; Falck, J. R.; Mioskowski, C. *Tetrahedron Lett.* **2002**, *43*, 2183–2185.

(69) Barton, D. H. R.; McCombie, S. W. *J. Chem. Soc. Perkin Trans. 1* **1975**, 1574–1585.

(70) Satoh, Y.; Yamada, T.; Onozaki, Y.; Kawamura, D.; Hayakawa, I.; Kigoshi, H. *Tetrahedron Lett.* **2012**, *53*, 1393–1396.

(71) Chenault, J.; Dupin, J.-F. E. *Synthesis (Stuttg).* **1987**, *5*, 498–499.

(72) Kang, B. Ph.D. Thesis, Simon Fraser University, 2012.

(73) Ghosh, A. K.; Li, J. *Org. Lett.* **2009**, *11*, 4164–4167.

(74) Draper, J. A.; Britton, R. *Org. Lett.* **2010**, *12*, 4034–4037.

(75) Bräse, S.; Wertal (nee Nüske), H.; Frank, D.; Vidović, D.; de Meijere, A. *European J. Org. Chem.* **2005**, 4167–4178.

(76) Coxon, J. M.; Dansted, E.; Hartshorn, M. P. *Org. Synth.* **1977**, *56*, 25.

(77) Hoye, T. R.; Jeffrey, C. S.; Tennakoon, M. a; Wang, J.; Zhao, H. *J. Am. Chem. Soc.* **2004**, *126*, 10210–1.

(78) Wang, X.; Bowman, E. J.; Bowman, B. J.; Porco, J. a *Angew. Chem. Int. Ed. Engl.* **2004**, *43*, 3601–5.

(79) Samsel, E. G.; Kochi, J. K. *J. Am. Chem. Soc.* **1986**, *108*, 4790–4804.

(80) Escoula, B.; Hajjaji, N.; Lattes, A. *J. Chem. Soc. Chem. Commun.* **1984**, *18*, 1233–1234.

(81) d'Hooghe, M.; Van Brabandt, W.; Dekeukeleire, S.; Dejaegher, Y.; De Kimpe, N. *Chemistry* **2008**, *14*, 6336–6340.

(82) Mancuso, A. J.; Huang, S.-L.; Swern, D. *J. Org. Chem.* **1978**, *43*, 2480–2482.

(83) Schmit, A. L. Ph.D. Thesis, University of Minnesota, 2011.

(84) Hong, S. H.; Sanders, D. P.; Lee, C. W.; Grubbs, R. H. *J. Am. Chem. Soc.* **2005**, *127*, 17160–17161.

(85) Mitsunobu, O.; Yamada, M. *Bull. Chem. Soc. Jpn.* **1967**, *40*, 2380–2382.

(86) Zhang, K.-Y.; Borgerding, A. J.; Carlson, R. M. *Tetrahedron Lett.* **1988**, *29*, 5703–5706.

(87) Ranatunga, S.; Kim, J. S.; Pal, U.; Del Valle, J. R. *J. Org. Chem.* **2011**, *76*, 8962–8976.

(88) Kirk, K. L. *Org. Process Res. Dev.* **2008**, *12*, 305–321.

(89) Ametamey, S. M.; Honer, M.; Schubiger, P. A. *Chem. Rev.* **2008**, *108*, 1501–1516.

(90) Fried, J.; Sabo, E. F. *J. Am. Chem. Soc.* **1954**, *76*, 1455–1456.

(91) Liang, T.; Neumann, C. N.; Ritter, T. *Angew. Chem. Int. Ed. Engl.* **2013**, *52*, 8214–8264.

(92) Barker, T. J.; Boger, D. L. *J. Am. Chem. Soc.* **2012**, *134*, 13588–13591.

(93) Lee, E.; Kamlet, A. S.; Powers, D. C.; Neumann, C. N.; Boursalian, G. B.; Furuya, T.; Choi, D. C.; Hooker, J. M.; Ritter, T. *Science* **2011**, *334*, 639–642.

(94) Watson, D. a; Su, M.; Teverovskiy, G.; Zhang, Y.; García-Fortanet, J.; Kinzel, T.; Buchwald, S. L. *Science* **2009**, *325*, 1661–1664.

(95) Braun, M.-G.; Doyle, A. G. *J. Am. Chem. Soc.* **2013**, *135*, 12990–12993.

(96) Xia, J.-B.; Zhu, C.; Chen, C. *J. Am. Chem. Soc.* **2013**, *135*, 17494–17500.

(97) Liu, W.; Huang, X.; Cheng, M.-J.; Nielsen, R. J.; Goddard, W. A.; Groves, J. T. *Science* **2012**, *337*, 1322–1325.

(98) Bloom, S.; Pitts, C. R.; Miller, D. C.; Haselton, N.; Holl, M. G.; Urheim, E.; Lectka, T. *Angew. Chem. Int. Ed. Engl.* **2012**, *51*, 10580–10583.

(99) Amaoka, Y.; Nagatomo, M.; Inoue, M. *Org. Lett.* **2013**, *15*, 216–2163.

(100) Chambers, R. D.; Parsons, M.; Sandford, G.; Bowden, R. *Chem. Commun.* **2000**, 959–960.

(101) Rueda-Becerril, M.; Sazepin, C. C.; Leung, J. C. T.; Okbinoglu, T.; Kennepohl, P.; Paquin, J.-F.; Sammis, G. M. *J. Am. Chem. Soc.* **2012**, *134*, 4026–4029.

(102) Leung, J. C. T.; Chatalova-Sazepin, C.; West, J. G.; Rueda-Becerril, M.; Paquin, J.-F.; Sammis, G. M. *Angew. Chem. Int. Ed. Engl.* **2012**, *51*, 10804–10807.

(103) Teare, H.; Robins, E. G.; Arstad, E.; Luthra, S. K.; Gouverneur, V. *Chem. Commun.* **2007**, 2330–2332.

(104) Tzirakis, M. D.; Lykakis, I. N.; Orfanopoulos, M. *Chem. Soc. Rev.* **2009**, *38*, 2609–2621.

(105) Renneke, R. F.; Pasquali, M.; Hill, C. L. *J. Am. Chem. Soc.* **1990**, *112*, 6585–6594.

(106) Hill, C. L. *J. Mol. Catal. A Chem.* **2007**, *262*, 2–6.

(107) Hill, C. L. *Synlett* **1995**, 127.

(108) Tanielian, C. *Coord. Chem. Rev.* **1998**, *178-180*, 1165–1181.

(109) Protti, S.; Ravelli, D.; Fagnoni, M.; Albini, A. *Chem. Commun.* **2009**, 7351–7353.

(110) Lykakis, I. N.; Tanielian, C.; Seghrouchni, R.; Orfanopoulos, M. *J. Mol. Catal. A Chem.* **2007**, *262*, 176–184.

(111) Duncan, D. C.; Netzel, T. L.; Hill, C. L. *Inorg. Chem.* **1995**, *34*, 4640–4646.

(112) Dondi, D.; Fagnoni, M.; Albini, A. *Chem. Eur. J.* **2006**, *12*, 4153–4163.

(113) Ravelli, D.; Zema, M.; Mella, M.; Fagnoni, M.; Albini, A. *Org. Biomol. Chem.* **2010**, *8*, 4158–4164.

(114) Ochiai, M.; Yoshimura, A.; Hoque, M. M.; Okubo, T.; Saito, M.; Miyamoto, K. *Org. Lett.* **2011**, *13*, 5568–5571.

(115) Stavber, S.; Planiniek, Z.; Zupan, M. *J. Org. Chem.* **1992**, *57*, 5334–5337.

(116) Shimizu, T.; Hiranuma, S.; Nakata, T. *Tetrahedron Lett.* **1996**, *37*, 6145–6148.

(117) Suginome, H.; Yamada, S. *Tetrahedron Lett.* **1984**, *25*, 3995–3998.

(118) Minch, M. J. *Concepts Magn. Reson.* **1994**, *6*, 41–56.